

Role of the complement system and HtrA1 in microglia and age-related macular degeneration



Inaugural - Dissertation

zur

Erlangung des Doktorgrades
der Mathematisch-Naturwissenschaftlichen Fakultät
der Universität zu Köln

vorgelegt von

Isha Akhtar-Schäfer
aus Köln

Köln 2019

Berichterstatter/in

Prof. Dr. Elena Rugarli

Prof. Dr. Thorsten Hoppe

Tag der mündlichen Prüfung: 15. Januar 2019

Für meine Eltern

“If the extremity of the ivory handle of a dissecting knife be pushed against this surface, a breach is made in it, and a membrane of great delicacy may be separated and turned down in folds over the choroid coat, presenting the most beautiful specimen of a delicate tissue which the human body affords.”

An Account of a Membrane in the Eye by Arthur Jacob (1790–1874)

Contents

I Summary.....	1
II Zusammenfassung	2
1 Introduction.....	3
1.1. The mammalian retina.....	4
1.2. Age-related macular degeneration	6
1.2.1. Genetic risk factors	9
1.2.2. Complement system activation in the retina during AMD	10
1.2.3. Risk locus ARMS2/HTRA1	14
1.3. Microglia	17
1.3.1. Microglia activation and its role in AMD.....	18
1.3.2. Microglia modulation as therapy strategy	20
1.4. Aims of the study	24
2 Material and Methods	25
2.1. Material	26
2.1.1. Mice	26
2.1.2. Cells and bacteria.....	26
2.1.3. Media	27
2.1.4. Buffers and solutions	28
2.1.5. Antibodies.....	29
2.1.6. Enzymes.....	30
2.1.7. Kits.....	30
2.1.8. Cloning constructs and cloning primers	31
2.1.9. RNAscope probes and qRT-PCR primers	32
2.1.10. Cell culture compounds and reagents	33

2.1.11. Devices.....	34
2.1.12. General consumables	35
2.1.13. Software	36
2.2. Methods.....	36
2.2.1. Murine model of dry AMD.....	36
2.2.1.1. Bright light induced retinal damage	36
2.2.1.2. SD-OCT	37
2.2.1.3. Retina preparation	37
2.2.1.4. Ex vivo electroretinogram	37
2.2.2. Histologic analysis.....	38
2.2.2.1. Preparation of fixed frozen cryo sections.....	38
2.2.2.2. RNA-Scope	38
2.2.2.3. Immunostaining.....	39
2.2.2.4. Fluorescence microscopy	39
2.2.3. Cell culture.....	39
2.2.3.1. Maintenance and passage of cells	39
2.2.3.2. Primary microglia cell culture.....	40
2.2.3.3. Treatment regime	40
2.2.3.4. Nitrite measurement	41
2.2.3.5. Morphological analysis	41
2.2.4. Expression of recombinant eukaryotic proteins.....	42
2.2.4.1. Cloning.....	42
2.2.4.2. Transfection.....	44
2.2.4.3. Affinity chromatography	44
2.2.4.4. Enzymatic activity assay	45
2.2.5. PAI-1 promoter assay	45
2.2.6. Transcript analysis	46
2.2.6.1. RNA isolation and quantification.....	46
2.2.6.2. Reverse transcription.....	47
2.2.6.3. Quantitative reverse transcriptase PCR.....	47
2.2.7. Protein analysis.....	48
2.2.7.1. Protein isolation and quantification.....	48
2.2.7.2. Western blot	48
2.2.8. Statistical analysis.....	49

3	Results	50
3.1.	Light induced retinal damage as rodent model for dry AMD	51
3.1.1.	ERG in light damaged retinal explants	51
3.1.2.	HF in SD-OCT after LD	54
3.2.	Complement system activation in microglia during retinal degeneration.....	56
3.2.2.	Expression of anaphylatoxin receptors in activated microglia <i>in vitro</i> ..	56
3.2.3.	Expression of anaphylatoxin receptors in activated microglia <i>in vivo</i> ..	57
3.3.	Involvement of HtrA1 in microglial inflammation during retinal degeneration	60
3.3.1.	Expression of HtrA1 in the retina during retinal degeneration	60
3.3.2.	Effects of AMD-associated HtrA1 variants on microglial activity	61
3.3.2.1.	Expression and enzymatic activity of HtrA1 variants.....	62
3.3.2.2.	Effects of HtrA1 variants on TGF- β signaling.....	63
3.3.2.3.	Effects of HtrA1 variants on TGF- β response elements	68
4	Discussion.....	70
4.1.	Light-induced retinal degeneration as model for dry AMD.....	71
4.2.	Role of C3aR and C5aR in microglia during inflammation.....	73
4.3.	Effect of HTRA1 variants on TGF- β signaling in microglia	75
4.4.	Perspective	78
	Bibliography.....	79
	List of Abbreviations.....	104
	List of Figures	107
	List of Tables.....	108
	Attachments	109
	Acknowledgements.....	110
	Erklärung	111
	Lebenslauf	112

I Summary

Age-related macular degeneration (AMD) is a retinal degenerative and neovascular disease and the most common cause of blindness in the elderly. Advanced AMD includes the late stages geographic atrophy (GA) and choroidal neovascularization (CNV). A characteristic hallmark of AMD is the chronic over-activation of the innate immune system leading to devastating neuron demise and the promotion of pathologic vessel growth. Microglia, the resident immune cells of the retina, are significant drivers of this tissue harming inflammation during AMD. Interestingly, immunomodulatory approaches attenuating pathologic microgliosis have demonstrated beneficial effects on disease progression.

Genome wide association studies (GWAS) identified single nucleotide polymorphisms (SNPs) in genes of the complement system and AMD. Uncontrolled complement activation, owing to genetic mutations, results in increased expression of the anaphylatoxins C3a and C5a, which promote disease progression. However, the underlying mechanism of complement anaphylatoxins remains elusive. Hence, the role of microglia and the C3a and C5a mediated retinal degeneration was investigated. Indeed, activated microglia were found to have increase expression of the anaphylatoxin receptors C3aR and C5aR during inflammatory conditions. Furthermore, microglia were found to be the sole cells in the retina to express C3a and C5a receptors during degeneration. Hence, inhibition of microglial anaphylatoxin receptors represents an exploitable therapy strategy.

Furthermore, a strong correlation between polymorphisms on the gene for high-temperature requirement A serine peptidase 1 (HTRA1) and AMD was found. HtrA1 is known to inhibit transforming growth factor β (TGF- β) signaling, a pathway involved in the induction of a homeostatic microglia state. Hence, the effect of AMD-associated variants of HtrA1 on microglial activation was studied. For this purpose, TGF- β and HtrA1 variants, including the wildtype and AMD-associated isoform, were applied on pro-inflammatory microglia. As expected, TGF- β exerted protective anti-inflammatory effects on challenged microglia. However, HtrA1 variants did not alter transcript expression of TGF- β response genes and neither induced a reactive microglial phenotype. This study shows HtrA1 did not change the quiescent state of microglia secondary to TGF- β stimulation.

II Zusammenfassung

Die altersabhängige Makuladegeneration (AMD) ist eine degenerative Erkrankung der Netzhaut, welche zugleich die häufigste Ursache für Erblindung bei älteren Menschen ist. Die fortgeschrittene Form der AMD umfasst die trockene atrophische und die feuchte neovaskuläre Form. Ein Merkmal der AMD ist die chronische Aktivierung des angeborenen Immunsystems, die zu einem verheerenden Neuronensterben und der Förderung des pathologischen Gefäßwachstums führt. Die Immunzellen der Netzhaut, die Mikrogliazellen, sind wichtige Treiber dieser Entzündungsreaktion. Interessanterweise konnte man durch immunomodulatorische Ansätze die pathologische Mikrogliose abschwächen, welche sich positiv auf das Fortschreiten der Krankheit auswirkte.

Genetische Assoziationsstudien identifizierten Mutationen in Genen des Komplementsystems, welche zur AMD Manifestation beitragen. Eine unkontrollierte Komplementaktivierung aufgrund genetischer Mutationen führt zu einer erhöhten Expression der Anaphylatoxine C3a und C5a, die das Fortschreiten der Krankheit fördern. Der zugrundeliegende Mechanismus von Komplement-Anaphylatoxinen bleibt jedoch schwer fassbar. Daher wurde die Rolle der Mikrogliazellen und der Anaphylatoxine untersucht. Tatsächlich wiesen aktivierte Mikrogliazellen eine erhöhte Expression der Anaphylatoxin-Rezeptoren C3aR und C5aR auf. Darüber hinaus wurde festgestellt, dass Mikrogliazellen als einzige Zellart in der Retina Rezeptoren für C3a und C5a exprimieren. Daher stellt die Hemmung von Anaphylatoxin-Rezeptoren eine Therapiestrategie dar.

Darüber hinaus wurde eine starke Korrelation zwischen Polymorphismen auf dem Gen für die Serinprotease HTRA1 und der AMD gefunden. Es ist bekannt, dass HtrA1 den Signalweg des Wachstumsfaktors TGF- β , welcher die Mikrogliose reduziert, hemmt. Daher wurde die Wirkung von AMD-assoziierten Varianten von HtrA1 auf die Mikrogliazell-Aktivierung untersucht. Zu diesem Zweck wurden aktivierte Mikroglia mit TGF- β - und HtrA1-Varianten behandelt. Wie erwartet, wirkt TGF- β entzündungshemmend. Jedoch zeigten die HtrA1-Varianten keinen Einfluss auf die Antwortgene von TGF- β und den dadurch induzierten homöostatischen Mikrogliazell-Phänotypen. Diese Studie zeigt, dass AMD-assoziierte Mutationen im HtrA1 Protein keinen Einfluss auf Mikrogliazellen haben.

1 Introduction

1.1. The mammalian retina

The retina is the sensory part of the eye receiving and processing visual stimuli from the environment. It lines the posterior part of the eye and exhibits a highly organized, layered structure with more than 60 distinct retinal cell types (Hoon et al, 2014; Masland, 2001) (Fig. 1 A). The cells in the retina convert this visual information into action potentials and forward it through the optic tract to the visual cortex, in the occipital lobe, of the brain.

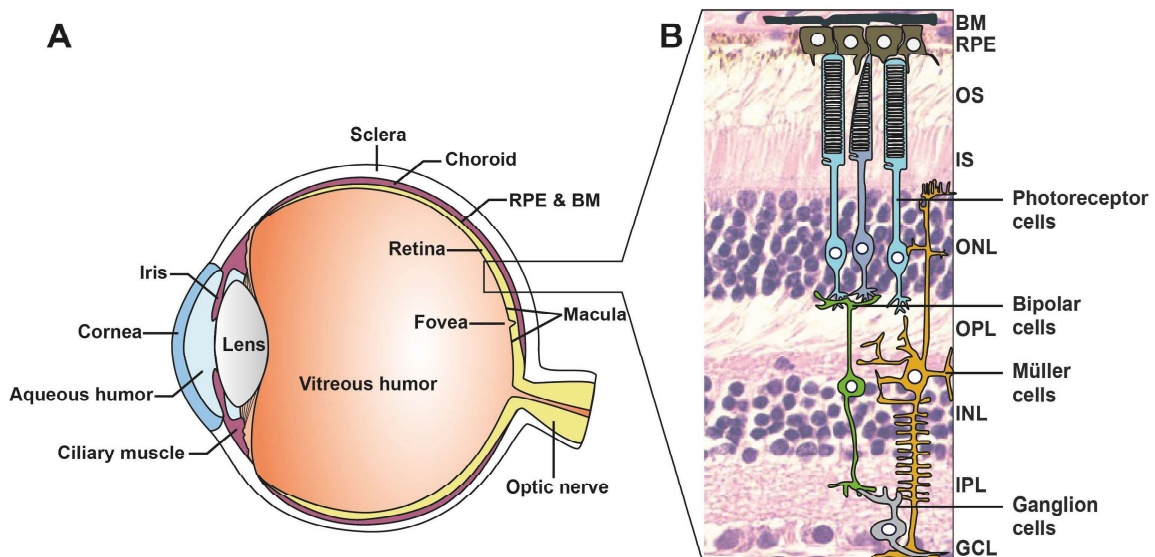


Figure 1 Schematic overview of the human eye and the structure of the retina
(A) The vertebrate eye cup develops from the neural tube, in particular the diencephalon. The light sensitive neural retina lines the posterior part of the eye and is attached to the retinal pigment epithelium (RPE) and Bruch's membrane (BM). **(B)** H&E stained cross section of human retina exhibits layered structure corresponding to different cell components as illustrated schematically. Retinal cells include rod and cone photoreceptor cells (blue), bipolar cells (green), Müller cells (orange), and retinal ganglion cells (grey). These cells are distributed across six layers: OS: outer segments; IS: inner segments; ONL: outer nuclear layer; OPL: outer plexiform layer; INL: inner nuclear layer; IPL: inner plexiform layer; GCL: ganglion cell layer. Axons of the ganglion cells form the optic nerve. Schematic retinal cells modified from Karlstetter et al. (Karlstetter et al, 2010).

The neural tube, in particular the developing diencephalon, gives rise to the vertebrate eye cups (Lamb et al, 2007). The approximately 0.5 mm thick sensory retina can be divided into distinct macroscopic layers of nerve cell bodies and synapses corresponding to diverse

component cells (Kolb, 1995) (Fig. 1 B). The outer nuclear layer (ONL) contains the nuclei of the photoreceptor cells, the inner nuclear layer (INL) contains the bipolar-, horizontal- and amacrine nuclei. The ganglion cell layer (GCL) is the innermost layer of nuclei. Those nuclear layers are divided by the outer plexiform layer (OPL) and the inner plexiform layer (IPL) where synaptic contacts occur. The photoreceptor outer segments (OS) of the rod and cone photoreceptor cells are attached to the apical surface of the retinal pigment epithelium (RPE). The basal surface of the RPE faces the underlying Bruch's membrane (BM). Aside from forming the blood retina barrier (BRB) the RPE is essential for the proper functioning of the neural retina and performs crucial housekeeping tasks including transport of nutrients, removal of waste products, phagocytosis of shed photoreceptor outer segments, and visual pigment regeneration (Bonilha, 2014; Cunha-Vaz et al, 2011).

Light enters the eye and travels through the vitreous and, the layers of the retina until it is captured by the OS of the cone and rod cells. Cone cells are responsible for day and color vision (photopic vision) whereas rod cells are responsible for vision in dim light (scotopic vision). The human retina has around 6 million cone cells, which are most densely represented in the macula. Three types of cone cells exhibit differing absorption properties due to the distinct opsins. The mean wavelengths of maximal absorption are 437 nm, 533 nm and 564 nm wavelength for the blue, green and red pigment, respectively (Bowmaker & Dartnall, 1980). The far more sensitive rod cells respond to a single photon and outnumber the cone cells by 20-fold, situated mainly in the periphery of the eye (Luo et al, 2008). Those cells contain rhodopsin, which is the main protein responsible for vision (Stein et al, 1982). Absorption of a single photon isomerizes the chromophore and ligand of rhodopsin, from 11-*cis*-retinal to all-*trans*-retinal and hence activates the phototransduction cascade followed by hyperpolarization of the photoreceptor membrane and decrease of glutamate release at the synaptic terminal (Lamb & Pugh, 2006). Next, the chemical output is integrated by interneurons (bipolar, horizontal and amacrine cells) and transmitted to ganglion cells (Jager, 2005). The axons of the ganglion cells form the optic nerve and optic tract which enters the lateral geniculate bodies. From here the geniculocalcarine tract projects into the primary visual cortex (Swienton & Thomas, 2014).

1.2. Age-related macular degeneration

AMD is the most frequent retinal degenerative and neovascular disease as well as the most common cause of irreversible vision loss in the elderly, especially among Caucasians. Epidemiologic facts on AMD are highly alarming, with more than 150 million people worldwide suffering from early forms, beginning with distortion of central vision and around 10 million people developing the late stages where high-resolution central vision is lost and patients are considered legally blind (Fig. 2) (Friedman et al, 2004; Wong et al, 2014).



Figure 2 Early, intermediate and late AMD symptoms of diseased individuals
Early AMD causes slightly blurred central vision. With disease progression central vision then becomes shadowed until a blind spot develops concomitant with difficulty in seeing colors and fine details. Figures from Dissertation Vierkotten (2011).

Early to intermediate stages of AMD are characterized by hypo- and hyper-pigmentation of the RPE and the appearance of drusen in the macular region which can be visualized in a fundus picture (Fig. 3) (Ferris et al, 2005). Drusen are extracellular aggregates located in the sub-RPE space (between the BM and the basal lamina of the RPE) (Abdelsalam et al, 1999; Buschini et al, 2011). AMD is a progressive disease where disease severity correlates with the size and number of drusen. Advanced AMD includes two late stages manifestations: geographic atrophy (GA) and the exudative, neovascular form (nAMD). In GA focal loss of photoreceptors and the underlying RPE is apparent (Fig. 3). Characteristic for nAMD is blood vessel growth from the subretinal space into the retina where the vascular network not only forms in an unregulated manner, but also becomes leaky (Fig. 3) (McLeod et al, 2009). In contrast to the slow progressing atrophic AMD form, the exudative form results in acute vision loss through edema formation and bleeding of new blood vessels which invade the

neural retina, accounting for more than 90 % central vision loss in AMD patients (Colijn et al, 2017; Weih et al, 2000). New vessel formation is driven by the angiogenic factor vascular endothelial growth factor (VEGF). Patients are therefore treated with monthly intravitreal injections of antibodies directed against VEGF, however, treatment success is not guaranteed (Cummings & Cunha-Vaz, 2008). Moreover, no treatment options are currently available for patients suffering from GA.

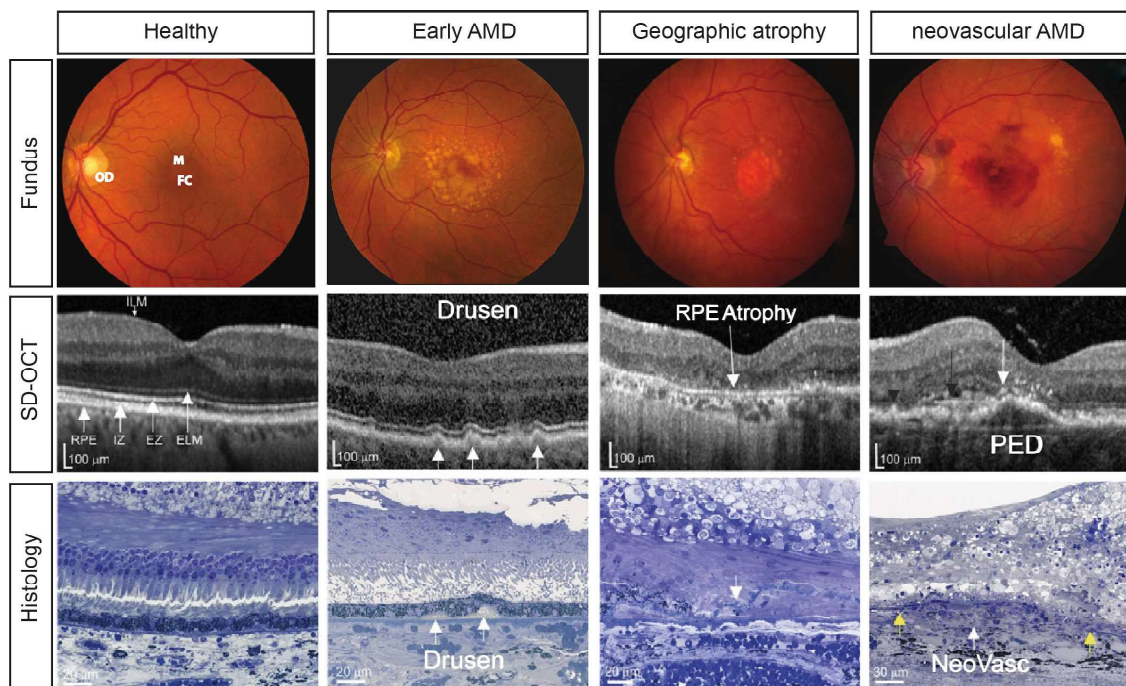


Figure 3 Fundus and SD-OCT photographs and histology of healthy and diseased eyes. Retinal fundus photographs of healthy individual shows no abnormality in the macula region. Regular layered structure can be seen though SD-OCT (white arrow point to the RPE and the external limiting membrane, ELM), and in histologic sections. Early to intermediate stage of AMD are characterized by the appearance of drusen which are visible in SD-OCT pictures (white arrows). Late stage AMD either develops into geographic atrophy (G) or neovascular AMD (nAMD). GA is characterized by atrophic RPE and absence of these cells in histologic sections. In nAMD drusen are still present along with subretinal hemorrhages which may result in pigment epithelial detachment (PED). Appearance of hyperreflective foci in SD-OCT images has been observed (white arrow). Fragmentation of the BM facilitates ingrowth of newly built blood vessels. OD: optic disc; M: macula; FC: fovea centralis; IZ: interdigitation zone; EZ: ellipsoid zone. Fundus pictures adapted from Swaroop et al. (Swaroop et al, 2009). SD-OCT and histology pictures from Toomey et al. (Toomey et al, 2018a).

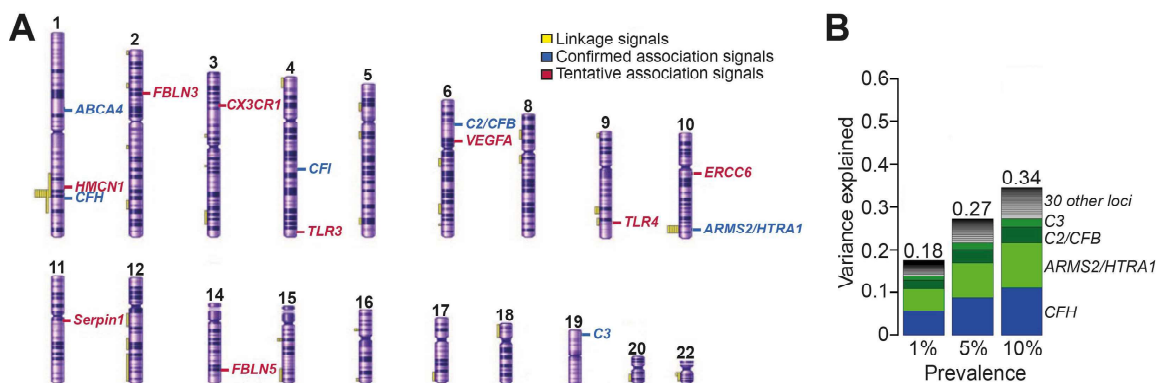
Recently, ophthalmic imaging was facilitated by the wide use of noninvasive high-resolution spectral domain optical coherence tomography (SD-OCT). This tool aids to acquire cross-sectional images of the retina in real time by means of echo time delay and magnitude of backscattered light. These images deliver data on the thickness and intactness of retinal layers and even more the appearance of drusen (Smith & Chauhan, 2015) (Fig. 3). Monitoring the retina of wet AMD patients demonstrated the presence of small, dense particles referred to as hyper-reflective foci (HF) (Altay et al, 2016; Framme et al, 2010).

AMD is a multifactorial disease with both, genetic and non-genetic factors contributing to disease ontogenesis, progression and manifestation. Age is considered as the most significant risk factor for AMD as the prevalence for late stage AMD peaks in individuals older than 80 years (Fritsche et al, 2014; Klein et al, 2010; Swaroop et al, 2009). The aging retina is not spared from the progressive decline in function which affects every other organ in the human body. Advanced age is accompanied by increased retinal vulnerability to disease due to changes in both, the highly active photoreceptor cells and the phagocytic RPE (Mitter et al, 2012). These cells contribute to the generation of metabolic by-products which are cleared rapidly under physiologic conditions (Datta et al, 2017). However, aged cells are less effective in dealing with the accumulating metabolic waste which becomes apparent as depositions in the form of drusen (Wang et al, 2009a).

Secondary to aging, smoking was found to significantly increase the risk of developing AMD most likely owing to oxidative insults (Espinosa-Heidmann et al, 2006; Khan et al, 2006). Furthermore, abdominal obesity significantly increases the risk factor for developing AMD while diets rich in antioxidant are associated with a decreased risk (Adams et al, 2011; Tan et al, 2008). Dysbiosis in gut microbes induced by high fat diet is known to facilitate intestinal permeability and hence allow translocation of pathogens which are associated to exacerbated CNV (Andriessen et al, 2016). Due to comprehensive association studies of smoking and fatty diet, current management of early and intermediate AMD include lifestyle and dietary modifications e.g. cessation of tobacco use, increased dietary intake of antioxidants and control of body-mass index (Jager et al, 2008).

1.2.1. Genetic risk factors

Despite the fact, that change of lifestyle reduces the likelihood of disease progression, one major contributor cannot be modified: genetic heritability is a substantial contributor evidenced by a number of twin and familial aggregation studies (Fig. 4 A) (Hammond et al, 2002; Seddon et al, 1997; Seddon et al, 2005). In a study by Seddon et al., authors found that genetic factors account for up to 71 % of the variation in the overall severity of AMD (Seddon et al, 2005). Using genome wide association studies (GWAS) a total of 52 variants in 34 loci were identified which are highly associated with AMD (Fritsche et al, 2013; Fritsche et al, 2016). Strikingly, variants on chromosome 1q32, coding for complement factor H (CFH), have a strong and indisputable association (Edwards et al, 2005; Haines et al, 2005; Klein et al, 2005; Raychaudhuri et al, 2011; Zarepari et al, 2005). These results were followed by genetic association studies that found further associated variants in genes coding complement proteins (Seddon et al, 2013; Ven et al, 2013; Zhan et al, 2013). Another locus in chromosome 10q26 harboring high-temperature requirement A serine peptidase 1 (HTRA1) and age-related maculopathy susceptibility 2 (ARMS2) demonstrated one of the strongest replicable association with AMD (Fig. 4 B) (DeAngelis et al, 2008; Dewan et al, 2006; Yang et al, 2006).



1.2.2. Complement system activation in the retina during AMD

Studies have shown that the retina expresses a variety of complement proteins, receptors and regulators despite the fact that it is an immune privileged organ (Anderson et al, 2010). The complement system, consisting of numerous small proteins and factors, when triggered, activates in a cascade fashion through at least one of its three pathways (Fig. 5). The classical pathway is induced when antibodies bind to their corresponding antigens (Janeway CA Jr et al, 2001). The mannose-binding lectin (MBL) pathway is triggered by the binding of lectin to mannose residues on the surface of microorganisms (Fujita, 2002). The alternative pathway is spontaneously and continuously activated (Pangburn & Muller-Eberhard, 1984; Zipfel et al, 2007). Two critical steps result in the activation of the complement pathways, namely the cleavage of complement factor 3 (C3) and factor 5 (C5) by convertases that are generated upon activation of the before mentioned pathways. This results in the generation of C3a, C3b, C5a and C5b. C3b participates in opsonizing pathogens or dead cells and promoting their phagocytosis in a non-inflammatory manner. Of note, deposition of C3b on intact cell surfaces is prevented by regulators (Gal et al, 2007; Gros et al, 2008). Furthermore, C3b participates in the formation of C5 convertases (Pangburn & Rawal, 2002). Secondly, C5b initiates the terminal pathway by the assembly of C6, C7, C8 and C9 forming the membrane attack complex (MAC) (Morgan, 1999; Muller-Eberhard, 1986). MAC is a lipophilic transmembrane channel leading to pore formation on the cell surface and eventually cell lysis (Bhakdi & Trantum-Jensen, 1988; Lueck et al, 2011). Lastly, the anaphylactic peptides C3a and C5a aid in the recruitment and activation of innate immune cells, and furthermore, serve as antimicrobial and antifungal factors (Nordahl et al, 2004; Ward, 2009). Importantly, complement system activation is tightly regulated by a group of soluble and membrane-bound complement factors. For instance, surface bound complement receptor 1 (CR1) and decay-accelerating factor (DAF) as well as soluble CFH dissociate C3 convertases (Lambris, 1988). C1-inhibitor (C1INH) also inactivates MASP1 and MASP2 proteases, preventing classical pathway and MBL mediated complement activation (Davis et al, 2008). Furthermore, CD59 is known to block MAC assembly (Kimberley et al, 2007).

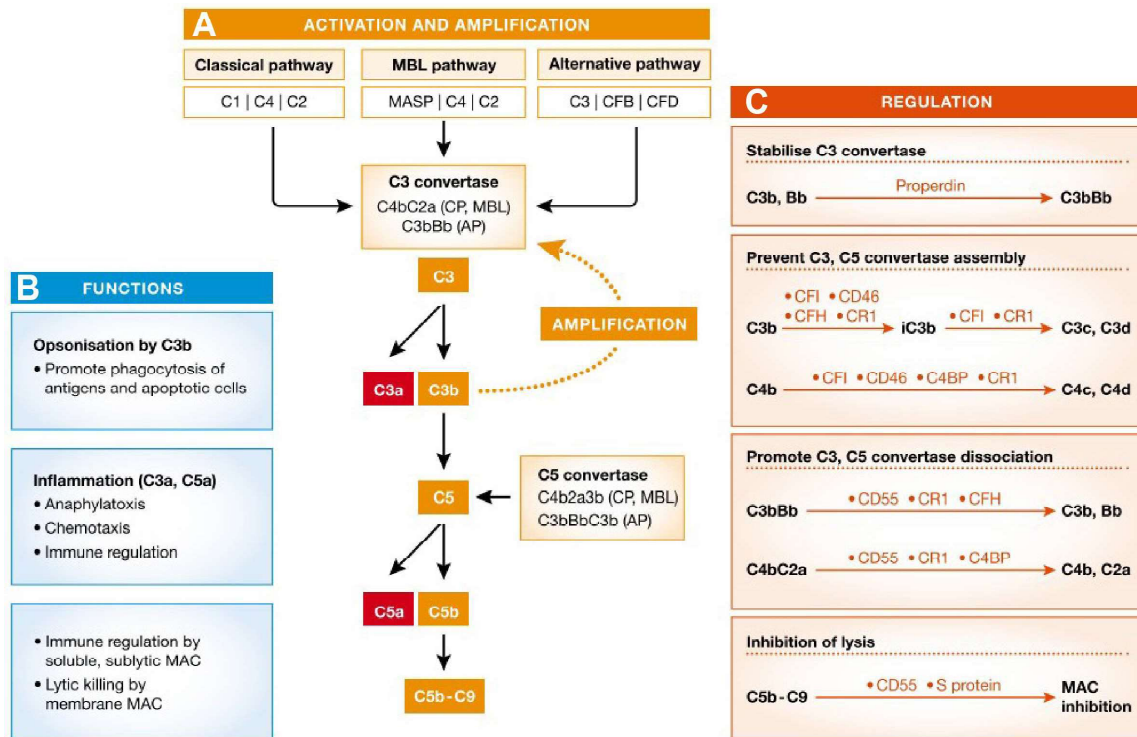


Figure 5 Complement activation, regulation, and immune functions

(A) The complement system is activated through three pathways: the classical pathway (CP), the MBL pathway and the alternative pathway (AP). The activation of these pathways is followed by assembly of C3 convertases, which cleave C3 into C3a and C3b. (B) C3b can serve as opsonin and also form C3bBb to amplify complement activation through AP. Next, C5 is cleaved into C5a and C5b by the generated C5 convertases. C5b initiates the terminal pathway, through recruitment of C6 - C9 to the target surface and generation of MAC. Furthermore, the anaphylatoxins C3a and C5a are actively involved in immune responses. (C) Activation of the complement cascade is regulated through several fragments: For instance properdin stabilizes C3bBb. Conversely CFI, CFH, CD46, CR1, C4BP and CD55 inhibit convertase assembly or may even promote convertase dissociation. MAC assembly is inhibited by CD55 and S protein. Figure from Akhtar-Schäfer et al. (Akhtar - Schäfer et al, 2018).

More importantly, retinal cells themselves produce complement factors. In an elaborative study Anderson and colleagues were able to detect a number of complement genes in the RPE/choroid interface and the neural retina (Anderson et al, 2010). Interestingly, only complement components of the classical and alternative pathways seemed to be produced by retinal cells while factors of the lectin pathway may find their way to the RPE through systemic circulation. Additionally, protein expression analyses demonstrated the presence of

regulatory proteins including CD46, CD55, CD59 and CFH (Chen et al, 2007; Fett et al, 2012; Vogt et al, 2006). Furthermore, receptors for the anaphylatoxins C3a and C5a were detected in the inner retina and the INL, respectively (Vogt et al, 2006). Interestingly, few genes associated with the classical and the alternative complement pathways were upregulated in the aging retina (Chen et al, 2010). Similarly, expression of MAC in choriocapillaris was found to potentiate with increasing age (Chirco et al, 2016). These findings support the hypothesis of complement system activities which are induced during aging, most likely as a result of increasing retinal dyshomeostasis (Chen & Xu, 2015; Xu & Chen, 2016).

Also, involvement of the complement system in AMD disease pathogenesis is beyond dispute. This has been proven through two major aspects: (1) polymorphisms in a number of complement genes associated with AMD, as previously mentioned, and (2) the presence of various complement components in drusen of AMD patients (Crabb et al, 2002; Gold et al, 2006; Mullins et al, 2001).

With being the first major susceptibility gene CFH is a much validated risk locus for developing AMD (Edwards et al, 2005; Hageman et al, 2005; Haines et al, 2005; Klein et al, 2005). A single nucleotide polymorphism (SNP) in exon 9, rs1061170, accounts for a tyrosine to histidine mutation at position 402 (Y402H) (Edwards et al, 2005; Hageman et al, 2005; Klein et al, 2005). Carrying the mutated allele increases the risk for developing AMD by a ratio of 2.5 or 6.2 for the heterozygous or homozygous form, respectively (Conley et al, 2006). A closer look at the functional consequences of the Y402H variant demonstrated a reduced binding and regulatory activity leading to uncontrolled alternative pathway activation (Skerka et al, 2007). Similarly, missense mutations in the complement genes encoding for CFI, C3 and C9 confirmed associations with AMD (Helgason et al, 2013; Maller et al, 2007; Seddon et al, 2013; Zhan et al, 2013). Furthermore, the authors were able to show that the C3 risk allele results in a change of lysine to glutamine at position 155 leading to resistance towards proteolytic inactivation by CFH and CFI, and eventually excessive alternative complement activation (Seddon et al, 2013). Certainly, the impact of mutations needs further evaluation in order to uncover the underlying defective mechanism.

To find answers genetically engineered mice are being widely used. For instance, reduced CFH activity was translated into a mouse model by knocking out Cfh (Cfh^{-/-}) and analyzing the retina at 2 years of age (Coffey et al, 2007). Indeed, these mice exhibited features of AMD and, more importantly, C3 accumulation in the retina concomitant with BM thinning. Similarly, younger Cfh^{-/-} mice (9 months) that were exposed to open environment had reduced photoreceptor numbers when compared to controls kept in a pathogen free environment (Hoh Kam et al, 2013). A chimeric mouse, which resembles the human variant more, was generated by replacing the WT form with the Y402H variant of CFH (Ufret-Vincenty et al, 2010). These mice exhibited lipofuscin and C3d accumulation along with macrophage infiltration into the retina.

Identified SNPs in complement related genes cause uncontrolled complement activation which has been observed in AMD patients in many cases. For instance, increased MAC deposition was found in the choroid and in drusen of AMD cases (Mullins et al, 2011; Mullins et al, 2014). Furthermore, the regulators CFB, CFH and CFI, the components C3, C5, C6, C7, C8 and C9 as well as the anaphylatoxins C3a and C5a were found to be present in the drusen of patients (Anderson et al, 2010; Crabb et al, 2002; Gold et al, 2006; Johnson et al, 2001; Nozaki et al, 2006). Drusen components including C-reactive protein, lipofuscin and amyloid- β also serve as complement system activators (Sparrow et al, 2012; Zhou et al, 2006; Zhou et al, 2009). In summary, complement system regulators and activators, as well as complement factors themselves are part of identified drusen constituents which drive overshooting complement activation. In agreement with these results are studies on complement system inhibitors which potently suppress CNV in animal models (Bora et al, 2010; Lipo et al, 2013; Nozaki et al, 2006). Based on these findings, several clinical studies focus on complement inhibition in AMD (Akhtar - Schäfer et al, 2018; Xu & Chen, 2016). For instance, lampalizumab, the humanized IgG Fab fragment directed against CFD, the rate limiting enzyme in alternative pathway activation was tested in clinical trials (Loyet et al, 2014). However, despite promising preclinical results drug administration did not result in GA reduction (Holz et al, 2018).

1.2.3. Risk locus ARMS2/HTRA1

As previously mentioned, GWAS identified a strong correlation between polymorphisms on chromosome 10q26 locus and the progression of AMD (Fisher et al, 2005; Jakobsdottir et al, 2005). This locus harbors significant association across a high linkage disequilibrium region containing the gene for ARMS2 and the adjacent gene HTRA1 (Fig. 6 A) (Wang, 2014). A strong association was identified for the non-synonymous SNP rs10490924, which resulted in an amino acid substitution of alanine with serine (A69S) in ARMS2 (Rivera et al, 2005). However, ARMS2 is a primate-specific gene only, hindering the analysis in rodents due to lack of a homologous gene (Francis et al, 2008; Pahl et al, 2012). Nevertheless, a humanized mouse with human ARMS2 and A69S ARMS2 variant expression in the entire body of a mouse did not cause any significant phenotype in mice (Nakayama et al, 2014). Furthermore, analyzing variants other than rs10490924 across this region led to the identification of rs11200638, which is situated in the promotor region of HTRA1 (Yang et al, 2006). Strikingly, further analysis demonstrated enhanced transcription of HTRA1 in individuals homozygous for the risk allele (Dewan et al, 2006; Yang et al, 2006). Consequently, high HtrA1 protein levels were found in retinae with AMD (Tuo et al, 2008; Yang et al, 2006). HtrA1 enrichment was also found in drusen deposits, the RPE and the aqueous humor of AMD patients (Melo et al, 2017; Tosi et al, 2017). Strikingly, mice overexpressing HtrA1 exhibited altered composition of BM proteins including fibronectin, fibulin 5 and elastin, thus facilitating BM fragmentation and vessel growth into the avascular retina, which is characteristic for exudative AMD (Kumar et al, 2014; Vierkotten et al, 2011). Other authors reported polypoidal choroidal vasculopathy –like phenotype in mice with HtrA1 overexpression (Jones et al, 2011). Global HtrA1 overexpression along with exposure to cigarette smoke resulted in CNV, photoreceptor demise and the appearance of HF (Nakayama et al, 2014). Apart from CNV formation HtrA1 overexpression in the RPE induced degradation of intracellular tubulin, impaired phagocytosis of shed photoreceptor debris and accelerated premature senescence, prohibiting homeostatic function and inducing photoreceptor demise as it is seen in AMD (Melo et al, 2017; Supanji et al, 2013).

Increased susceptibility to nAMD was further found to be associated with two synonymous SNPs in exon 1 (DeAngelis et al, 2008). The SNPs rs1049331 and rs2293870 result in no amino acid change at A34A and G36G, respectively. However, reduced binding to insulin-like growth factor 1 (IGF-1) was observed, likely explained by a frequent-to-rare codon conversion, leading to reduced translation of HTRA1 mRNA (Jacobo et al, 2013). Furthermore, Friedrich et al. reported that this AMD-associated isoform of HtrA1 exhibits reduced binding to TGF- β in microglia (Friedrich et al, 2015). This finding points towards increased TGF- β signaling, however, the pathophysiological relevance needs further scrutinizing.

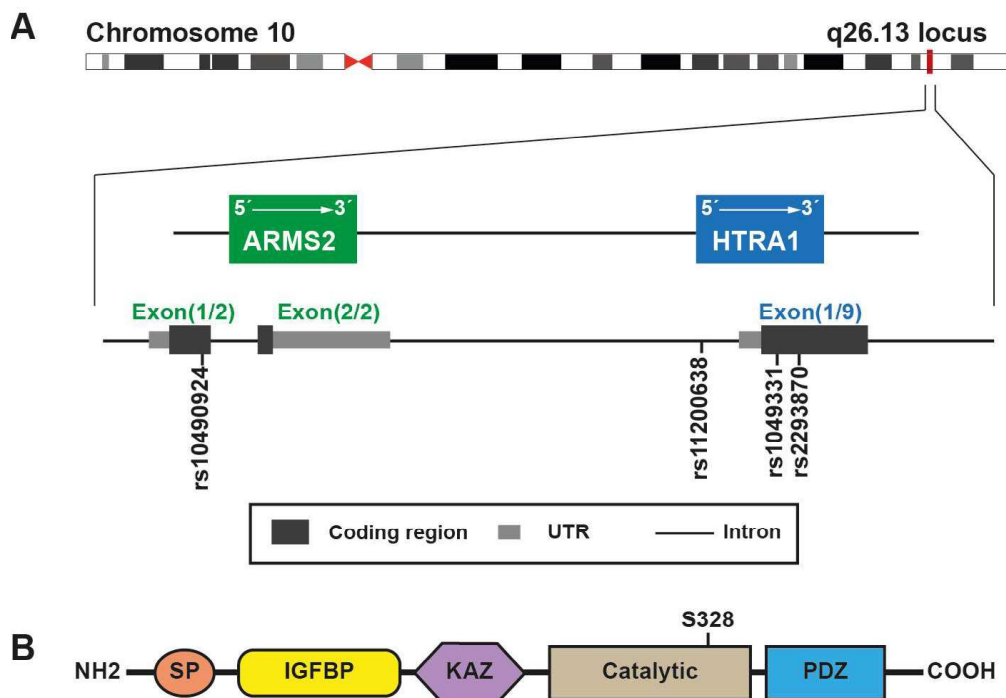


Figure 6 The 10q26 locus, harboring ARMS2/HTRA1 and the structure of HtrA1
(A) Schematic overview of the AMD-associated region on chromosome 10q26 exhibiting high linkage disequilibrium. **(B)** Protein domains of HtrA1. SP: signal peptide domain cleaved in mature secreted protein. Next, IGFBP (insulin growth factor binding protein) domain, which is followed by KAZ (kazal-like domain). The catalytic domain contains histidine, asparagine and serine (S328), which form a catalytic triad. C-terminal contains the PDZ (postsynaptic density of 95 kDa, Discs large and zonula occludens 1) region. UTR: untranslated region.

HtrA1 belongs to an evolutionarily conserved family of trypsin-like serine proteases (Clausen et al, 2011; Clausen et al, 2002). Four homologs have been described and divided into two groups. HtrA1, 3 and 4 consists of a N-terminal signal sequence for secretion, IGFBP-like module, a kazal-like module (KAZ), a protease domain, and a C-terminal PDZ domain, while HtrA2 is a mitochondrial protein with a transmembrane anchor and a cleavable N-terminal domain (Fig. 6 B) (Eigenbrot et al, 2012). The 51-kDa HtrA1 protein is ubiquitously expressed (De Luca et al, 2003) and involved in numerous processes including protein quality control (Krojer et al, 2008; Strauch & Beckwith, 1988), chaperone function (Krojer et al, 2008; Malet et al, 2012), extracellular matrix homeostasis, as well as modulation of cell growth, proliferation, and migration (Canfield et al, 2007; Chien et al, 2009a; Chien et al, 2009b; Schmidt et al, 2016). The variety of functions implicate an essential role for proper physiological processes, and indeed, a number of diseases are associated with malfunctioned protein expression including cancer (Baldi et al, 2002; Chien et al, 2004; Shridhar et al, 2002), arthritis (Grau et al, 2006; Milner et al, 2008), ischemic cerebral small-vessel disease (CARASIL) (Graham et al, 2013; Hara et al, 2009), and Alzheimer's disease (Grau et al, 2005; Munoz et al, 2018; Tennstaedt et al, 2012). Interestingly, loss of HtrA1 has been found to cause CARASIL and facilitate cancer growth, while elevated expression is evident in arthritis (Beaufort et al, 2014; Hara et al, 2009; Hou et al, 2013). One major commonality across these pathologies comprises the modulation of signaling pathways by cleaving or sequestering the pleiotropic cytokine TGF- β (Graham et al, 2013; Launay et al, 2008; Oka et al, 2004). TGF- β is a well-defined regulator of angiogenesis and vascular homeostasis but also immune regulation (Goumans et al, 2009; Li et al, 2006; Santarpia et al, 2015; ten Dijke & Arthur, 2007). Hence, disturbances in TGF- β availability gives rise to a wide range of diseases. In fact, HtrA1 is expressed in areas of active TGF- β signaling and thus, controls its availability, shapes maturation and survival of neurons, as well as angiogenesis (De Luca et al, 2004; Launay et al, 2008; Oka et al, 2004). However, it remains elusive whether increased expression of HtrA1 alters TGF- β signaling in the retina during AMD pathogenesis.

1.3. Microglia

The term microglia was first coined a century ago by the Spanish neuroscientist Río Hortega who, not only separated these cells from astrocytes, but was also able to provide evidence of their morphological transformations during pathology. Fortunately, four of his original papers have been made available in translated English versions (Sierra et al, 2016). Microglia belong to the group of mononuclear phagocytes which furthermore include circulating blood monocytes, tissue resident macrophages and dendritic cells but differ in ontogeny, location, function and phenotype (Chow et al, 2011; Guilliams et al, 2014). Fate-mapping studies showed that macrophages are derived from blood-born monocytes, while microglia originate from primitive myeloid progenitors in the extra-embryonic yolk sac (Ginhoux et al, 2010). Microglia migrate into the central nervous system (CNS) before the blood-brain barrier is established and once the tissue is matured, this population is maintained in the brain parenchyma and the retina throughout the entire life span (Réu et al, 2017). This autonomous self-renewing cell population replenishes from two distinct sources in the brain and retina during adulthood. Upon elimination of microglia by using selective colony stimulating factor 1 receptor (CSF1R) inhibitors, researchers found that replenished cells in the brain were derived from surviving microglia which transiently express nestin during repopulation (Elmore et al, 2014; Huang et al, 2018b). Similarly, microglia in the retina repopulated from residual microglia in the optic nerve, ciliary body and iris macrophages (Huang et al, 2018a). Moreover, repopulated microglia exhibit the broad functionalities of naive cells during physiologic and pathologic conditions (Zhang et al, 2018).

Once microglia migrate into the retina and the tissue is matured, the cells represent the resident immune cells. The cell bodies remain situated in the IPL and OPL (Hume et al, 1983). Strikingly, their long protrusions span the entire nuclear layers (Karlstetter et al, 2015). Due to their dynamic nature, microglia are able to monitor the complete retinal environment. Among the most important role is the constant surveillance of retinal homeostasis. Furthermore, microglia are indispensable for synaptic pruning and signal transmission (Schafer et al, 2012; Wang et al, 2016b).

1.3.1. Microglia activation and its role in AMD

Two major characteristics make microglia indispensable for retinal homeostasis and integrity. First, the retina is the highest oxygen-consuming organ of the body and constituted of cell types, such as photoreceptor cells and the RPE that are intensely metabolically active to guarantee proper vision through lifetime (Chiu & Taylor, 2011; Wong-Riley, 2010). As previously mentioned, with increasing age there is reduced functionality of retinal cells, making them less effective in dealing with the accumulating metabolic waste (Damani et al, 2011; Mitter et al, 2014; Wang et al, 2009a). Secondly, the sensory retina represents an immune privileged organ, with little to no regenerative capacity after injury and inflammation accompanied by tissue distortion (Jiang et al, 1993; Streilein, 2003). These circumstances require constant surveillance making microglia the first line of defense in the retinal parenchyma. Importantly, microglia need tight regulation since their activation may pose threat to the surrounding host tissue. Hence, indispensable cross-talk with Müller cells and retinal neurons limits unnecessary immune activation in the healthy retina (Harada et al, 2002; Langmann, 2007).

Throughout life the retina is challenged by noxious insults including endogenous and exogenous pathologic stimuli which are sensed by microglia via surface receptors or pattern recognition receptors (PRRs) (Kettenmann et al, 2011; Kigerl et al, 2014; Masuda et al, 2017; Wang et al, 2016a). In the event of such insults microglia sense the damage- or pathogen-associated molecular patterns (DAMPs/ PAMPs) and react by retracting their surveilling processes and becoming amoeboid (Fig. 7 A) (Karlstetter et al, 2015; Karperien et al, 2013). Furthermore, they migrate to the site of damage, while releasing pro-inflammatory cytokines and reactive oxygen species (ROS) which abrogate tissue damaging DAMPs and PAMPs (Fig. 7 B) (Ferrer-Martin et al, 2015). Synergistically, microglia enhance their phagocytic capacity to eliminate cellular waste (Mitchell et al, 2018; Wynn & Vannella, 2016). Under physiological conditions the insult is promptly neutralized and a return to homeostasis is achieved with only very little retinal remodeling (Chen et al, 2012; Rashid et al, 2018).

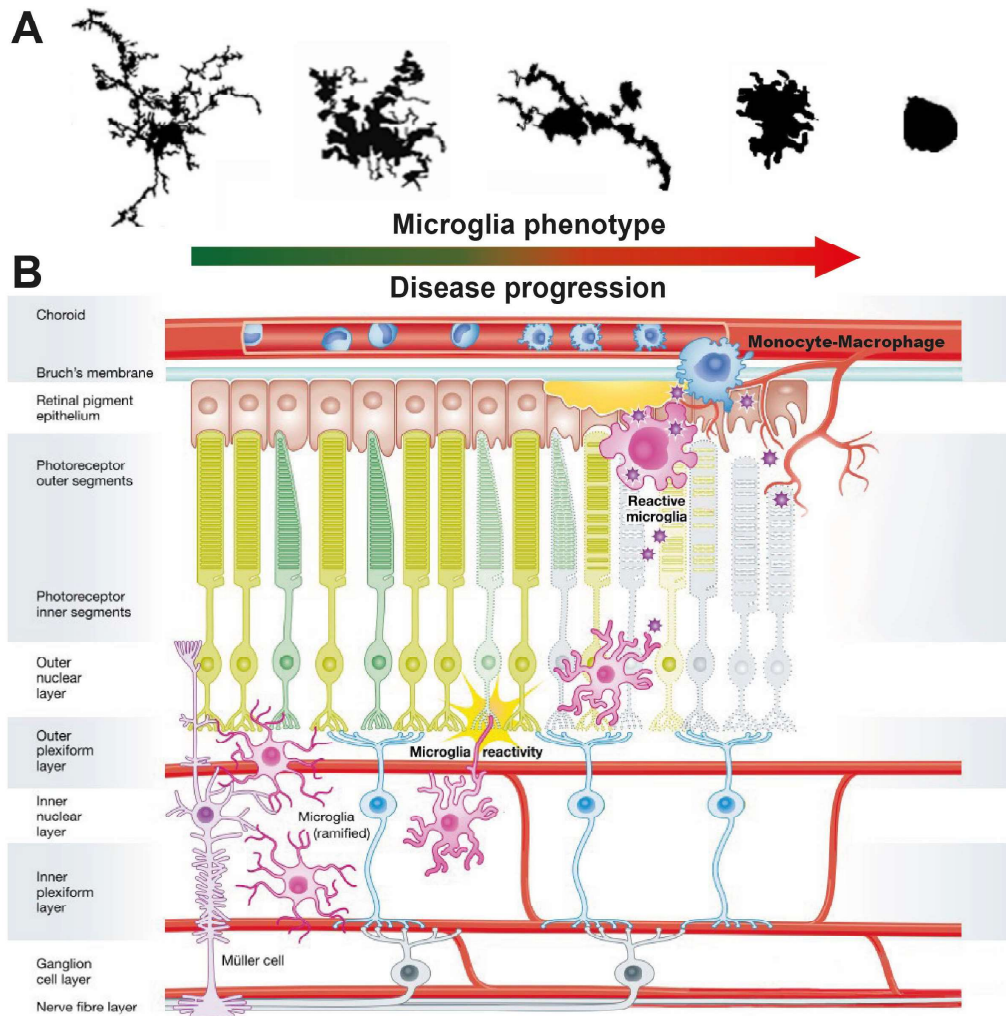


Figure 7 Microglia phenotype and retinal location during health and disease

(A & B) Under homeostatic conditions, microglia populate the plexiform layers and exhibit small cell bodies with ramified motile protrusions. Perturbations are rapidly sensed by microglia leading to a gradual shift towards an active phenotype. Disease progression is accompanied by gradual morphological transition of microglia towards amoeboid phagocytes. Upon BRB breach microglia recruit choroidal macrophages harming the retinal milieu and exacerbating the disease. Figures adapted from Karperien et al. (Karperien et al, 2013) and Akhtar-Schäfer et al. (Akhtar - Schäfer et al, 2018).

Transient microglia activation is beneficial since the toxicity associated with the immune response is outweighed by the initial noxious insult. However, numerous studies have shown that distressed conditions, owing to genetic predispositions, lead to chronic microglia activation, which causes non-resolving inflammation and terminal retinal damage due to the lack of regenerative capacity (Gupta et al, 2003). Eventually, microglia accumulate at the site

of damage and fail to return to their homeostatic state and even more attract choroidal macrophages (Caicedo et al, 2005; Sennlaub et al, 2013).

These abnormalities in microglial behavior are common hallmarks of AMD (Ardeljan & Chan, 2013). Despite being described as a disease of the macula-RPE-choroid interface and vascular complication, inflammation plays a major role in AMD disease progression (Ardeljan & Chan, 2013; Bhutto & Luttly, 2012; Karlstetter et al, 2015). Analysis of transcriptome profiles from AMD and healthy human donor eyes showed significant involvement of inflammatory responses along with released chemokine and complement activation in all AMD phenotypes (Newman et al, 2012). Elevated cytokine levels, including C-C motif chemokine 2 (CCL2), which is involved in monocyte recruitment, were detected in ocular fluids from nAMD patients (Fauser et al, 2015; Robbie et al, 2016). Strikingly, bloated phagocytic microglia were found in close association with drusen in AMD patients (Gupta et al, 2003). Drusen constituents include proteins associated with established roles in mediating immune responsiveness, suggesting that macular drusen in AMD portrays potent pro-inflammatory stimulus (Buschini et al, 2011; Doyle et al, 2012). Indeed, the widespread accumulation of drusen components as seen in AMD is a potent chemoattractant stimulus for microglia (Penfold et al, 2001).

1.3.2. Microglia modulation as therapy strategy

During retinal degeneration overshooting microglial reactivity leads to tissue damage and exacerbation of disease severity. However, microglia depletion cannot be a promising therapeutic strategy, since microglia are indispensable for the maintenance of synaptic structures in the adult CNS as well as in the retina (Parkhurst et al, 2013; Wang et al, 2016b). With that being said, immunomodulatory compounds, which should exclusively dampen the pro-inflammatory response of microglia while preserving their crucial homeostatic functions, are needed.

The analysis of immune-modulating compounds *in vivo* requires preclinical studies with rodent models where cardinal features of AMD are being mimicked (Luckoff et al, 2017).

For instance, the commonly used light-induced photo-oxidative damage model stems from the evidence that extended exposure to light involves the risk for developing retinal degeneration such as in AMD patients (Taylor et al, 1992; Tomany et al, 2004). Similar effects are mimicked in albino rodents, by exposing them to intense visible light for an extended period of time and thereby inducing significant loss of photoreceptor cells and thinning of the ONL (Wenzel et al, 2005). This is accompanied by a vigorous change in microglia morphology and translocation to the outer retina (Fig. 7 and 8). Furthermore, subretinal microglia exhibit not only enhanced release of pro-inflammatory factors including $\text{Il-1}\beta$, $\text{Tnf-}\alpha$, Il-6 , Ccl2 and iNos but also increased phagocytic capacity resulting in photoreceptor degeneration, which is evident through thinning of the ONL (Scholz et al, 2015a; Scholz et al, 2015b; Wang et al, 2014). Similarly, laser-induced CNV is extensively applied in rodent research to study nAMD (Ambati et al, 2013; Lambert et al, 2013). It results in the rupture of the BM and penetration of choroidal capillaries into the avascular retina within a short time. Due to the laser burn a focal inflammatory reaction concomitant with recruitment and accumulation of reactive amoeboid microglia along with infiltrating mononuclear phagocytes is evident (Combadiere et al, 2007; Karlstetter et al, 2017; Luckoff et al, 2016). Moreover, infiltrating mononuclear phagocytes secrete pro-inflammatory cytokines and the pro-angiogenic factor Vegf which results in exacerbation of disease progression and severity (Combadiere et al, 2007; Luckoff et al, 2016).

In order to prevent retinal degeneration and neovascularization immunomodulatory strategies investigated in preclinical studies involve targeting activating and inhibiting cell surface receptors (e.g. Interferon- β , $\text{IFN-}\beta$) and modulating intracellular molecules (e.g. translocator protein, TSPO) (Akhtar - Schäfer et al, 2018; Karlstetter et al, 2015; Langmann, 2007). For instance, downstream signaling of the $\text{IFN-}\beta$ receptor (interferon- α/β receptor, Ifnar) proved to be crucial for microglial homeostasis since its deletion led to elevated microglial reactivity (Prinz et al, 2008; Teige et al, 2003). In the laser-induced CNV model in mice, systemic administration of $\text{IFN-}\beta$ not only inhibited microglial reactivity and macrophage recruitment, but also reduces vascular leakage and neoangiogenesis (Luckoff et al, 2016). Conversely, global deletion of Ifnar as well as conditional deletion of microglial $\text{IFN-}\beta$ signaling in mice resulted in an aggravated disease phenotype. Likewise, ligands binding to TSPO, a

transmembrane protein located on the outer mitochondrial membrane in microglia, induce beneficial effects by limiting the magnitude of microglial activation responses (Girard et al, 2012; Wang et al, 2014). The synthetic TSPO ligand XBD173 demonstrated anti-inflammatory effects, by markedly inhibiting amoeboid microglia accumulation in the outer retina accompanied by no thinning of the ONL in the light-induced retinal degeneration model (Fig. 8). These effects likely involve the increased conversion of cholesterol to pregnenolone, and then to progesterone, a neuroprotective neurosteroid (Cai et al, 2018; Karlstetter et al, 2014).

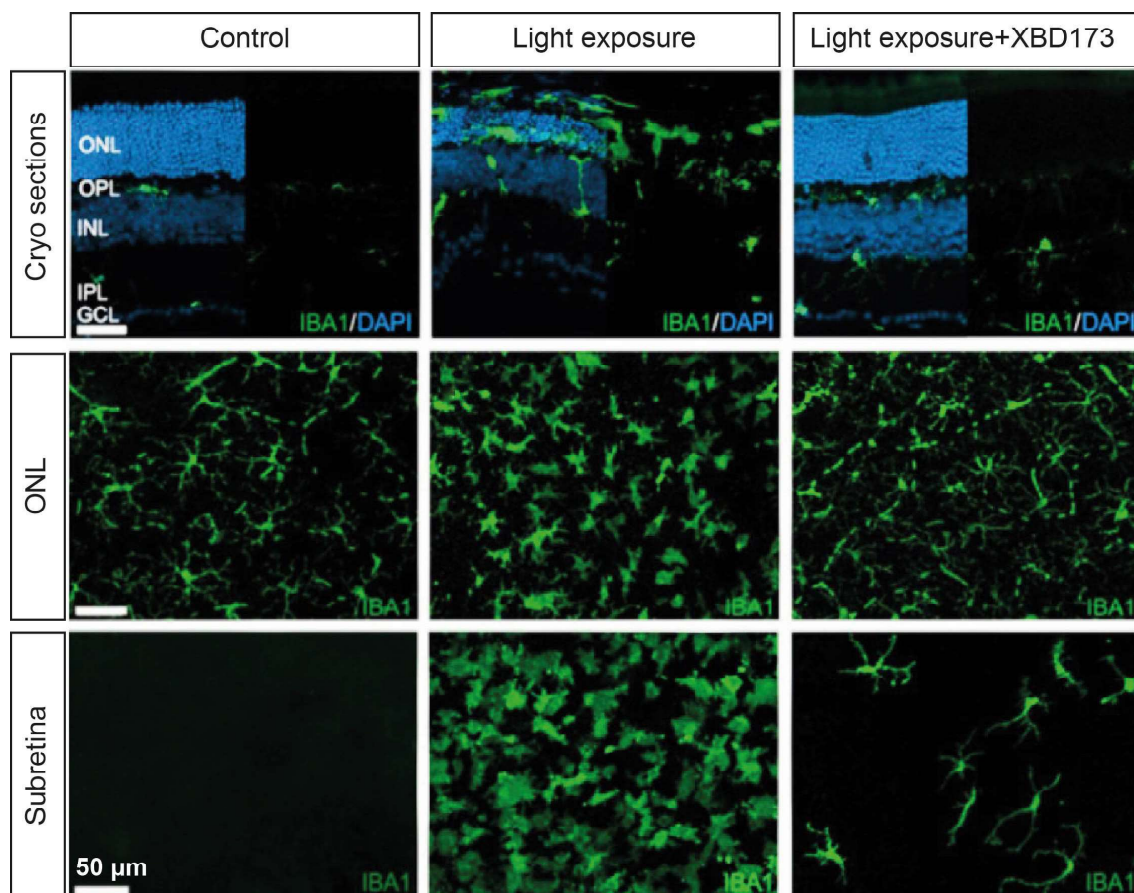


Figure 8 XBD173 treatment of light-exposed mice prevents microglia reactivity

In retinal cryo sections microglia are visualized by staining ionized calcium binding adapter protein 1 (Iba1). During physiologic conditions ramified microglia remain in the plexiform layers. Photo-oxidative damage induced by exposure to bright white light leads to degeneration of photoreceptor cells concomitant with migrating and bloated microglia in the OPL and subretinal layer. Application of the immunomodulatory compound XBD173 markedly preserves retinal morphology concomitant with reduced appearance of amoeboid microglia in the ONL and the subretinal space. Figures adapted from Scholz et al. (Scholz et al, 2015a).

Immunomodulatory therapy represents an overarching approach to treat AMD along with other retinal degenerative diseases (Akhtar - Schäfer et al, 2018). Since AMD is a complex disease with various causes, the integration of associations from solid genetic findings could aid to identify novel targets for immunotherapy.

Indeed, there is much evidence that the complement system participates in microglia activation. Already, in a very early study van der Schaft observed the presence of complement factors around the RPE while he was searching for macrophage attractants in post mortem eyes of nAMD patients (van der Schaft et al, 1993). Interestingly, the AMD associated Y402H variant of Cfh was shown to promote microglia accumulation more potently than the common variant (Calippe et al, 2017). Similarly, the drusen constituents C3a and C5a not only induce VEGF expression, but also attract microglia (Nozaki et al, 2006). Consequently, genetic ablation of their respective receptors, C3aR and C5aR, reduced VEGF expression and CNV formation. Identifying the mechanistic principle behind anaphylatoxin mediated inflammation would aid to find novel targets for immunomodulatory therapies.

In case of HTRA1, the second most prominent risk locus associated with AMD, TGF- β signaling likely represents the key element. Alterations in TGF- β availability and receptor signaling pathway have been shown in several other diseased forms where disturbances in HtrA1 level are involved, as mentioned above. In the retina TGF- β belongs to the inhibitory factors released by the RPE into the subretinal-space where it displays immunosuppressive effects on the innate immune system by modulating microglia (Karlstetter et al, 2010; Karlstetter et al, 2015; Zamiri et al, 2007). Strikingly, TGF- β proved to be a potent silencer of neuroinflammation by dampening microgliosis (Gong et al, 2012; Spittau et al, 2015; Spittau et al, 2013; Zhou et al, 2012; Zhou et al, 2015).

Upon ligand binding TGF- β receptor type II (Tgf- β RII) phosphorylates and thus, activates TGF- β receptor type I serine/threonine kinase activity (Huse et al, 1999; Yamashita et al, 1994). This is followed by the phosphorylation of the intracellular signaling mediators Smad2 and Smad3 (Massague & Wotton, 2000). Consequently, these Smad proteins form a complex with Smad4, translocate to the nucleus where TGF- β target gene expression initiates (Zhang & Derynck, 1999). The profound regulatory effects of TGF- β on cell fate and survival

are evident in TGF- β deficient mice which suffer from uncontrolled inflammation, organ failure and early death (p20), making further analysis in adult tissue impossible (Shull et al, 1992). However, severe microgliosis in neonatal Tgf- β $-/-$ mice gave some first hints towards the importance of this signaling pathway in microglia (Brionne et al, 2003). An alternative mouse model involves the conditional knockout of Tgf- β RII under the control of the microglial marker Cx3Cr1 (Goldmann et al, 2013). These mice exhibit no abnormal developmental deficits, and more importantly, unaffected number of microglia (Zöller et al, 2018). However, these TGF- β deficient microglia demonstrate an over-activated phenotype concomitant with increased CCL2 secretion which may result in further mononuclear phagocyte recruitment. Thus, the question arises whether elevated HtrA1 expression results in aggravation of microglia mediated inflammation by inhibiting TGF- β signaling. Whether the AMD-associated variants change the function of HtrA1 in the retina remains inconsistent and largely elusive.

1.4. Aims of the study

SNPs in complement genes were found to induce an increase in complement activation. Similarly, AMD-associated SNPs in HTRA1 correlate with an increase in HtrA1 protein expression in retinæ of AMD patients. There is adequate evidence, that these alterations owing to genetic mutations may exacerbate microgliosis, a common hallmark during retinal degeneration. Hence, the present study dealt with the question whether microglia are affected by increased complement activation and increased HtrA1 levels.

Firstly, the role of microglia and the C3a and C5a mediated retinal degeneration was investigated. Furthermore, it was investigated whether HtrA1 induces neuroinflammation by sequestering TGF- β and thus facilitates microglial reactivity and tissue damaging inflammation. Consequently, the response of microglia to AMD-associated HtrA1 levels and variants during inflammation with particular focus on TGF- β signaling was evaluated. The study provides new insights for a better understanding of genetic associations and disease formation with particular focus on the immune response as a therapy target.

2 Material and Methods

2.1. Material

2.1.1. Mice

Table 1 Mouse strain, eye drops and systemic anesthesia.

Mice	Origin and husbandry
BALB/cJ and C57BL/6J	Male and female animals used for this work were housed in an air-conditioned environment at 20-24 °C on a 12 hours light-dark schedule. Mice had access to phytoestrogen-free food and water ad libitum.
Eye drops	Manufacturer, Cat. No.
Hylo-Vision Gel sine eye drops	OmniVision
Phenylephrin 2.5 % / Tropicamid 0.5 %	Pharmacy University Hospital Cologne
Anesthetic solution - Formula	Manufacturer
8.5 ml of 0.9 % isotonic NaCl	Fresenius Kabi
1 ml Ketaminehydrochloride (Ketaset)	Zoetis
0.5 ml Xylazinehydrochloride (Rompun) use 0.1 ml /10 g bodyweight	Bayer HealthCare

2.1.2. Cells and bacteria

Table 2 Cell lines and bacteria strain.

Cell lines	Origin
BV-2 murine microglia like cells	Dr. Ralph Lucius, Christian Albrechts University, Kiel, Germany
SV40 immortalized human microglia	Applied Biological Materials Inc., Richmond, BC, Canada
human embryonic kidney (HEK)293 cells	Institute of Biochemistry II, University of Cologne, Germany
Bacteria strain	Origin
DH5α	<i>Escherichia Coli</i> (E. Coli)

2.1.3. Media

Table 3 Reagents and formula for cell culture and lysogeny broth (LB) media/plates.

Reagents	Manufacturer, Cat. No.
Agar-Agar	Merck, #101614
Ampicillin sodium salt	Roth, #K029.2
Chloramphenicol	Calbiochem, #220551
Dulbecco's Modified Eagle Medium (DMEM)	Sigma-Aldrich, #D6429
DMEM/F-12 GlutaMAX	ThermoFisher Scientific, #31331
Dulbecco's Phosphate-Buffered Saline (DPBS)	Gibco, #14190
Fetal Calf Serum (FCS)	Gibco, #10270-106
Hank's Balanced salt Solution (HBSS)	Gibco, #14025092
Kanamycin sulfate	Sigma-Aldrich, #K4000
Penicillin/Streptomycin	Gibco, #15140-122
Pepton from casein	Roth, #8986
Puromycin dihydrochloride	Gold Biotechnology, #P-600-1
Sodium chloride (NaCl)	Merck, #106400
Trypsin/EDTA	Sigma-Aldrich, #T3924
Yeast extract	AppliChem, #A1552
Cell culture media	Formula
BV-2, SV40 and primary micorglia culture	DMEM 10 % FCS 10 % Penicillin/Streptomycin
HEK293	DMEM/F-12 GlutaMAX 10 % FCS and then 2 % FCS 4 µg/ml Puromycin
Lysogeny broth (LB) media	Formula
LB-media	10 g/l Yeast extract 20 g/l NaCl 20 g/l Peptone
LB ampicillin media (LB-amp)	100 µg/ml Ampicillin in LB-media
LB-amp agar plates	14 g/l Agar-Agar in LB-amp
LB chloramphenicol media (LB-chlor)	20 µg/ml Chloramphenicol in LB-media
LB-chlor agar plates	14 g/l Agar-Agar in LB-chlor
LB kanamycin media (LB-kan)	50 µg/ml Kanamycin in LB-media
LB-kan agar plates	14 g/l Agar-Agar in LB-kan

2.1.4. Buffers and solutions

Table 4 Buffers and solutions prepared as indicated.

Buffer/Solution	Formula	Manufacturer, Cat. No.
1x PBS, pH 7.4	137 mM NaCl	
	2.7 mM Potassium chloride (KCl)	Amresco, #E404
	10 mM Disodium phosphate (Na_2HPO_4)	1 tablet/100 ml dH_2O
	1.8 mM Monopotassium phosphate (KH_2PO_4)	
1x TBE	1 M Tris, pH 7.5	Roth, #4855.3
	1 M Boric acid	Sigma-Aldrich, #B6768
	20 mM EDTA	Merck, #108421
1x TBS-T	150 mM NaCl	see above
	200 mM Tris	see above
	0.1 % v/v Tween-20	see above
10% NBF	10 % v/v Formalin (~4 % Formaldehyde)	Sigma-Aldrich, #F8775
	34 mM Monosodium phosphate (NaH_2PO_4)	Merck, #6346
	46 mM Na_2HPO_4 , dibasic anhydrous	Roth, #P030.1
6x Loading dye	60 % v/v Glycerine	Roth, #3783.1
	20 mM EDTA	see above
	0.25 % w/v Bromphenol blue	Sigma-Aldrich, #B-6131
Antibody solution	2 % w/v Bovine serum albumin (BSA)	Amresco, #0332
	0.1 % v/v Triton X-100	Sigma-Aldrich, #T8787
	0.2 % w/v Sodium azide (NaN_3) in 1xPBS	Roth, #K305.1
Blotto	1 % w/v Milk powder	Roth, #T145.3
	0.01 % v/v Tween-20 in 1x PBS	Merck, #822184
Digestion buffer	10 mM Tris-HCL pH 7.8	see above
	0.1 mM NaN_3	see above
Membrane blocking buffer	5 % w/v Milk powder in TBS-T	see above
RIPA buffer	50 mM Tris-HCl pH 7.4	see above
	150 mM NaCl	see above
	1 % v/v NP-40	Calbiochem, #492016
	0.5 % w/v Sodium deoxycholate	Sigma-Aldrich, #D6750
	0.1 % w/v Sodium dodecyl sulfate (SDS)	Serva, #20765.03
	2 mM Phenylmethanesulfonyl fluoride (PMSF)	Applchem, #A0999
	cOmplete™ mini protease inhibitor	Roche, #11836153001
Running buffer	192 mM Glycine	AppliChem, #1067
	250 mM Tris	see above
	0.1 % w/v SDS	see above
Transfer buffer	192 mM Glycine	see above
	250 mM Tris	see above
	20 % v/v Methanol	Chemosolution, #1437.2511
Stripping buffer	192 mM Glycine, pH 2.2	see above
	0.0001 % w/v SDS	see above
	0.01 % v/v Tween-20	see above

Table 5 Self prepared gels.

Gels	Formula	Manufacturer, Cat. No.
Agarose gel	1.5 % w/v Agarose	Biozyme, #840004
	0.5 µg/ml Ethidium bromide in TBE	Sigma-Aldrich, #46067
Running gel	12 % (or 10%) v/v Acrylamide	Roth, #A124.1
	0.4 M Tris pH 8.8	see above
	0.1 % w/v SDS	see above
	0.1 % w/v Ammonium persulfate (APS)	Sigma-Aldrich, #A3678
	0.01 % v/v TEMED	Roth, #2367.1
Stacking gel	5 % v/v Acrylamide	see above
	0.125 M Tris pH 6.8	see above
	0.1 % w/v SDS	see above
	0.1 % w/v APS	see above
	0.005 % v/v TEMED	see above

2.1.5. Antibodies

Table 6 List of primary and secondary antibodies, stains and fluorophores.

Antibodies, stains and fluorophores	Dilution	Manufacturer, Cat. No.
Rabbit anti-HtrA1, polyclonal	1:500	Pineda (Vierkotten et al., 2011)
Rabbit anti-HTRA1/PRSS11, polyclonal	1:500	Novusbio, #NBP2-23869
Rabbit anti-Iba1, polyclonal	1:500	Wako, #01-1074
Rabbit anti-phospho-Samd2, monoclonal	1:1000	Cell Signaling Technology, #3108
Rabbit anti-Samd2, monoclonal	1:1000	Cell Signaling Technology, #5339
Strep-Tactin®-HRP Conjugate	1:10000	IBA Lifesciences, #2-1502-001
Alexa Fluor® 488 goat anti-rabbit IgG, polyclonal	1:1000	Life Technologies, #A11008
goat anti-rabbit IgG-HRP, polyclonal	1:4000	Agilent Dako, #P0448
DAPI (4',6-Diamidino-2-Phenylindole)	0.1 µg/ml	Invitrogen, #D1306
Phalloidin-TRITC	0.1 µg/ml	Sigma-Aldrich, #P1951
TSA® Plus Cyanine 3	1:1500	PerkinElmer, #NEL744E001KT
TSA® Plus Fluorescein	1:1500	PerkinElmer, #NEL741E001KT

2.1.6. Enzymes

Table 7 Enzymes, reaction buffers and PCR reagents.

Enzymes, buffers and reagents	Manufacturer, Cat. No.
Recombinant DNase I	Roche, #04536282001
Q5® High-Fidelity DNA Polymerase	New England BioLabs, #M0491S
Q5® Reaction Buffer	New England BioLabs, #B9027S
FastDigest BglII	ThermoFisher Scientific, #FD0083
FastDigest BamHI	ThermoFisher Scientific, #FD0974
FastDigest NheI	ThermoFisher Scientific, #FD0973
FastDigest KpnI	ThermoFisher Scientific, #FD0524
FastDigest XhoI	ThermoFisher Scientific, #FD0694
10x Fast Digest Buffer	Supplied with the enzymes
10x Fast Digest Green Buffer	Supplied with the enzymes
dNTP-Set	Genaxxon, #M3015
MassRuler DNA Ladder	ThermoFisher Scientific, #SM0403

2.1.7. Kits

Table 8 Commercially available kits.

Kits systems	Manufacturer, Cat. No.
CellTiter 96® Cell Proliferation Assay	Promega, #G4000
EnzChek Protease Assay Kits	ThermoFisher Scientific, #E6638
Griess Reagent System	Promega, #G2930
LightCycler® 480 Probes Master	Roche Applied Science, #04707494001
NucleoSpin® Plasmid	Macherey-Nagel, #740588
NucleoSpin® RNA	Macherey-Nagel, #740955
NucleoSpin® Gel and PCR Clean-up	Macherey-Nagel, #740609
ONE-Glo™ Luciferase Assay System	Promega, #E6110
Pierce™ BCA Protein Assay Kit	ThermoFisher Scientific, #23225
Rapid DNA Ligation Kit	ThermoFisher Scientific, #K1422
RevertAid RT Kit	ThermoFisher Scientific, #K1691
RNAscope® Fluorescent Version 2	Advanced Cell Diagnostics (Bio-technique), #323110
RNAscope® H ₂ O ₂ and Protease Reagents	Advanced Cell Diagnostics (Bio-technique), #322381
RNAscope® Target Retrieval Reagents	Advanced Cell Diagnostics (Bio-technique), #322000
RNAscope® Wash Buffer Reagents	Advanced Cell Diagnostics (Bio-technique), #310091
SignalFire™ Elite ECL Reagent	Cell Signaling Technology, #12757

2.1.8. Cloning constructs and cloning primers

Table 9 Origin of gene sequence and plasmids used for cloning.

Gene of interest	Origin	Restriction sites
hHTRA1 WT	Plasmid, kanamycin resistance; GeneArt	NheI - BamHI
hHTRA1 SNP	Plasmid, kanamycin resistance; GeneArt	NheI - BamHI
hHTRA1 S328A	Plasmid, kanamycin resistance; GeneArt	NheI - BamHI
mHtra1 WT	Prof. Choi Oka, NAIST, Ikoma, Japan	NheI - BglII
mHtra1 S328A	Prof. Choi Oka, NAIST, Ikoma, Japan	NheI - BglII
hPAI-1	RPCI-11 Human BAC clone (E. Coli), chloramphenicol resistance	KpnI - XhoI
Plasmids	Origin	Method
Expression plasmid	Prof. Manuel Koch, Biochemistry II, University of Cologne, Germany	Eukaryotic protein expression
pGL4.10 [luc2]	Promega, Cat. No.: E665A	Promotor expression analysis
pSV- β -Galactosidase	Promega, Cat. No.: E1081	Luciferase control vector

Table 10 Cloning primers for human (h) and murine (m) constructs.

Forward (F) and reverse (R) primer contain the restriction sites indicated in capital letters.

Target gene	Amplicon length	Primer
hHTRA1	1377 bp	F 5'-aaaaGCTAGCagctgtcccggccggccgctcggcgccctt-3'
		R 5'-tggtGGATCCctatgggtcaattcttcgggaatc-3'
mHtra1	1377 bp	F 5'-acaaGCTAGCttgccgtcggggaccggccgctc-3'
		R 5'-tggtAGATCTctaggggtcgatttcttcaggaatc-3'
hPAI-1	903 bp	F 5'-cccGGTACCAagcttttaccatggtaccacct-3'
		R 5'-cccCTCGAGcagctgctggaggggggc-3'

Table 11 Sequencing primers.

Target gene	Forward primer	Reverse primer
hHTRA1	5'-tctttctccttgcctggcc-3'	5'-gcgataaagtattatattatggcgca-3'
	5'-cctctgtgtgtgccag-3'	5'-gcaccgttcttcagctcaac-3'
	5'-ggaagcccgtttccctca-3'	5'-gctcctgagatcacgtctgg-3'
	5'-ggctctccgccaatgatgtca-3'	5'-gtggctccatgaaccacctc-3'
mHtra1	5'-cctgtgcgtgtgccag-3'	5'-actgttgggatcttctgcc-3'
	5'-gccattggaagcccctttc-3'	5'-ttcagctcaacctgacccg-3'
	5'-caacggacagtctgtgtgtca-3'	5'-acggctccttcagctctttgg-3'
hPAI-1	5'-taaccctgtgtccgttca-3'	5'-ccacgtgtccagactctctc-3'
	5'-tagacaatcacgtggctggc-3'	5'-gtgtgtgtgtgtgtgtgtg-3'
	5'-gtggggctggaacatgagtt-3'	5'-ggcgtgtgggtcttcttga-3'

2.1.9. RNAscope probes and qRT-PCR primers

Table 12 RNAscope® probes for murine target genes.

Target gene	Channel	Cat. No.	Accession No.
Htra1	C1	423711	NM_019564.3
Aif	C1	319141	NM_019467.2
Aif	C3	319141-C3	NM_019467.2
C3ar	C3	476751-C3	NM_009779.2
C5ar	C3	439951-C3	NM_007577.4

Table 13 Primers and Roche probes used for quantitative RT-PCR.

Target gene	Forward primer	Reverse primer	Probe No.
hC3AR	5'-gaagccttcagctactgtctcag-3'	5'-agaattactgggggctcattc-3'	#76
hC5AR	5'-ggagggaccttcgatectc-3'	5'-gggggtgtataattgaaggagt-3'	#54
hGAPDH	5'-gcccaatacgaacaaatcc-3'	5'-agccacatcgctcagaca-3'	#60
hTNF- α	5'-cagcctcttctccttctgat-3'	5'-gccagagggtgattagaga-3'	#29
mArginase-1	5'-gaatctgcatgggcaacc-3'	5'-gaatcctggtacatctgggaac-3'	#2
mAtp5b	5'-ggcacaatgcaggaaagg-3'	5'-tcagcaggcacatagatagcc-3'	#77
mC3	5'-accttacctcggcaagttct-3'	5'-ttgtagagctgctggtcagg-3'	#76
mC3ar	5'-gtggctcgcagatcatca-3'	5'-aagactccatggctcagtcac-3'	#1
mC5ar	5'-gcatccgtcgtgtgtac-3'	5'-tgctgttatctatgggtcca-3'	#63
mHtra1	5'-agtgggtcaggattcatcga-3'	5'-gtgaccacgtgagcattgt-3'	#88
miNos	5'-ctttgccacggacgagac-3'	5'-tcattgtactctgagggtga-3'	#13
mKlf10	5'-agccaacctgctcaactc-3'	5'-ggcttttcagaaattgtccatt-3'	#67
mPai-1	5'-aggatcgaggtaaacgagagc-3'	5'-gcgggctgagatgacaaa-3'	#69
mTnf- α	5'-ctgtagcccacgtcgtagc-3'	5'-ttgagatccatgccgttg-3'	#78
mYm-1	5'-aagaacactgagctaaaaactctcct-3'	5'-gagaccatggcactgaacg-3'	#88

2.1.10. Cell culture compounds and reagents

Table 14 List of cytokines and compounds for cell culture and other reagents.

Cytokines and reagents	Manufacturer, Cat. No.
Recombinant murine interferon- γ (IFN- γ)	PreproTech, #315-05
Recombinant human TGF- β	PreproTech, #100-21
Lipopolysaccharides (LPS) from <i>E. coli</i>	Sigma-Aldrich, #L4391
Phorbol-12-myristate-13-acetate (PMA)	Sigma-Aldrich, #1585
Zymosan A from <i>Saccharomyces cerevisiae</i>	Sigma-Aldrich, #Z4250
Ames' Medium	Sigma-Aldrich, #A1420
β -mercaptoethanol	Sigma-Aldrich, #M-7154
Buffer Standard AVS TITRINORM, pH 10	VWR, #85680.295
Buffer Standard AVS TITRINORM, pH 7	VWR, #32045.295
Buffer Standard AVS TITRINORM, pH 4	VWR, #32044.292
Citric acid	Sigma-Aldrich, #C0759
Collagen I, bovine	Gibco, #A10644
D-desthiobiotin	Sigma-Aldrich, #D1411
D-saccharose	Roth, #4621.1
Dimethylsulfoxid (DMSO)	Serva, #20385.01
Ethanol 70 %	Applichem, #A2192
Ethanol	Applichem, #A3678
Fluorescence Mounting Medium	Dako, #S302380-2
FuGENE® HD	Promega, #E2311
Gelatin-Sepharose® 4B	GE Healthcare, #17-0956-01
Goat Serum	Abcam, #AB7481
HistoFix 4 %	Roth, #P087.4
Hydrochloric acid (HCL) 37 %	Roth, #X942
Isopropanol	Merck, #100995
Laemmli sample buffer	Bio-Rad, #161-0747
Magnesiumchloride	Sigma-Aldrich, #68475
Methanol	Chemosolution, #1437.2511
Nitrophenyl- β -D-galactopyranoside (ONPG)	Sigma-Aldrich, #N1127
PageRuler™ Prestained Protein Ladder	ThermoFisher Scientific, #26616
Poly-D-lysine	Sigma-Aldrich, #P6407
RNase away	Molecular Biopro., #70003
Sodium carbonate	Roth, #P028.1
Strep-Tactin® Sepharose® 50 % suspension	Iba Lifesciences, #2-1201-010
Tissue Tek OCT-Compound	Sakura, #4583
TransIt-LT1 Transfection reagent	Mirus, #MIR 2305
Trypan blue	Biochrom AG, #L6323

2.1.11. Devices

Table 15 List of laboratory devices.

Devices	Manufacturer
Adventurer Pro balance	Ohaus®
ApoTome.2	Zeiss
AxioCam ICc 1 camera	Zeiss
AxioCam MRm camera	Zeiss
Bacterial incubator	VWR International
Centrifuge 5415 R	Eppendorf
Centrifuge Mini Star	VWR International
Cryostat CM3050	Leica
ERG recording system	custom-built
Explorer R Ex 124 balance	Ohaus®
Galaxy 170S CO ₂ incubator	New Brunswick Scientific
Heraeus Labofuge 400 R	Thermo Scientific
HybEZ™ II Hybridization System	Advanced Cell Diagnostics
Illuminance meter T-10A	Konica Minolta
Imager.M2 microscope	Zeiss
Infinite®F200 Pro plate reader	Tecan
Intas Gel iX20 Imager	Intas
Light damage device	custom-built
LightCycler® 480 Instrument II	Roche Applied Science
Matrix™ Multichannel pipette	ThermoFisher Scientific
Mini-Protean® Tetra System	Bio-Rad
MiniTrans-Blot® Cell Module	Bio-Rad
MSC-Advantage hood	Thermo Scientific
MultiImageII	Alpha Innotech
NanoDrop 2000 Spectrophotometer	Thermo Scientific
Neubauer counting chamber	OptikLabor
Orbital incubator S1500	Stuart®
PCR workstation	VWR International
peQSTAR 2x cyclor	peQlab
See-saw rocker SSL4	Stuart®
Spectralis™ HRA+OCT	Heidelberg Engineering
Thermomixer compact	Eppendorf
TissueLyser LT	Qiagen
TW20 watherbath	Julabo
VisiLight® binocular	VWR International
Vortex-genie®	Scientific Industries™

2.1.12. General consumables

Table 16 General consumables (not in alphabetical order).

Consumables	Manufacturer, Cat. No.
Nitrocellulose membrane 0.45 µm	Bio-Rad, #1620115
1-mL syringe	BD, #309628
20G needle	BD, #301300
Amicon® Ultra-15 filter units 30k	Merck, #UFC903008
Gloves	Dermagrip, #100176
Microtome blades C35 TYPE	Feather, #207500003
PCR stripes	Kisker Biotech, #G003-SF
1.5 ml micro tube	Sarstedt, #72.690
1.5 ml black micro tube	Roth, #AA80.1
2 ml micro tube	Sarstedt, #72.689
15 ml reaction tube	Sarstedt, #62.554.502
50 ml reaction tube	Sarstedt, #62.554.254
Biosphere R filter tips 2.5 µl	Sarstedt, #70.1130.212
Biosphere R filter tips 200 µl	Sarstedt, #70.760.211
Biosphere R filter tips 1000 µl	Sarstedt, #70.762.211
30 µl Impact 384 tips	Thermo Scientific, #7431
T75 culture flask	Sarstedt, #83.3911.002
Nunc® TripleFlasks	Sigma-Aldrich, #F8542
6-well cell culture plates	Sarstedt, #83.3920
12-well cell culture plates	Sarstedt, #83.3921
96-well microtiter plate	Sarstedt, #83.3924
96-well black microtiter plates	ThermoFischer Scientific, #611F96BK
96-well white microtiter plates	Costar, #3912
Cell scraper	Sarstedt, #83.1830
FrameStar® 384-well plates with seal	4titude, #4ti-0382
Tissue-Tek® Cryomold® Molds	VWR, #R 4557
Cover glasses 18x18 mm	Th.Geyer, #7695023
Superfrost Plus™ microscope slides	ThermoFischer Scientific, #J1800AMNT

2.1.13. Software

Table 17 List of software programs.

Software	Manufacturer
AlphaView FluorChem FC2	Cell Biosciences
CS1 Adobe Creative Suite	Adobe Systems
EndNote X8	Thomson Reuters
GraphPad Prism version 6.07	GraphPad Software, Inc.
ImageJ 1.50i	National Institutes of Health
Intas GDS 3.39 software	IntasScience Imaging
LightCycler® 480 software 1.5.1	Roche Applied Science
Nanodrop2000/2000c	ThermoFisher Scientific
Office Suite 2010	Microsoft Corporation
Spectralis HRA+OCT Software	Heidelberg Engineering
Tecan i-control 1.9	PerkinElmer
Zen 2012	Zeiss

2.2. Methods

2.2.1. Murine model of dry AMD

2.2.1.1. Bright light induced retinal damage

Bright light induced retinal damage (LD) was performed in BALB/cJ mice according to previous description (Grimm & Reme, 2013; Grimm et al, 2000). Prior to LD mice were dark-adapted for 16 hours. Pupil dilatation was induced by topical application of Phenylephrin 2.5 % / Tropicamid 0.5 % under dim red light. Subsequently, mice were exposed to bright white light with an intensity of 15,000 lux for 1 hour. After light exposure, the animals were housed in dark-reared conditions overnight and then maintained under normal light conditions for the remaining experimental period of 4 hours, 1, 2, 3 and 4 days.

2.2.1.2. SD-OCT

Animals were anesthetized by intraperitoneal injection of Rompun/Ketavet (see 2.1.1), and their pupils were dilated by topical application of Phenylephrin 2.5 % / Tropicamid 0.5 % before image acquisition. Spectral domain optical coherence tomography (SD-OCT) was performed on both eyes with a commercially available Spectralis™ HRA+OCT to investigate structural changes in the retina after light exposure (Fischer et al, 2009). Of particular interest was the presence of hyperreflective foci (HF).

2.2.1.3. Retina preparation

Mice were sacrificed by cervical dislocation and the eyes were quickly enucleated by making small incisions in the inner and outer corner of the eye. In that way the eye could be lifted with a curved forceps making it easier to disconnect the bulb from the optic nerve and the underlying tissue. For RNA and electroretinogram (ERG) analysis the retina was isolated from the remaining part of the bulb in a petri dish filled with PBS. Using a 27 gauge needle the cornea was punctured to release the pressure of the bulb. Next, the cornea was cut away with a micro scissors. Through the resulting opening the lens was removed leaving the retina exposed with the ganglion cell layer pointing upwards. In order to detach the retina completely, the choroid/sclera along with the retina were cut away right beneath the ora serrata. By cutting away the optic nerve the retina could be peeled away and completely freed from the underlying tissue. The isolated retinæ were subjected to ERG analysis and RNA isolation.

2.2.1.4. Ex vivo electroretinogram

Mice were dark adapted before sacrificing and enucleation of the eyes for 16 hours. Preparation of the retina took place in dim red light. Both eyes were immersed in a glass petri dish filled with Ames' medium and the retina was isolated. Next, the retina was mounted into a recording chamber and perfused at a rate of 1 ml/minute with oxygenated Ames' solution. Scotopic ERG recordings were elicited at 37 °C by 500 ms white flashes of light applied every 3 minutes and sampled at a rate of 100 Hz via two Ag/AgCl electrodes placed on either side of the retina. The flash intensity was set to 6.3 mJ and successively increased to 200,

630, 2000 and 20 000 mlx at the retinal surface using calibrated neutral density filters. Recordings were amplified and band-limited between 1 and 300 Hz (Neumaier et al, 2018).

2.2.2. Histologic analysis

2.2.2.1. Preparation of fixed frozen cryo sections

Enucleated eyes were fixated in 10 % NBF over night at 4 °C followed by dehydration in 30 % sucrose solution for 1 hour. Subsequently, eyes were embedded in TissueTek O.C.T., quick-frozen on dry ice and stored at -20 °C for short term and at -80 °C for long term. Cryo sections of 12 µm thickness were prepared using a cryostat. Sections were mounted on microscope slides and stored at -80 °C until further use for RNA and protein analysis.

2.2.2.2. RNA-Scope

RNA-scope in situ hybridization was performed according to the protocol provided by Advanced Cell Diagnostic. Kits used for this procedure were RNAscope® Fluorescent Version 2 and RNAscope® H₂O₂ and Protease Reagents. Briefly, retinal cryo sections were baked in a dry hybridization oven for 1 hour at 60 °C. Next, sections were washed twice in PBS at room temperature for 5 minutes. Subsequently, the sections were treated with hydrogen peroxide for 10 minutes at room temperature. Then, slides were heated at 98 °C in target retrieval buffer for 5-15 minutes. To cool the slides down, they were immediately transferred to a dish containing distilled water for few seconds, followed by incubation in 100 % ethanol for 3 minutes. Slides were allowed to dry completely before adding Protease Plus and placing them in the hybridization oven at 40 °C for 30 minutes. Next, RNA probes were applied and allowed to hybridize at 40 °C for 2 hours. It is noteworthy, that probes from two different channels allow simultaneous visualization of two genes. Finally, the signal was amplified by hybridizing the probes with preamplifiers and amplifiers at 40 °C for 30 minutes each. Then, TSA® fluorophores were applied and dried in the hybridization oven at 40 °C for 30 minutes. Slides were counterstained with DAPI and cover slipped with fluorescence mounting medium.

2.2.2.3. Immunostaining

Cryo sections were thawed at room temperature and rehydrated in PBS for 5 minutes. Next, sections were blocked with blotto for 1 hour followed by incubation in primary antibody, diluted in primary antibody dilution solution, at 4 °C overnight. To avoid dehydration of the sections, a plastic paraffin film was mounted onto the sections. Next day, samples were washed three times with PBS and incubated with the secondary antibody, diluted in PBS, for 1 hour at room temperature, again followed by three washing steps in PBS. Since the secondary antibody is fluorescently labelled the sections were now kept in dark for the remaining protocol. The nuclei were stained with 0.1 mg/ml DAPI for 10 minutes at room temperature. After a final wash in 1x PBS sections were embedded with Dako fluorescent mounting medium.

2.2.2.4. Fluorescence microscopy

Fluorescent micrographs and z-stack images were acquired with an Imager.M2 microscope equipped with an ApoTome.2 and Image acquisition software ZEN.

2.2.3. Cell culture

2.2.3.1. Maintenance and passage of cells

All cell lines were cultured in T75 flasks at 37 °C in a humidified atmosphere of 5 % CO₂. Immortalized BV-2 murine microglia-like cells and SV40 human microglia-like cells were cultured in DMEM, high glucose with L-glutamine supplemented with 10 % FCS and 1 % penicillin/streptomycin. For passaging BV-2 cells were carefully scraped off in fresh media and split at a ratio of 1:5 every second days. SV40 cells were detached with trypsin/EDTA for 5 minutes at 37 °C. Next, cells were collected in fresh media and transferred to a 50 ml tube and pelleted at 1500 x g for 3 minutes. Finally, cells were split at a ratio of 1:3 every second day. Cells were seeded in collagen coated T75 flasks (~7 µg/cm²).

2.2.3.2. Primary microglia cell culture

Whole brains obtained from P0/1 C57BL/6J pups were washed in ice-cold HBSS. Vessels and meninges were removed from the brain surface using fine forceps and the binocular microscope. Next, brains were enzymatically dissociated. For this each brain was cut into small pieces and immersed in a micro tube containing 1 ml trypsin/EDTA followed by heating for 15 minutes at 37 °C. An equal amount of ice-cold FCS supplemented with DNase at a final concentration of 0.5 mg/ml was added. Brains were mechanically dissociated by resuspending with a 1000 µl and then a 200 µl pipet tip. The suspension was spun for 10 minutes at 500 x g. The supernatant was removed and the pellet was resuspended in DMEM containing 10 % FCS and 1 % penicillin/streptomycin. The cells were transferred to poly-D-lysine-coated T75 flasks (1 µg/cm²) with density of two brains/flask (e.g. when starting with six pups, seed the suspension in three flasks). The mixed glia culture was maintained at 37 °C in a humidified atmosphere of 5 % CO₂. Two consecutive days the cells were washed twice with PBS and fresh complete medium was added. After being in culture for 10 to 14 days primary microglia cells can be harvested from the adherent astrocyte cells. For that, microglia cells were detached by shaking at 250 rpm for 1 hour at 37 °C. The supernatant was then collected in a 50 ml reaction tube and microglia cells were pelleted by spinning at 800 x g for 10 minutes. Finally, cells were counted and seeded at a density of 2×10^5 in 6-well plates. The purity of microglia cell cultures was assessed by using an anti-Iba1 antibody, which is a microglia marker. Briefly, cells were seeded on poly-D-lysine coated cover glasses and fixed with 4 % HistoFix, washed with PBS and blocked in PBS containing 0.3 % v/v Triton X-100 and 10 % goat serum for 30 minutes. Subsequently, cells were washed and incubated with rabbit anti-Iba1 antibody diluted in PBS containing 0.1 % v/v Triton X-100 and 2.5 % goat serum for 1 hour. After washing the cells in PBS they were incubated in secondary antibody for 30 minutes. Finally, nuclei were stained with DAPI and cover slipped with fluorescence mounting medium.

2.2.3.3. Treatment regime

BV-2 cells were seeded in 6-well cell culture plates at a density of 3×10^5 (for gene and protein expression analysis), in 12-well cell culture plates at a density of 1×10^5 (for

morphologic analysis) and 5×10^5 (for nitric oxide release). SV40 cells were seeded in 6-well cell culture plates at a density of 3×10^5 for gene expression analysis.

To analyze complement activation in microglia BV-2 cells were stimulated with 50 ng/ml LPS and incubated for 3, 6 and 24 hours. SV40 cells were stimulated with 100 nM PMA and 50 μ g/ml Zymosan for 3, 6 and 24 hours. PMA was diluted in DMSO, which served as a vehicle control.

For the analysis of TGF- β receptor signaling primary microglia cells and BV-2 cells were either treated with IFN- γ (10 ng/ml), TGF- β (1 ng/ml) or both, as previously described (Zhou et al, 2015). IFN- γ and TGF- β treated BV-2 cells were additionally incubated with 50, 100 and 150 ng/ml of purified HtrA1 proteins for 24 hours. Cells were subjected to RNA analysis and morphologic analysis. For phospho-Smad2/Smad2 expression analysis, BV-2 cells were incubated with TGF- β and HtrA1 proteins for 3 hours. TGF- β was diluted in PBS containing 10 mM citric acid supplemented with 0.1 % BSA, which served as vehicle control.

2.2.3.4. Nitrite measurement

Nitric oxide (NO) concentrations were quantified in the culture medium of treated BV-2 cells by means of Griess reagent system. A total of 50 μ l supernatant from treated BV-2 cells were pipetted to each well of a clear 96-well microtiter plate and equal amount of sulfanilamide solution were added. After an incubation period of 10 minutes at room temperature and protection from light, 50 μ l of the NED solution (N-1-naphthylethylenediamine dihydrochloride under acidic conditions) was added. After 10 minutes, absorbance was measured at a wavelength of 540 nm on an Infinite®F200 Pro plate reader. NO-release was determined by comparison of the absorbance to the nitrite standard reference curve.

2.2.3.5. Morphological analysis

BV-2 cells were seeded on cover glasses in 12-well plates. Cells were treated as described above. After 24 hours, cells were fixed with 4 % HistoFix, washed with PBS and permeabilized in PBS containing 0.1 % v/v Triton X-100. Next, F-actin was fluorescently labeled under exclusion from light using phalloidin-TRITC. nuclei were stained with DAPI and cover slipped with fluorescence mounting medium.

2.2.4. Expression of recombinant eukaryotic proteins

2.2.4.1. Cloning

The outer reading frame (ORF) of the wildtype, protease-inactive and AMD-associated form of human (h) HTRA1 were ordered from GeneArt (Table 9). The ORF of the wildtype and protease inactive form of murine (m) Htra1 were a kind gift from Prof. Choi Oka (Oka et al, 2004). Protease-inactive mutants contained a substitution of serine at amino acid position 328 with alanine (termed S328A) while the human AMD-associated isoform carried two known SNPs in the coding exon 1 (rs1049331:C>T, and rs2293870:G>T). These less frequent alleles are synonymous SNPs and do not change the amino acid sequence at Ala34 and Gly36 (Jacobo et al, 2013). For eukaryotic expression the 1377 bp sequences (minus the endogenous signal peptide) of HTRA1 were amplified using cloning primers listed in table 10. The polymerase chain reaction (PCR) was set up and carried out as indicated in table 18 and 19. Of note, the annealing temperature decreased 1 °C/cycle during the first 10 cycles and remained constant at 59 °C for the remaining 29 cycles (touchdown PCR). This leads to higher specificity and yield, without the need for lengthy optimization (Korbie & Mattick, 2008).

Table 18 PCR to amplify the ORF of murine and human HTRA1 variants.

Reaction components	
Template DNA	50 - 100 ng
Forward primer	100 nM
Reverse primer	100 nM
dNTP's	200 nM
Q5 5x Reaction Buffer	10 µl
Q5 DNA Polymerase	0.3 µl
dH ₂ O	Up to 50 µl

Table 19 PCR program.

PCR step	Temperature	Time
Initial denaturation	98 °C	30 seconds
Denaturation	98 °C	5 seconds
Annealing	69 °C to 59 °C	20 seconds
Elongation	72 °C	55 seconds
Final extension	72 °C	2 minutes

Next, the PCR product was visualized on an agarose gel. The correct PCR product was identified by size analysis using the MassRuler DNA ladder. The band was excised and cleaned up using the NucleoSpin® Gel and PCR Clean-up kit. Subsequently, the DNA was digested at restriction sites NheI – BamHI and NheI – BglII as described in table 20.

Table 20 PCR product digestion.

Reaction components	
Cleaned up PCR product	20 µl
10x Fast Digest Buffer	5 µl
NheI	1 µl
BamHI (human)/ BglII (murine)	1 µl
dH ₂ O	Up to 50 µl

The reaction was incubated at 37 °C for 1 hour and subsequently cleaned up. Next, the insert was ligated into an expression plasmid containing a BMP40 signal peptide followed by a N-terminal double Strep II purification tag using the T4 ligase (Table 21).

Table 21 Insert and vector ligation.

Reaction components	
Vector DNA	1 µl
Insert DNA	3 µl
5 x ligation buffer	2 µl
T4 DNA Ligase	1 µl
dH ₂ O	Up to 10 µl

The resulting ligation products were transformed into DH5α cells, which are competent E-coli cells. First, 50 µl aliquots of DH5α cells were thawed on ice. Next, 10 µl of the ligated plasmid was added to the DH5α cells and incubated on ice for 30 minutes. Subsequently, the cells were heated to 46 °C for 1 minute, 300 µl LB-media was added and the suspension was

incubated at 37 °C for 1 hour to allow the cells to express resistance against ampicillin. The cells were streaked on LB-amp agar plates and incubated at 37 °C over night. Next day, 5 clones per plate were picked with a pipet tip, which was immersed in 5 ml of LB-amp media. The tubes containing the pipet tips were incubated at 250 rpm at 37 °C over night. Next day, DNA was isolated from the bacteria using NucleoSpin® Plasmid followed by a test digestion in order to control the size of the insert (Table 22). Positive clones were validated by DNA sequencing with the appropriate primers (Table 11).

Table 22 Test digestion.

Reaction components	
Template DNA	2 µl
10x Fast Digest Green Buffer	1 µl
NheI	0.2 µl
BamHI (human)/ BglII (murine)	0.2 µl
dH ₂ O	Up to 10 µl

2.2.4.2. Transfection

Expression plasmids were transfected into HEK293 cells, as previously described (Reuten et al, 2016). Briefly, HEK293 cells were cultured in DMEM/F-12 GlutaMAX supplemented with 10 % FCS when transfected with the expression plasmid using FuGENE® HD. Next day, 4 µg/ml puromycin was added to select for plasmid-positive cells. After reaching confluency, the cells were transferred to Nunc® TripleFlasks and FCS was reduced to 2 % to halt proliferation. Supernatant containing the secreted protein was collected every 48 hours for two consecutive weeks.

2.2.4.3. Affinity chromatography

For affinity chromatography, a Gelatine-Sepharose® pre-column and a Strep-Tactin® Sepharose column was prepared. The supernatant was filtered in order to eliminate any cell debris before loading onto the pre-column and column at 4 °C over night. Next, the recombinant protein was eluted in PBS containing 2.5 mM D-desthiobiotin. To minimize the concentration of D-desthiobiotin the buffer was changed using Amicon® Ultra-15 centrifugal filter units with a molecular weight cut-off at 30 kDa. The protein containing

solution was spun at 4500 x g for 10 minutes at 4 °C and the concentrate was diluted in PBS (size of Strep(II)-tagged murine and human HtrA1 proteins is around 57 kDa). This process was repeated two times to ensure complete removal of D-desthiobiotin. Protein concentration was determined via Pierce™ BCA Protein Assay Kit and samples were snap frozen and stored at –80 °C until further use. An antibody directed against murine and human HtrA1 was used to verify the identity of the purified proteins.

2.2.4.4. Enzymatic activity assay

Enzymatic activity of the purified proteins were assessed using the EnzChek Protease Assay Kits containing casein heavily labeled with green-fluorescent BODIPY® FL as a substrate (Thompson et al, 2000). Black 96-well microtiter plates were used to minimize background fluorescence. First, 90 µl of warm digestion buffer were pipetted into each well. Next, 10 µl HtrA1 enzymes, diluted in ice-cold digestion buffer, were added to each well. The reaction was initiated by adding 100 µl of BODIPY® FL casein diluted in ice-cold digestion buffer. The assay was performed with increasing concentrations of HtrA1 enzymes (2.5, 5, 10, 15, 20 and 25 µg/ml) while the substrate concentration remained constant at 5 µg/ml. The increase in relative fluorescence units (RFUs) was continuously monitored every 20 seconds for a 10 minute period at 37 °C using an Infinite®F200 Pro plate reader at excitation/emission wavelengths of 485/535 nm. Values were baseline corrected by subtracting the mean increase in RFU of the control conditions when no enzyme was added. The resulting slope for each concentration was calculated (RFU/s) and plotted against the enzyme concentration.

2.2.5. PAI-1 promoter assay

A 903 bp promoter sequence of the TGF-β response gene PAI-1 was amplified by PCR using a human male BAC clone as template. The amplified sequence was directionally cloned into the promoter-less pGL4.10 firefly luciferase reporter vector at restriction sites KpnI and XhoI as described in 2.2.4.1. Plasmids were transfected in BV-2 cells which were seeded the previous day in 12-well plates. Cells plated in antibiotic free medium were transfected for 24 hours with 0.5 µg of the reporter plasmid or promoterless pGL4.10 vector serving as a

negative control using the TransIT-LT1 Transfection reagent. Each transfection also consisted of 0.4 µg of β-galactosidase vector to normalize for transfection efficiency. Cell lysates were harvested by scraping in 250 µl of the 1 x Glo lysis buffer. To investigate effects of TGF-β and HtrA1 on promoter activity, cells were stimulated with TGF-β in fresh medium 24 hours after transfection and then incubated for further 6 hours. Cells were then lysed and their luciferase activity measured. For measurement of luciferase activity, 40 µl of the cellular extract was combined with 40 µl of the luciferase assay reagent and light emission was measured with the Infinite F200 pro reader. For normalization with β-galactosidase activity 50 µl of the cellular extract was combined with 50 µl of 13 mM ONPG and the absorbance was measured at 405 nm.

2.2.6. Transcript analysis

2.2.6.1. RNA isolation and quantification

Total RNA was extracted using the NucleoSpin® RNA Mini Kit according to the manufacturer's instructions. Prior to RNA extraction isolated retinæ were dissociated in 2 ml micro tubes containing the provided RA1 lysis buffer and stainless steel beads (5 mm mean diameter) using the TissueLyser LT for 40 seconds at 30 Hz. In case of treated cells, the cells were washed with PBS and lysed in RA1 lysis buffer. The lysis buffer inactivates RNases and creates appropriate binding conditions which favor adsorption of RNA to the silica membrane. Additionally, DNA which also binds to the silica membrane is degraded by the application of DNase. Subsequent washing aids to remove salts and other metabolites. RNA is eluted in a final step in 40 µl nuclease free water and stored at -80 °C.

RNA concentration was measured spectrophotometrically using NanoDrop 2000 in 1 µl eluted RNA. Nucleotides absorb ultraviolet light as a wavelength of 260 nm which means that the absorbance rate correlates with the RNA concentration. The ratio of absorbance at 260 nm and 280 nm is used to assess the purity of DNA and RNA. A 260/280 ratio of ~2.0 is considered as pure RNA, and thus was used for reverse transcription.

2.2.6.2. Reverse transcription

First-strand cDNA synthesis was performed with the RevertAid™ RT Kit according to the manufacturer's protocol. Up to 5 µg RNA can be transcribed while the supplied RiboLock RNase Inhibitor protects RNA from degradation. The synthesized cDNA was stored at -20 °C until further use.

2.2.6.3. Quantitative reverse transcriptase PCR

Quantitative amplifications of reverse transcribed (RT) cDNA were performed with the LightCycler® 480 Instrument II. The use of fluorescent signal allows quantitative examination of transcript levels. In the hydrolysis probe assays the Roche probe carries a fluorescent reporter and a quencher (Holland et al, 1991). The quencher is in close proximity of the fluorophore inhibiting fluorescent signal. Once the reaction is initiated the probe is hybridized to the target sequence and cleaved by the polymerase leaving the fluorophore unquenched. The fluorescence intensity increases with an increasing amount of target gene, and thus more probe cleavage. The reaction mixture contained the constituents indicated in table 23. The qRT-PCR was incubated at 95 °C to activate the polymerase and subjected to 40 cycles of amplification as indicated in table 24.

Table 23 qRT-PCR components.

Reaction components	
Template DNA	25-50 ng
Forward primer	1 µM
Reverse primer	1 µM
Roche probe	125 nM
LightCycler® 480 Probes Master	5 µl
dH ₂ O	Up to 10 µl

Table 24 qRT-PCR cycling conditions.

PCR step	Temperature	Time	
Initial denaturation	95 °C	5 minutes	
Denaturation	95 °C	15 seconds	40 cycles
Annealing	60 °C	1 minute	
End			

The qRT-PCR result was considered positive in case of amplification within 40 cycles, but crossing-point (Cp) values were recorded for only the first 35 cycles. Measurements were performed in duplicates and both positive and negative controls were used to confirm run validity. Advanced relative quantification was performed using the LightCycler® 480 software. The values were calculated by applying the absolute quantification/2nd derivative max method.

2.2.7. Protein analysis

2.2.7.1. Protein isolation and quantification

Cells were treated as described above and lysed in cold RIPA buffer. After an incubation period of 30 minutes on ice, samples were spun at maximum for 15 minutes at 4 °C and the supernatant was transferred into chilled tubes and stored at -80 °C until further use. Protein concentration of the samples was determined via bicinchoninic acid (BCA) assay according to the manufacturer's protocol. The principle of this method is that proteins can reduce Cu^{+2} to Cu^{+} in an alkaline solution which results in a purple color formation by bicinchoninic acid. The change in color correlates with the protein concentration in the sample. Change in color is determined spectrophotometrically by measuring the absorbance at 562 nm using the Infinite®F200 Pro plate reader. Protein concentration is then calculated on the basis of a BSA reference curve.

2.2.7.2. Western blot

Samples were denatured by adding Laemmli sample buffer and heating to 95 °C for 5 minutes. 20 µg of protein were separated by SDS-PAGE on 10 or 12 % gels (Table 5) with PageRuler™ Prestained Protein Ladder. Subsequently, proteins were transferred onto a 0.45 µm nitrocellulose membrane. The membrane was blocked in membrane blocking buffer for 1 hour. Next, the membrane was incubated with primary antibody diluted in membrane blocking buffer at 4 °C over night. Next day, blots were incubated with secondary antibody for 2 hours at room temperature. Blots were visualized using SignalFire™ Elite ECL Reagent and the MultiImage II system. For phosphor-Smad2/Smad2 analysis visualization of

Phospho-Samd2 (pSmad2) was followed by incubating the blots two times in stripping buffer for 10 minutes followed by blocking for 1 hour. Blots were then incubated with primary antibody against Samd2 and secondary goat anti-rabbit IgG-HRP as described above. Semi-quantitative densitometric analyses were carried out using ImageJ and ratios for pSmad2/Smad2 were plotted.

2.2.8. Statistical analysis

Normality of the data was assessed with D'Agostino-Pearson omnibus normality test. Real-time RT-PCR and HF data was analyzed using a one-way analysis of variance (ANOVA) followed by Tukey's multiple comparison test. For the ERG, Nitrite secretion, Luciferase activity and pSmad2/Smad2 Western blot analysis data did not follow a Gaussian distribution, and was analyzed using the non-parametric Kruskal-Wallis test, followed by Dunn's multiple comparison correction test using GraphPad Prism version 6.07 for Windows. $p \leq 0.05$ was considered statistically significant.

3 Results

3.1. Light induced retinal damage as rodent model for dry AMD

Exposure to white light was chosen as a model for retinal degeneration since it was shown to mimic features of GA in rodents (Grimm & Reme, 2013; Marc et al, 2008). Furthermore, reactive, amoeboid microglia were shown to be present in the outer retina (Scholz et al, 2015a; Scholz et al, 2015b). For the current study several end points were chosen to have a continuous monitoring of microglial reactivity with particular attention on the appearance of HF, complement activation and HtrA1 expression (Fig. 9). For this purpose SD-OCT images were taken and qRT-PCR analyses were carried out of control mice and at 4 hours, 1, 2, 3 and 4 days after LD. RNAscope staining was performed on cryo sections from eyes enucleated 1 and 3 days of LD. Furthermore, functional analyses were carried out to in explanted retinæ of control mice, 4 days and 7 days after LD.

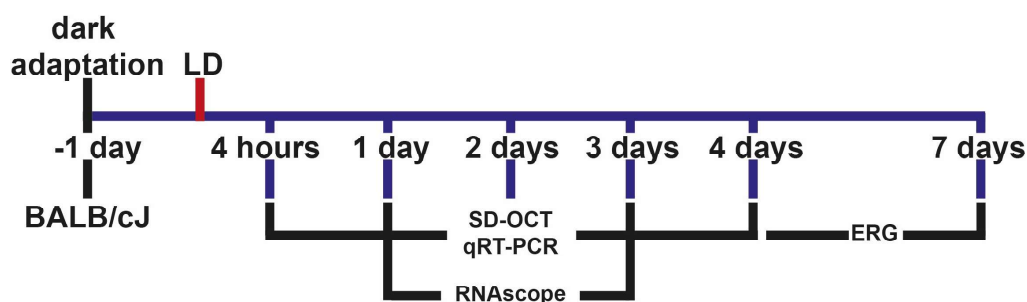


Figure 9 Experimental setup for light induced retinal damage (LD) in BALB/cJ mice
BALB/cJ mice were dark adapted one day before exposure to bright white light. As soon as 4 hours after LD mice were sacrificed and subjected to SD-OCT and qRT-PCR. Further time points were 1, 2, 3 and 4 days. Furthermore, RNAscope in situ hybridization were performed at 1 day and 3 days after LD. Additionally, *ex vivo* ERGs were recorded 4 and 7 days after LD.

3.1.1. ERG in light damaged retinal explants

The majority of the ERG signal originates from the photoreceptor cells and the bipolar cells. Scotopic ERG recordings aid to evaluate rod photoreceptor cell function and signal transduction in the retina. The scotopic ERG is carried out with dark adapted subject, when exposed to light stimulus. A corneal-negative potential is initially generated due to hyperpolarization of photoreceptor cells (a-wave). It is followed by a corneal-positive wave

reflecting mainly the depolarization of ON bipolar cells (b-wave). Reduced scotopic responses were recorded in patients suffering from early and late stage AMD (Gerth, 2009; Walter et al, 1999).

Severe loss of cone and rod photoreceptor cells are expected 4 days and 7 days post light damage. Hence, *ex vivo* ERG recordings were conducted at these time points. Stimulus intensity was increased successively in order to evaluate photoreceptor cell sensitivity. The a-wave amplitude was measured from the baseline to the negative peak and the b-wave was measured from the a-wave trough to the maximum positive peak. Implicit times for the a- and b-wave were measured as indicated (Fig. 10 A). Representative ERG traces from retina which received no LD, 4 days and 7 days after LD show differences in b-wave amplitude and implicit time at low stimulus intensities (Fig. 10 B). Differences in a-wave become more evident at higher stimulus intensities (Fig. 10 C, D). Furthermore, a more pronounced loss in b-wave amplitude is evident in the 4 days post LD retina.

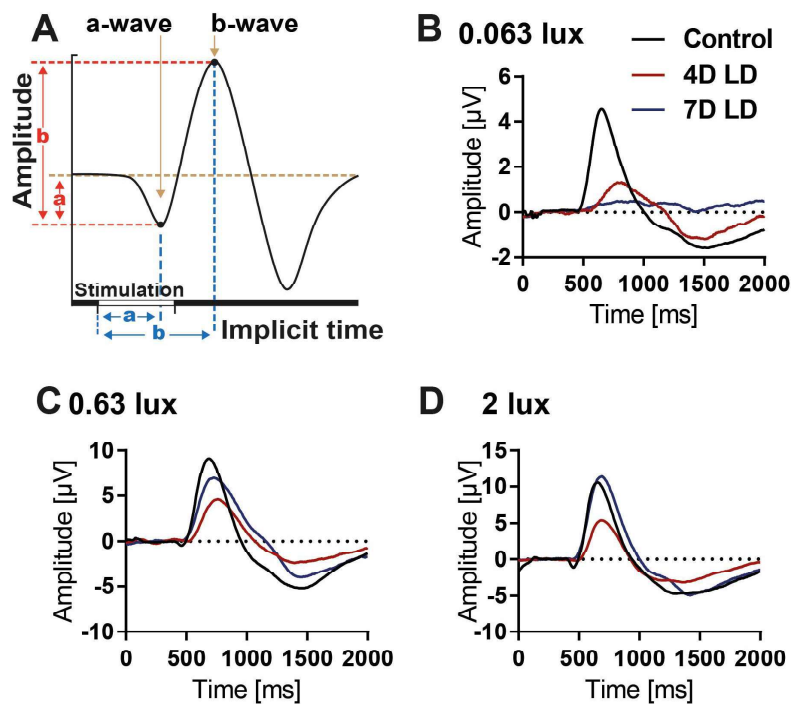


Figure 10 Representative ERG traces of retina from control and LD mice
(A) Schematic illustration of scotopic ERG pointing out amplitude and implicit times for a- and b-wave measured in the following section. Stimulus intensity to elicit scotopic ERG was successively increased. Representative traces for 0.063 (B), 0.63 (C) and 2 lux (D).

Quantification of a-wave and b-wave amplitude and implicit times demonstrates a reduction of a-wave amplitude after LD at higher stimulus intensities (Fig. 11 A). Interestingly, the b-wave amplitude is significantly reduced 4 days but not 7 days after LD when compared to control, indicating a recovery of signal originating from bipolar cells after 7 days of LD (Fig. 11 B). Furthermore, there is a decrease in a-wave implicit time which is significant at 7 days after LD (Fig. 11 C). Finally, a significant decrease in b-wave implicit time was observed at low stimulus intensities for 4 days after LD and at high stimulus intensities at 7 days after LD (Fig. 11 D).

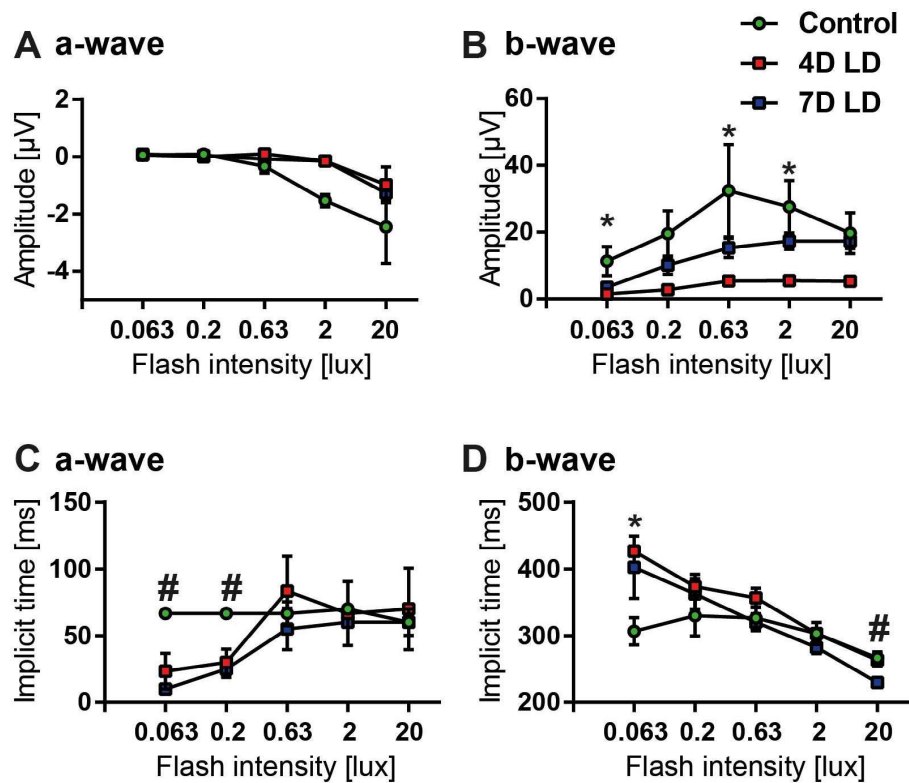


Figure 11 Analysis of a-wave and b-wave amplitude and implicit time after LD
(A) A reduction of a-wave amplitude is evident after LD at stimulus intensities 0.63, 2 and 20 lux.
(B) b-wave amplitude is significantly reduced 4 days (4D LD) but not 7 days (7D LD) after LD when compared to control.
(C) A significant decrease in a-wave implicit time was observed at 7D LD.
(D) A significant decrease in b-wave implicit time was observed at 0.036 lux stimulus intensity for 4D LD and at 20 lux at 7D LD. Values are presented as mean \pm SEM. N = 4/group, with * $p \leq 0.01$ when comparing 4 D LD to control and # $p \leq 0.01$ when comparing 7D LD to control.

3.1.2. HF in SD-OCT after LD

As mentioned above, one characteristic that was reported in SD-OCT scans of human AMD eyes were HF in outer retinal layers which regressed after treatment (Coscas et al, 2013). All OCT scans of control mice and those which received LD were analyzed for the presence of HF in the ONL. Staging of HF was based on the number of HF detected. SD-OCT scans were analyzed by two independent and blinded graders. Discrepancies between graders were solved by open adjunction. Similarly to human scans, HF were detected in mice which were subjected to LD (Fig. 12 A). Number of HF increased significantly after LD. However, it cannot be stated at what time the HF peak due to high standard deviations (Fig. 12 B).

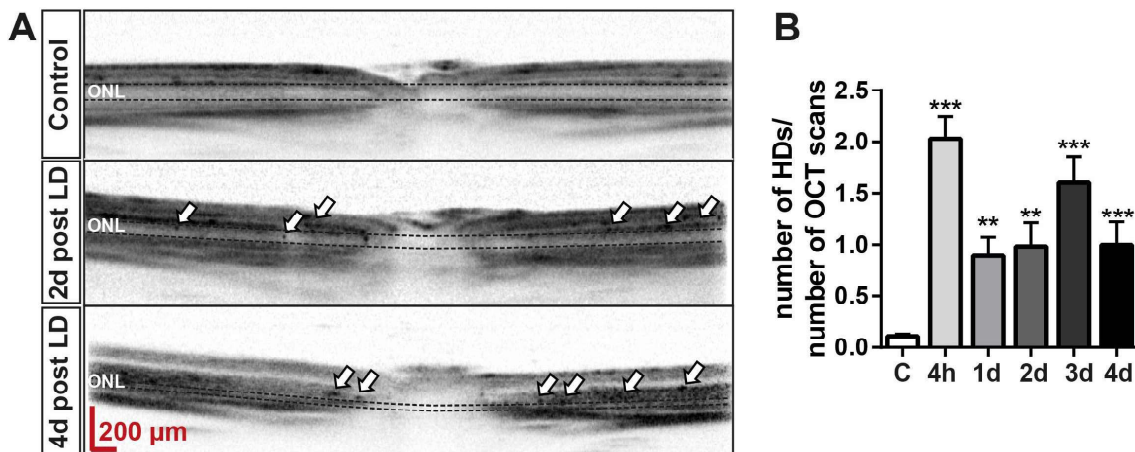


Figure 12 Representative OCT images and HF quantification
(A) OCT images of control mice and those receiving light damage (LD, 2 days and 4 days). HF are highlighted with white arrows. **(B)** HF from the ONL of both eyes were quantified by two independent blinded analysts. Number of HF increase significantly after light damage. Means were compared to control eyes. C= Control; Values are presented as mean ± SEM. N = 13-28, with ** $p \leq 0.01$ and *** $p \leq 0.001$.

The origin of these HF are a matter of debate. Interestingly, the size of HF in OCT scans matches the size of microglia (Saito et al, 2013). Thus, the location of HF in the OCT was retrieved in histological sections. These sections were stained with an antibody directed against Iba1, a microglia specific marker (Fig. 13 C). Despite some positive hints it is not certain whether the HF seen in the OCT scans are the Iba1-positive cells that were relocated in the cryo sections.

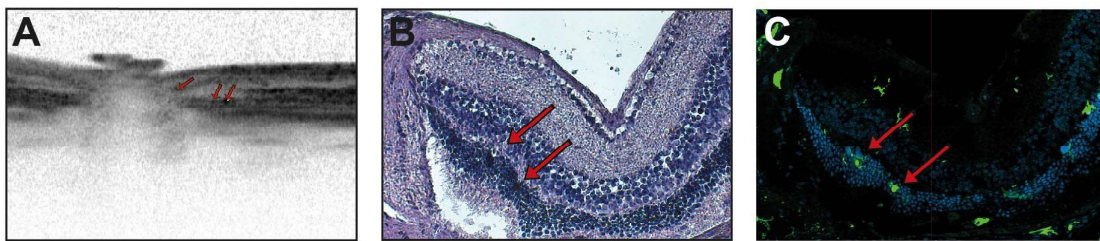


Figure 13 Origin of HF in degenerating retina

The location of HF in the OCT (A) was retrieved in histological sections which were subjected to HE-staining (B) and anti-Iba1 staining (C). It is not entirely sure, whether the HF seen in the OCT correspond to the spot seen in (B) and the Iba1-positive cells in (C).

3.2. Complement system activation in microglia during retinal degeneration

The first part of the project dealt with the role of the anaphylatoxin receptors C3aR and C5aR in microglia. Complement system activation is a major part of the innate immune system which additionally was found to play a role in microglial reactivity during retinal degeneration (Natoli et al, 2017). Upon inflammation C3 expression was found to be elevated in microglia, which should lead to increased C3a and C5a production. The question arises whether microglia play a role in anaphylatoxin signaling during degeneration in the retina. This could point towards a novel therapeutic target for patients suffering from GA which still lacks effective treatment options till today.

3.2.2. Expression of anaphylatoxin receptors in activated microglia *in vitro*

First, C3aR, C5aR and C3 expression was quantified via qRT-PCR in activated microglia *in vitro*. Here, an immortalized murine microglia-like cell line (BV-2) and a human microglia cell line (SV40) was chosen. BV-2 cells were stimulated with 50 ng/ml lipopolysaccharide (LPS) while SV40 cells were activated with 50 µg/ml Zymosan and 100 nM phorbol 12-myristate 13-acetate (PMA). LPS binds to Toll-like receptor 4 (TLR4), leading to rapid activation of an intracellular signaling network inducing a pro-inflammatory phenotype in microglia, evident by an increase in nitric oxide synthase (iNos) levels (Fig. 14 A) (Alexander & Rietschel, 2001). Zymosan is a glucan which activates microglia by binding to the dectin receptor 1. The effect is potentiated by the protein kinase C activator PMA, which leads to translocation of NF-κB, resulting in the increase of tumor necrosis factor-α (TNF-α) production (Fig. 14 E) (Song et al, 2015). Similarly, C3 transcript levels increased continuously over the period of 3, 6 and 24 hours in both cell lines (Fig. 14 B, F). Receptor expression of C3aR and C5aR were increased upon microglial activation, however the expression pattern differed across cell lines. BV-2 microglia exhibited a steep increase of

anaphylatoxin receptor expression after 3 hours, which dropped to baseline after 24 hours (Fig 14 C, D). SV40 microglia demonstrated a slower increase in receptor expression (Fig. 14 G, H).

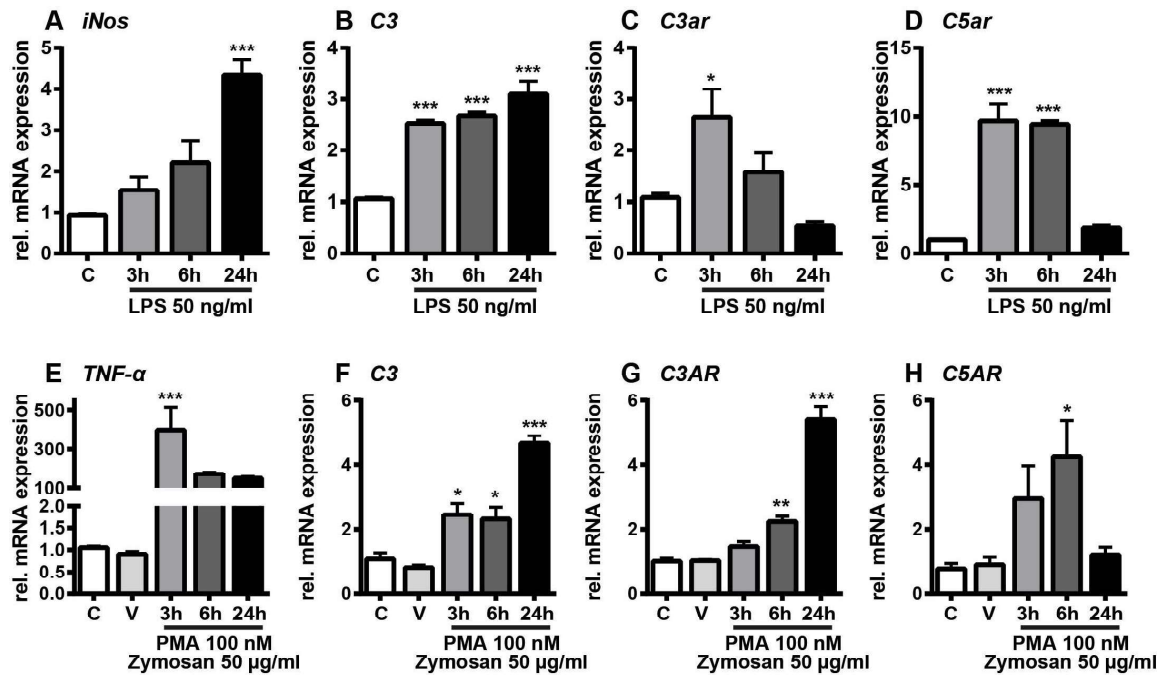


Figure 14 Expression of anaphylatoxin receptors in microglia upon activation in vitro. Activation of BV-2 (top row) and SV40 (bottom row) microglia were induced by LPS and a combination of zymosan/PMA, respectively. Stimulation led an increase in iNos, TNF-α and C3 expression (A, B, E, F). Receptor expression of C3ar and C5aR were increased upon microglial activation, however the expression pattern differed across cell lines. BV-2 microglia exhibited a step increase of anaphylatoxin receptor expression after 3 hours, which dropped to baseline after 24 hours (C, D). SV40 microglia demonstrated a slower increase in receptor expression (G, H). C= Control, V= DMSO, which served as a vehicle control. Values are presented as mean ± SEM. N= 4, with *p<0.05, **p<0.01 and ***p<0.001.

3.2.3. Expression of anaphylatoxin receptors in activated microglia *in vivo*

Next, gene expression levels of C3aR and C5aR were quantified in whole retinæ of mice which were subjected to LD. Expression of iNos was elevated at early time points after LD and dropped back to baseline levels after 3 days (Fig. 15 A). Similarly, expression of C3 was

transiently increased (Fig. 15 B). While C3aR expression could not be properly detected, levels of C5aR were also transiently increased at one and two days after LD when compared to control (Fig. 15 C, D).

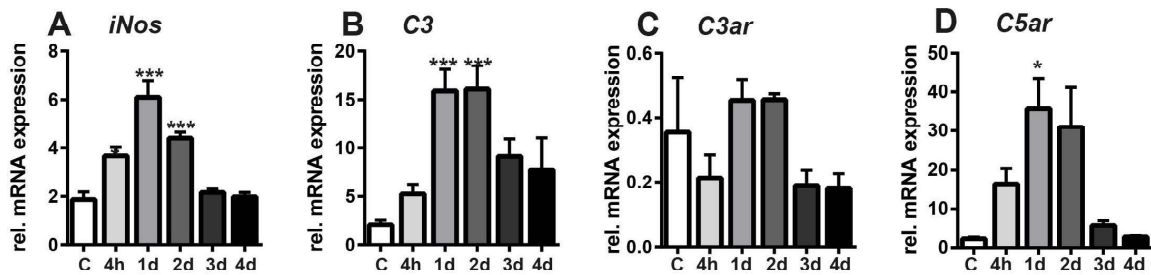


Figure 15 Transient increase in complement system activation upon retinal degeneration
(A) Expression of *iNos* was transiently elevated upon LD and dropped back to baseline levels after 3 days. **(B)** Expression of *C3* was transiently increased. While *C3aR* expression could not be properly detected, levels of *C5aR* were also transiently increased at one and two days after LD when compared to control **(C, D)**. C= Control. Values are presented as mean \pm SEM. N = 5-13/group, with * $p \leq 0.05$ and *** $p \leq 0.001$.

Since the qRT-PCR results give no hint on the expression site of *C3aR* and *C5aR* RNAscope in situ hybridization was carried out in control retina and retinae from mice which received LD. *C3aR* and *C5aR* were co-labeled with allograft inflammatory factor 1 (*Aif1*), a microglial marker. Increased expression was evident for both anaphylatoxin receptors 1 day post LD. In contrast, 3 days post LD expression of *C3aR* was still detectable, while *C5aR* expression was reduced (Fig. 16 and 17). Furthermore, co-expression could be confirmed for both anaphylatoxin receptors.

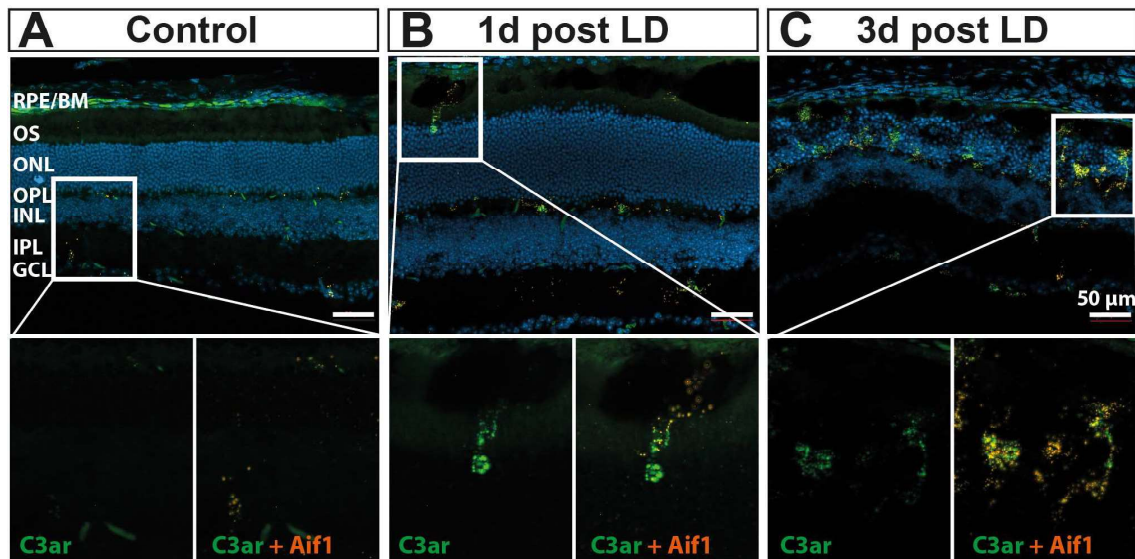


Figure 16 Co-localization of C3aR and microglia marker Aif1 during retinal degeneration (A) No expression of C3aR in control retina. However expression is increased and co-localizes with microglial marker Aif1 after LD (B, C).

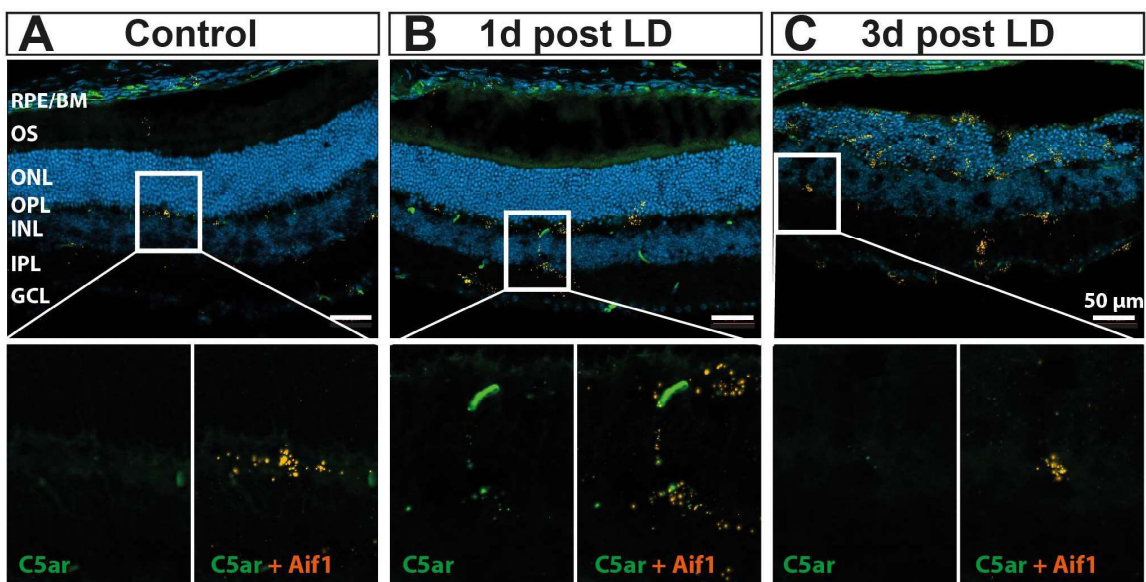


Figure 17 Co-localization of C5aR and microglia marker Aif1 during retinal degeneration (A) No expression of C5aR in control retina. (B) Increased expression of C5aR was observed at 1 day post LD. Expression site was primarily in microglia. (C) Reduced expression was observed at 3 days post LD expression.

3.3. Involvement of HtrA1 in microglial inflammation during retinal degeneration

The second part of the project deals with the effects of HtrA1 on microglial activation through the modulation of the TGF- β signaling pathway.

3.3.1. Expression of Htra1 in the retina during retinal degeneration

Firstly, the expression of Htra1 in the LD model was checked in order to validate the results seen in human patients. When mice were subjected to Htra1 in situ hybridization and qRT-PCR an increase of Htra1 gene synthesis after LD was evident (Fig 18). Again, Aif1 was used to check for microglial activation. A positive signal for Aif1 was visible in the OPL, which increased after LD. Furthermore, the expression of Htra1 did not overlap with Aif1, suggesting that microglia are not the sole expression site of Htra1 in the retina (Fig.18 A-C). Nevertheless, Htra1 may influence the immunomodulatory character of these cells by paracrine signaling.

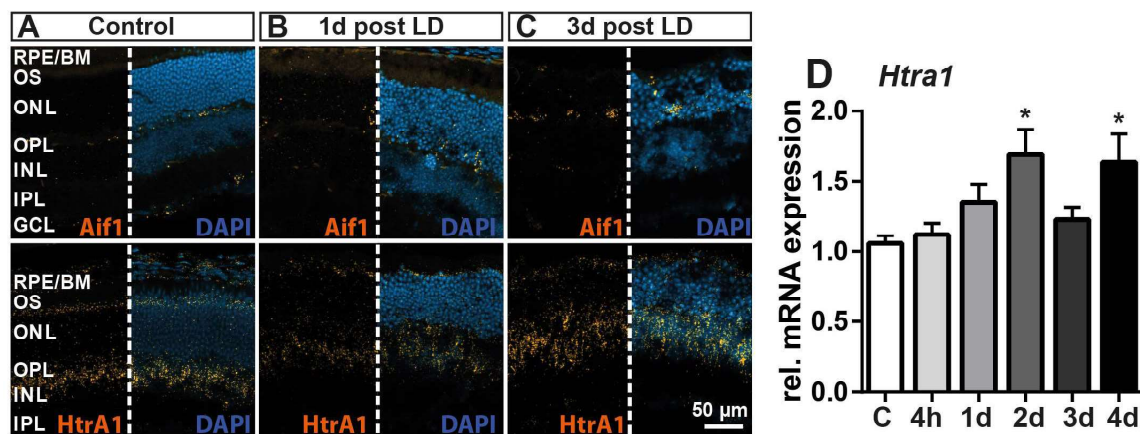


Figure 18 Gene expression of Aif1 and Htra1 after LD

(A) Aif1 shows positive signal of microglia which reside in plexiform layers. Upon LD change in microglia morphology and location is evident (B, C). Htra1 signal was enriched in the INL and the photoreceptor OS. Upon LD the signal of Htra1 intensifies as well as it spreads across the ONL. (D) Htra1 gene expression is increased after LD. C= Control. Values are presented as mean \pm SEM. N = 13-17/group, with * $p \leq 0.05$.

3.3.2. Effects of AMD-associated HtrA1 variants on microglial activity

In order to analyze the paracrine effect of HtrA1 on microglia *in vitro* experiments were conducted. For this purpose human AMD-associated HtrA1 isoforms were expressed. Additionally WT and protease-inactive form of human (h) and murine (m) HtrA1 were expressed. As indicated in 2.2.4.1 the protease-inactive mutants contained a substitution of serine at amino acid position 328 with alanine (termed S328A) while the human AMD-associated isoform carried two known synonymous SNPs in the coding exon 1 (rs1049331:C>T, and rs2293870:G>T). For simplification purposes, the human WT, protease inactive and the SNP-carrying form will be termed hWT, hS328A and hSNP, respectively. Similarly, the murine WT and protease inactive forms will be referred as mWT and mS328A, respectively. These variants were subjected to a protease and cell culture assays (Fig. 19). The protease assay served to determine the proteolytic activity while the cell culture and functional assays were used to evaluate the effect on TGF- β signaling and microglial activity.

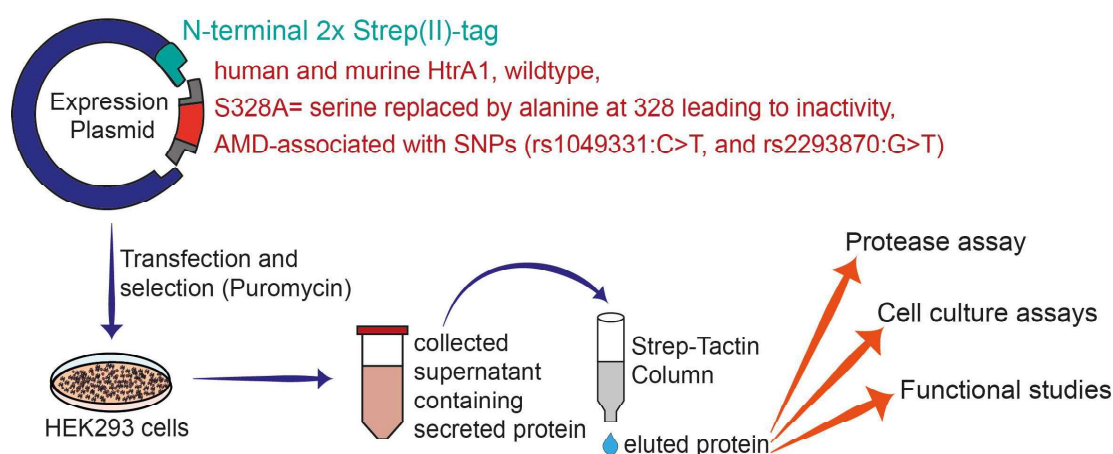


Figure 19 Work stream for HtrA1 expression, purification and *in vitro* analysis. Five HtrA1 proteins were expressed including the human and murine WT, S328A inactive forms and the human AMD associated form. The expression system used here led to a high yield of the purified HtrA1 which was subjected to the cell culture assays where the inhibitory effect on TGF- β signaling in microglia was evaluated.

3.3.2.1. Expression and enzymatic activity of HtrA1 variants

After expression and purification of N-terminally Strep(II)-tagged mWT, mS328A, hWT, hSNP and hS328A HtrA1 by affinity chromatography, recombinant proteins were immunoblotted and detected with an anti-HtrA1 antibody. Tagged HtrA1 variants were detected at approximately 57 kDa (Fig. 20 A). Smaller fragments were detected at 53, 43 and 37 kDa, however, the 37 kDa fragment was not present in the enzyme inactive samples mS328A and hS328A (highlighted with an asterisk). Hence, this could be attributed to autolytic cleavage, as previously described (Chien et al, 2006; Lorenzi et al, 2013). A quantitative protease assay using BODIPY-labelled casein was carried out in order to characterize the proteolytic properties of the expressed variants. A similar assay had already been applied to characterize HtrA2 (Cilenti et al, 2003). The assay demonstrated reproducible proteolytic activity for the mWT, hWT and hSNP forms whereas no increase in casein-proteolysis was evident in case of mS328A and hS328A as expected (Fig. 20 B). Interestingly, a higher proteolytic activity was observed for the hSNP isoform. These recombinant HtrA1 variants were then used for all further functional studies.

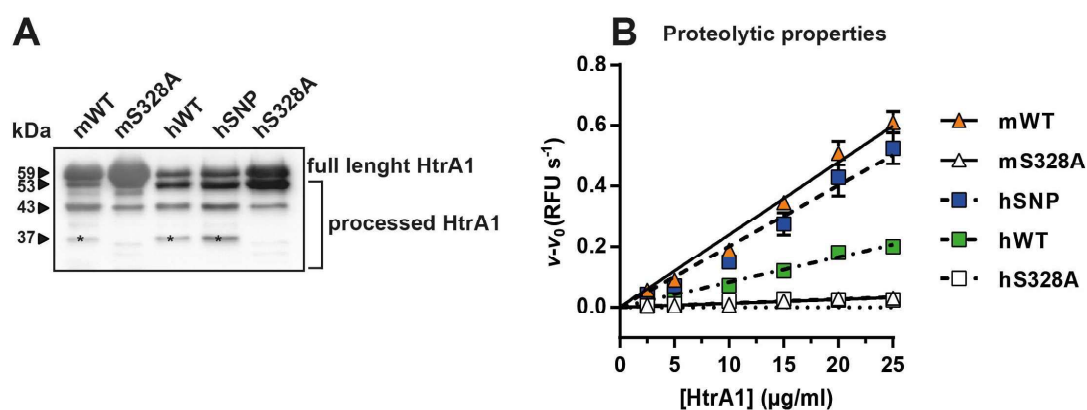


Figure 20 Immunoblot of HtrA1 variants and their proteolytic characterization

(A) Anti-HtrA1 immunoblot analysis of recombinantly expressed and purified Strep(II) tagged-HtrA1 variants from HEK293 cells shows bands at 57 kDa corresponding to the full length protein. Due to autolytic cleavage smaller fragments are present, though to a lesser extent in the mS328A and hS328A samples (marked with an asterisk). **(B)** Proteolytic activity was determined using BODIPY-FL-labelled casein as substrate. Slopes of the increase in RFU were plotted as a function of increasing enzyme concentrations. Shown are mean values \pm SEM. N = 3/group, performed in duplicates.

3.3.2.2. Effects of HtrA1 variants on TGF- β signaling

Next, the anti-inflammatory potential of TGF- β on activated primary murine microglia cells was assessed via qRT-PCR. Microglial activation was induced by application of IFN- γ . These pro-inflammatory microglia are characterized by the increased expression of pro-inflammatory cytokines Tnf- α and induction of iNos which catalyzes production of nitric oxide (NO) from L-arginine. In contrast, anti-inflammatory microglia demonstrate increased expression of arginase 1 (Arg1), which metabolizes L-arginine to produce L-ornithine and urea and hence competes with iNos. Furthermore, anti-inflammatory microglia exhibit increased expression of chitinase-like protein 3 (Ym1) (Raes et al, 2005). Primary microglia cells were cultured in serum-free media and treated with TGF- β (1 ng/ml), IFN- γ (10 ng/ml) or both for 24 hours. Treatment of primary microglia cells with TGF- β led to a significant increase in its response genes Pai-1 and kruppel like factor 10 (or TGF- β -inducible early growth response protein 1; Klf10), as well as Arg1 (Fig. 21 A,B). At the same time, Arg1 expression was increased while no increase in Ym1 was observed (Fig. 21 C, D). Stimulation with IFN- γ induced a significant up-regulation of iNos and Tnf- α concomitant with a reduction in Arg1 and Ym1 (Fig. 21 C-F). Upon co-treatment with TGF- β the pro-inflammatory reactive phenotype of microglia was reduced by decreasing iNos and Tnf- α transcripts, concomitant with an increase in Pai-1, Klf10 as well as an increase in Arg1 and Ym-1. The anti-inflammatory effect of TGF- β on IFN- γ challenged murine primary microglia was furthermore assessed by morphologic analysis. Here, cells were labeled using phalloidin-TRITC. Additionally, cells were stained using Iba1, to confirm the purity of the primary microglia culture (Fig. 22). IFN- γ stimulated cells exhibited an amoeboid shape with shortened and thickened processes when compared to untreated conditions (Fig. 22 C). Co-treatment with TGF- β demonstrated increased numbers of spindle-like and long-shaped microglia representing a more quiescent phenotype (Fig. 22 D).

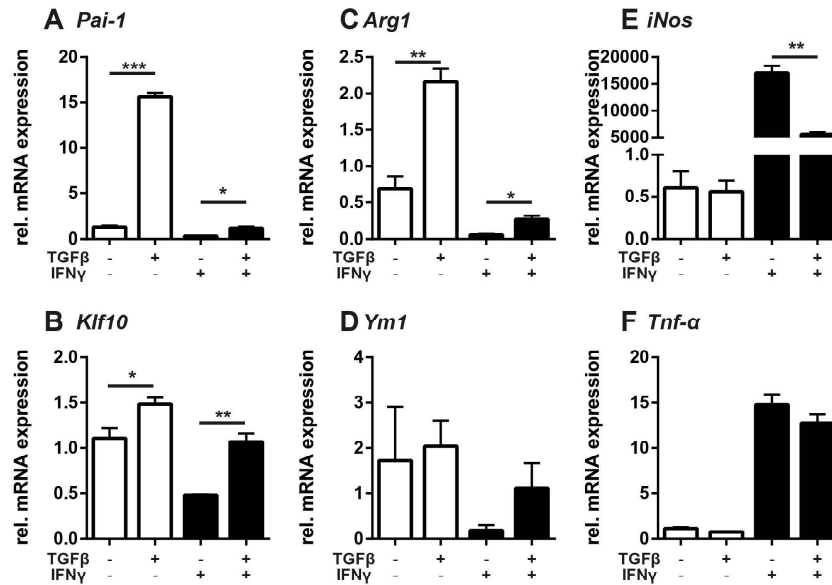


Figure 21 TGF- β induced quiescence in challenged primary murine microglia cells
Treatment of primary microglia cells with 1 ng/ml TGF- β led to a significant increase in the TGF- β response genes *Pai-1* and *Klf10* (**A**, **B**) as well as alternative activation markers *Arg1* and *Ym1* (**C**, **D**). Treatment with 10 ng/ml IFN- γ induced a significant up-regulation of *iNos* and *Tnf- α* and reduction in the alternative activation marker *Arg1* and *Ym1* (**C-F**). Upon co-treatment of microglia cells TGF- β reduced the pro-inflammatory reactive phenotype of microglia cells and induced a significant decrease in *iNos* concomitant with an increase in *Arg1*. Values are presented as mean \pm SEM. N = 3/group, with * $p \leq 0.05$, ** $p \leq 0.01$ and *** $p \leq 0.001$.

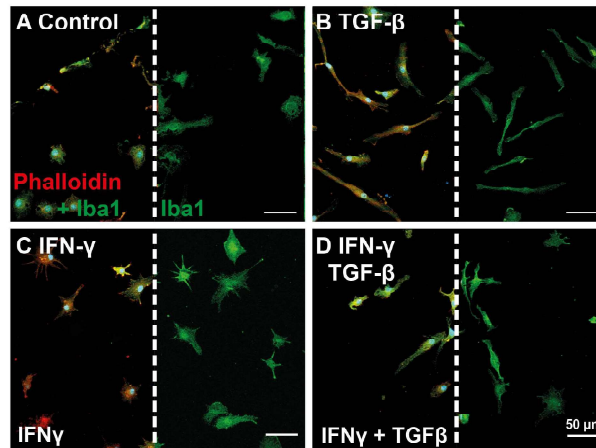


Figure 22 Primary microglia cell morphology upon treatment with IFN- γ and TGF- β
(**A-D**) Primary murine microglia cells were stained with *Iba1* and phalloidin-TRITC to confirm culture purity. (**B**) TGF- β stimulation (1 ng/ml) induced a spindle-like and long-shaped morphology in unchallenged cells. (**C**) Stimulation with 10 ng/ml IFN- γ induced an amoeboid shape with shortened and thickened processes when compared to untreated conditions. (**D**) Co-treatment with TGF- β demonstrated increased numbers of long-shaped ramified microglia representing a more quiescent phenotype.

The immune-modulatory property of TGF β could be confirmed in the BV-2 microglia cell line for Pai-1, Arg1 and iNos, which demonstrated the most significant differences in the primary microglia cells (Fig. 23).

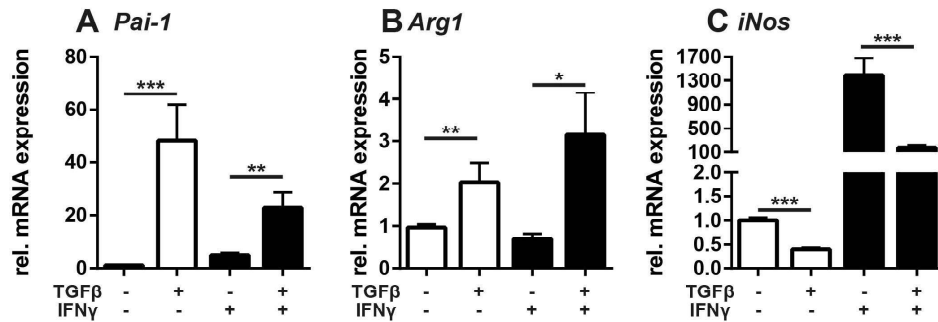


Figure 23 BV-2 cells mirror primary microglial activity

(A, B) Treatment of BV-2 cells with 1 ng/ml TGF- β led to a significant increase in Pai-1 and Arg1. Treatment with 10 ng/ml IFN- γ induced a significant up-regulation of iNos and reduction in the alternative activation marker Arg1 (B, C). Upon co-treatment TGF- β reduced the pro-inflammatory reactive phenotype of microglia and induced a significant decrease in iNos concomitant with an increase in Arg1. Values are presented as mean \pm SEM. N = 9/group, with *p \leq 0.05, **p \leq 0.01 and ***p \leq 0.001.

The following experiments were carried out in BV-2 cells which demonstrated similar results as seen in primary microglia cells from mouse. Since the aim was to investigate whether exogenous stimulation with HtrA1 variants alter the anti-inflammatory effect of TGF- β on challenged BV-2 cells the expressed variants in increasing concentrations were applied to cells treated with IFN- γ and TGF- β . Concentrations of HtrA1 ranging from 50 ng/ml to 150 ng/ml were used, which correspond to the elevated HtrA1 levels in the aqueous humor of patients with nAMD (Tosi et al, 2017). When mWT was applied a significant decrease in Pai-1 and Arg1 but intriguingly also in iNos with the lowest concentration was observed (Fig. 24 A-C). Furthermore, application of 150 ng/ml mS328A led to no significant changes, except for the case of Pai-1. Surprisingly, when the human forms were applied no significant changes were observed in gene expression levels (Fig. 24 D-F). These results point towards a lack of effects of HtrA1 on TGF- β induced microglial quiescence.

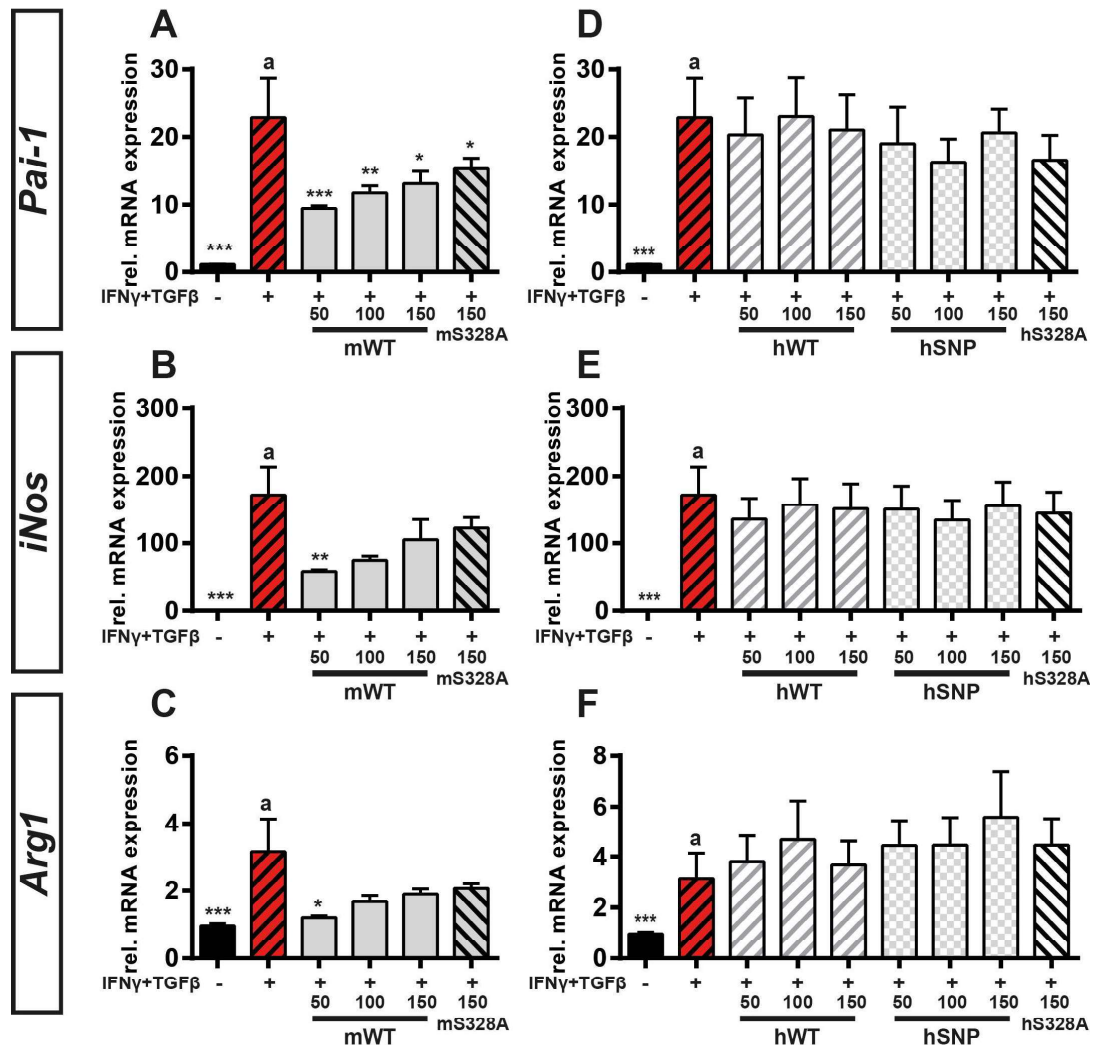


Figure 24 HtrA1 stimulation do not inhibit TGF- β induced microglial quiescence
Application of mWT led to a significant decrease in *Pai-1* and *Arg1* but intriguingly also in *iNos* with the lowest concentration (A-C). Application of human forms led to no significant changes in gene expression levels of *Pai-1*, *iNos* and *Arg1* (D-F). Values are presented as mean \pm SEM. N = 9/group, with * $p \leq 0.05$, ** $p \leq 0.01$ and *** $p \leq 0.001$ when compared to IFN- γ +TGF- β indicated with an (a).

Overactivated glial cells can produce neurotoxic oxidant molecules such as NO (Boje & Arora, 1992). Congruently, an increase in NO release of IFN- γ -challenged BV-2 cells was observed, which was blocked upon co-treatment with TGF- β (Fig. 25 A). Again, HtrA1 variants were applied to the cells. However, no differences in NO release were evident when murine and humane HtrA1 variants were applied and compared to IFN- γ + TGF- β conditions. Furthermore, the morphological changes of microglia were evaluated. As already seen in

primary microglia cells, IFN- γ stimulated cells exhibited an amoeboid shape with shortened and thickened processes (Fig. 25 C). Co-treatment with TGF- β demonstrated increased numbers of spindle-like and long-shaped microglia representing a more quiescent phenotype (Fig. 25 D). However, co-treatment with HtrA1 variants did not change the TGF- β - induced spindle-like morphology of BV-2 cells (Fig. 25 E-F).

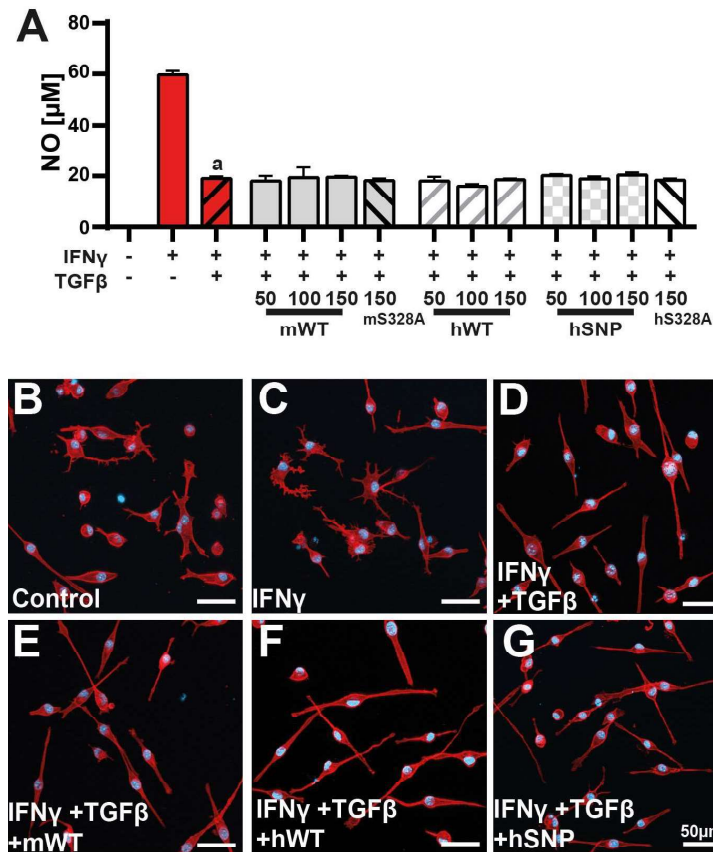


Figure 25 HtrA1 variants do not alter NO levels and morphology

(A) Quantification of NO release from BV-2 microglia treated with 10 ng/ml IFN- γ in the absence or presence of 1 ng/ml TGF- β and HtrA1 variants in increasing concentrations. IFN- γ -induced elevated release of NO was blocked by TGF- β . Co-treatment with HtrA1 variants did not change the levels of NO release when compared to IFN- γ +TGF- β . Values are presented as mean \pm SEM. N = 4/group, with no significant differences when compared to IFN- γ +TGF- β indicated with an (a). (B-G) Representative images of phalloidin-TRITC labeled microglia treated with 10 ng/ml IFN- γ in the absence or presence of 1 ng/ml TGF- β and 150 ng/ml HtrA1 variants for 24 hours. Upon IFN- γ treatment microglia exhibited an amoeboid shape to a greater extent when compared to untreated control cells (C). Co-treatment with TGF- β induced a spindle-like and long-shaped microglia representing a more quiescent phenotype (D). Pre-incubation with HtrA1 did not alter TGF- β induced effects on BV-2 microglia cells (E-G).

3.3.2.3. Effects of HtrA1 variants on TGF- β response elements

To examine whether the HtrA1 variants affect TGF- β signaling a reporter assay for microglia was designed. For this, the TGF- β responsive region of the human PAI-1 promotor was cloned into the pGL4.10 luciferase reporter vector (Fig. 26 A). Plasmids were transfected into BV-2 microglia, which were then stimulated with TGF- β and HtrA1 variants. An increase in promotor activity was evident, when the cells were stimulated with 0.5 ng/ml and 1 ng/ml TGF- β (Fig. 26 B). However, no differences were observed when transfected cells were co-incubated with 150 ng/ml HtrA1 variants.

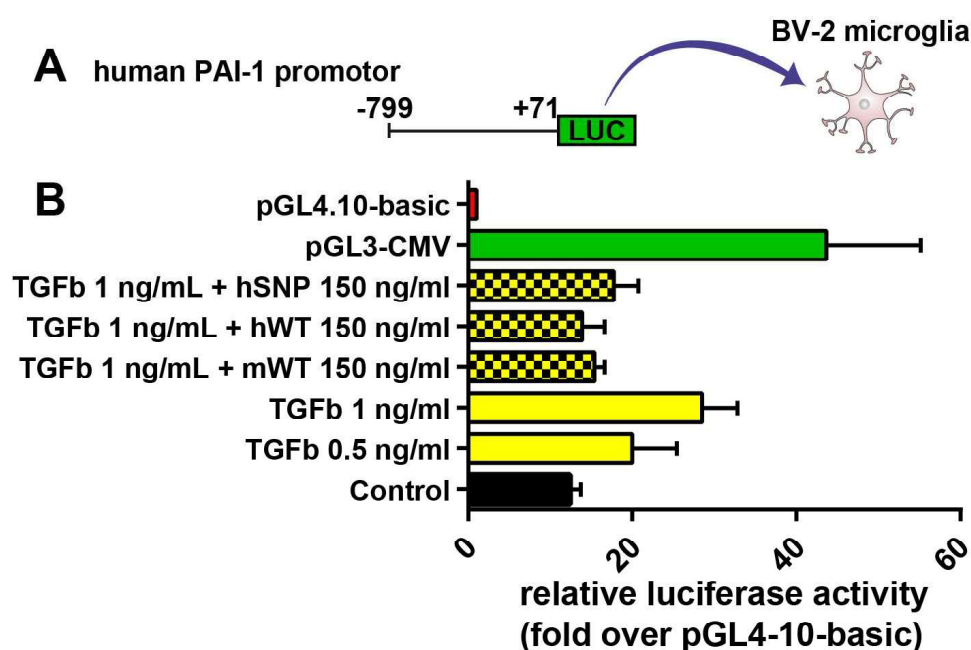


Figure 26 HtrA1 variants do not influence TGF- β induced PAI-1 promotor activity
(A) Promotor assay with TGF- β response gene PAI-1 in BV-2 microglia. **(B)** Stimulation of transfected microglia with 0.5 ng/ml and 1 ng/ml TGF- β led to an increase in luciferase activity. Co-treatment with HtrA1 variants did not result in significant reduction in PAI-1 promotor activity. Values are presented as mean \pm SEM. N = 4/group, performed in duplicates with no significant differences.

Upon binding of TGF- β to the TGF- β receptors Smad2 proteins are phosphorylated. Hence, the influence of HtrA1 variants on the levels of pSmad2 in TGF- β treated BV-2 cells was

evaluated. Western blot analyses showed that no pSmad2 was detectable in microglia that were not treated with TGF- β . In contrast, application of 1 ng/ml TGF- β led to a significant increase in pSmad2 levels (Fig. 27 A, B). However, co-treatment with any of the HtrA1 variants in increasing concentrations did not reduce the level of pSmad2 indicating that HtrA1 does not influence TGF- β signaling in BV-2 microglia cells (Fig. 27 A-C).

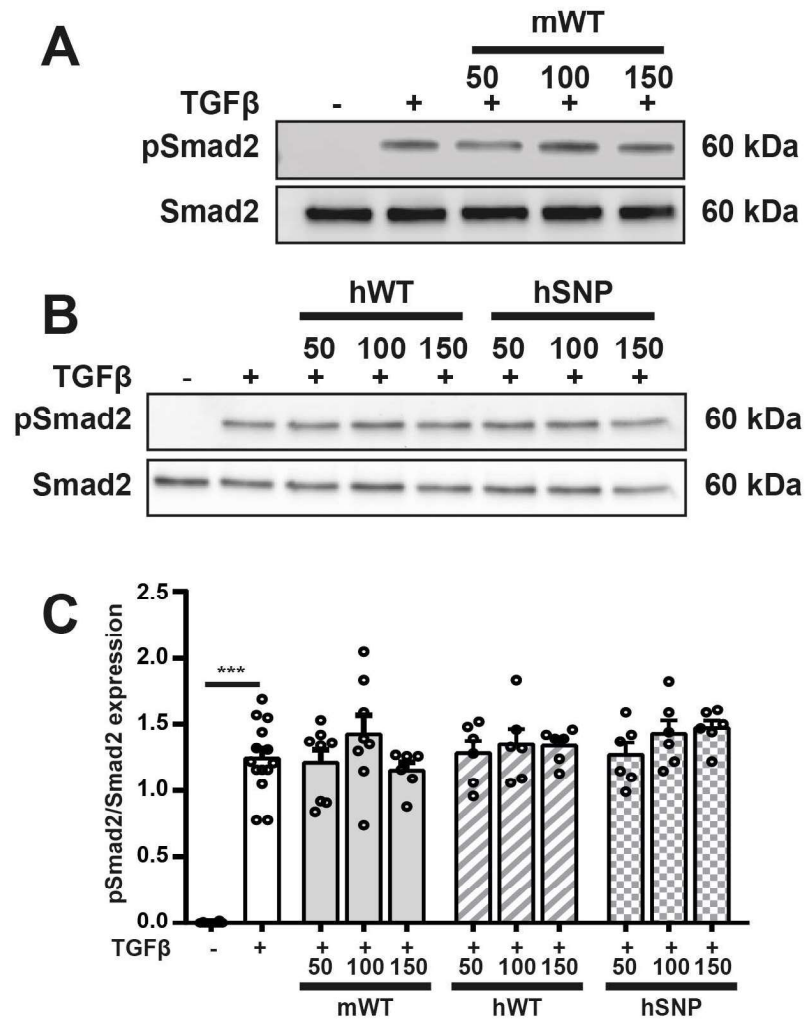


Figure 27 Effect of HtrA1 variants on paracrine TGF- β signaling

BV-2 cells were treated with TGF- β in the presence and absence of murine (**A**) and human (**B**) HtrA1 variants in the concentration of 50, 100 and 150 ng/ml for 3 hours. Representative Western blots from at least six independent experiments are shown. Densitometric analysis of Western blots shown in A and B (**C**). Treatment of microglia cells with 1 ng/ml TGF- β resulted in significant increase in pSmad2. However, stimulation with HtrA1 variants did not change levels of pSmad2. Values are presented as mean \pm SEM. $N \geq 6$ /group, with *** $p \leq 0.001$.

4 Discussion

The initial microglia response is vital and beneficial for retinal homeostasis. However, overshooting reactivity owing to environmental risk factors and genetic mutations need to be controlled in order to preserve retinal integrity during AMD disease pathogenesis. Hence, therapeutic approaches should aim to preserve the homeostatic function of microglia. On the search for novel immunomodulatory compounds the present study focused on genetic studies which found high correlation between polymorphisms in factors of the complement system and AMD as well as serine protease HTRA1 variants and AMD. The aim was to evaluate the role of complement anaphylatoxin receptors C3aR and C5aR in the retina during degeneration with particular focus on microglia. Similarly, the potential of HtrA1 to inhibit microglial TGF- β signaling *in vitro* was tested.

4.1. Light-induced retinal degeneration as model for dry AMD

In order to study AMD disease pathogenesis and to develop therapeutic compounds multiple animal models have been developed. However, being a complex disease involving genetic and environmental risk factors, as well as the anatomy of the human macula, it remains a challenge to mimic the features seen in AMD in rodent models. Despite the plethora of rodent models, none was yet found which echoes the human form in all its facets (Pennesi et al, 2012). Genetic models, which employ for instance the deficient CFH activity, only exhibit a disease phenotype after 2 years (Coffey et al, 2007). Similarly, mice over-expressing HtrA1 demonstrate AMD like features after one year when additionally exposed to cigarette smoke (Nakayama et al, 2014). In another HtrA1 overexpressing mouse only very subtle changes were visible when applying transmission electron microscopy (Vierkotten et al, 2011).

The inducible LD model for rodents has proven to be useful tool for the evaluation of photoreceptor demise and microgliosis. The steady and synchronized cell death and fast progression provides the opportunity to test therapeutic compounds. Since extended exposure to light involves the risk for developing retinal degeneration such as in AMD patients, the LD model itself is not artificial (Taylor et al, 1992; Tomany et al, 2004). The susceptibility

for light-induced damage depends on the retinoid isomerohydrolase (RPE65) protein. RPE65 is expressed in the RPE and crucial for the retinoid cycle where it is involved in regeneration of 11-cis-retinal from all-trans-retinal (Moiseyev et al, 2005). It has been found that C57BL/6J mice have a reduced LD susceptibility when compared to BALB/c mice. This is explained by an Rpe65 variation present in C57BL/6J mice where methionine instead of leucine is present at amino acid position 450 (L450M) (Wenzel et al, 2001). As a consequence, levels of Rpe65 are very low, resulting in decreased rhodopsin regeneration kinetics. In contrast, the Rpe65 M450L sequence is present in most species, which have a fast regeneration kinetic for rhodopsin and a high susceptibility towards LD (Danciger et al, 2000). Similarly, in BALB/c mice high amounts of the Rpe65 protein were detected (Wenzel et al, 2001). Most likely, the excessive bleaching of rhodopsin results in accumulation of retinoid metabolites and toxic byproducts which ultimately lead to photoreceptor demise (Wenzel et al, 2005).

Photoreceptor death can functionally be assessed by recording scotopic and photopic ERGs. The *ex vivo* ERG measurements of retinæ from mice subjected to LD demonstrated a reduction of a-wave and b-wave amplitude and implicit times when compared to control. The scotopic a-wave, which reflects rod photoreceptor function, remained significantly reduced, while interestingly, the b-wave amplitude recovered to some extent at 7 days post LD. Reduction in a-wave amplitude and implicit time stem from a reduced sensitivity of photoreceptor cells towards the stimulus, as expected after LD. The signal of the b-wave originates mainly from the depolarization of bipolar cells postsynaptic to photoreceptor cells and affected by other neuronal and glial cells. This restored signal hints towards increased input from surviving cone photoreceptor cells as it is was described in zebrafish (McGinn et al, 2018). However, these speculations need further validation.

Furthermore, the presence of HF in SD-OCT scans was analyzed. Indeed, HF were detected in mice which were subjected to LD. Similar to human AMD patients, the number of HF increased significantly after LD. However, no correlation between HF number and damage severity was evident. Even more, HF number demonstrate high standard deviations making it an unsuitable marker for disease severity in the rodent LD model. In contrast, in studies with AMD patients a positive correlation between HF number and disease severity as well

as inflammation was seen (Frizziero et al, 2016; Niu et al, 2017). Reasonably, the question on the origin of these HF arises. Despite the attempts undertaken here it remains uncertain whether the HF seen in the OCT scans are the Iba1-positive spots that were relocated in the cryo sections. The sizes of the HF in OCT scans match the size of MP (Saito et al, 2013) but also of migrating RPE cells (Christenbury et al, 2013; Coscas et al, 2013; Pang et al, 2015). To be entirely certain, further advancement of the SD-OCT tool is required. The combination of transgenic mouse lines with fluorescent labeling of microglia and the possibility to detect these in the B-scans could provide better evidence. Only then, immunomodulatory and microglia targeted therapy could be easily assessed using non-invasive SD-OCT imaging.

4.2. Role of C3aR and C5aR in microglia during inflammation

Unrestrained complement activation due to polymorphisms in genes coding for complement factors is considered as a risk factor for developing AMD. Particularly, enrichment of the anaphylatoxins C3a and C5a resulting from excessive alternative pathway activation is evident in AMD patients (Reynolds et al, 2009; Schick et al, 2017). Interestingly, complement activation further augments immune responses in the retina which aggravates neuron demise. Receptors for these anaphylatoxins are Gi protein coupled (Rollins et al, 1991) and are mainly expressed on myeloid cells (Benard et al, 2004; Gasque et al, 1998; Lacy et al, 1995).

In the current study, increased C3aR and C5aR expression was evident in two independent microglia cell lines upon stimulation with pro-inflammatory agents. Furthermore, increased expression of C3, C3aR and C5aR were observed upon LD when compared to control. Expression peaked in the first two days following LD and decreased on the third and fourth day post LD. Interestingly, the sole expression site of C3aR and C5aR in the retina was found to be in microglia. These results are in line with earlier observations where, during inflammatory conditions, e.g. experimental allergic encephalitis, C3aR and C5aR expression was elevated on microglia and infiltrating macrophages (Davoust et al, 1999; Müller-Ladner et al, 1996; Van Beek et al, 2000). Hence, in very recent studies, researchers tested the

therapeutic potential of anaphylatoxin receptor blockers in nAMD models, though mostly concentrating on C5aR. C5a was found to increase and mediate VEGF secretion in a human retinal pigmented epithelial cell line (Cortright et al, 2009). Furthermore, it was found, that CNV resulted in an increase of IL-17 production by C5aR-expressing T-cells (Coughlin et al, 2016). Systemic administration of anti-C5a-blocking antibodies blunted IL-17 levels concomitant with reduced CNV size (Brockmann et al, 2015; Coughlin et al, 2016). More interestingly, two recently published studies investigated the potential of C5a elimination in models for dry AMD, since C5a was also found to be a chemoattractant for microglia (Song et al, 2017; Toomey et al, 2018b). Song and colleagues compared the number of Iba1-positive microglia in the retina of C3aR- and C5aR-deficient mice. Prior LD no difference in microglia number was evident. However, microglial response following LD was impaired in mice lacking C5aR but not C3aR (Song et al, 2017). Similarly, in mice lacking Cfh which were fed with high fat diet and developed dry AMD-like features, anti-C5a therapy resulted in reduced microglia recruitment. However, other AMD-like pathologies, including RPE damage and functional vision loss were not changed after immunotherapy targeting C5a (Toomey et al, 2018b).

The present results suggest that not only C5aR, but also C3aR should serve as a target for an immunomodulatory approach, since the latter also serves as a chemoattractant for microglia. Additionally, Schraufstatter and colleagues found that C3aR translocates into the nucleus following C3a stimulation (Schraufstatter et al, 2009). Subsequently, prolonged phosphorylation and nuclear translocation of the mitogen-activated protein kinase (MAPK) extracellular signal-regulated kinase (ERK) 1/2 was found, which leads to the induction of pro-inflammatory gene expression (Dang et al, 2014; Kyriakis & Avruch, 2001; Schulte & Fredholm, 2003). Hence, a dual therapy approach would imply the inhibition of microglia recruitment concomitant with a suppression of pro-inflammatory gene expression when blocking C3aR and C5aR.

4.3. Effect of HTRA1 variants on TGF- β signaling in microglia

Numerous studies found strong correlation between polymorphisms located in the HTRA1 gene and AMD (Fritsche et al, 2016). However, limited understanding of the pathophysiological role hinders the correct interpretation of genetic data. Faulty HtrA1 expression and the subsequent dysregulated TGF- β signaling have been identified as the underlying mechanism of multiple diseases (Oka et al, 2004). Being a potent silencer of microgliosis, neutralization of TGF- β by HtrA1 could explain tissue-harming inflammation, which is a major characteristic seen in the retina of AMD patients. Here, the effect of AMD-associated HtrA1 isoforms on microglia was tested. Surprisingly, the results show no involvement of HtrA1 in the TGF- β signaling pathway of microglia.

In order to adapt the situation found in AMD patients first eukaryotic wildtype, proteolytic inactive and AMD-associated HtrA1 variants were expressed and purified. The immunoblot demonstrated bands corresponding to the full length protein concomitant with smaller fragments which were partly absent in the enzymatic inactive variant and thus could be attributed to autolytic cleavage. Also, several smaller fragments were present across all variants, which were in agreement with earlier observations (Lorenzi et al, 2013; Risør et al, 2014). Furthermore, variants, apart from mS328A and hS328A, were proteolytically active, as expected. Interestingly, increased catalytic activity of hSNP was observed. This result contrasts earlier findings by Jacobo et al., who reported reduced activity of the same isoform when compared to the WT protein (Jacobo et al, 2013). It is noteworthy, that the activity assay was carried out differently. Jacobo et al. used conditioned media from transiently transfected HEK293T cells that contained HtrA1, supplemented it with protease inhibitors and tested for the ability to proteolyze FITC-labeled casein. Rather, similar proteolytic activity across all active isoforms was expected, since earlier examinations have demonstrated comparable catalytic activities of full-length HtrA1 and HtrA1 lacking the N-domain, where the synonymous SNPs are located (Eigenbrot et al, 2012). The reproducible increase in enzymatic activity for the hSNP isoform can thus be attributed to the risk alleles. Secondly, IFN- γ challenged primary murine microglia were treated with TGF- β in order to induce TGF- β dependent microglial quiescence. Here, TGF- β treatment significantly

inhibited IFN- γ -mediated iNos and Tnf- α mRNA production and morphological shift towards an amoeboid phenotype. Similar findings were observed in the BV-2 murine microglia cell line. The anti-inflammatory effect of TGF- β involves the downregulation of the STAT1 and STAT2, the downstream effectors of type II interferon receptors, while negative regulators of the IFN- γ pathway, including SOCS2 and SOCS6, were increased (Platanias, 2005; Zhou et al, 2015). Furthermore, TGF- β scavenges INF- γ mediated NO release via negative regulating of MAPK including ERK and p38 downstream signaling (Herrera-Molina et al, 2012). Furthermore, importance of TGF- β signaling in ocular physiology was demonstrated in a study, where deletion of TGF- β signaling in newborn mice induced microgliosis concomitant with abnormal vessel including retinal hemorrhages and microaneurysms (Braunger et al, 2015).

Faulty regulation of TGF- β signaling by HtrA1 was discovered to be the underlying pathomechanism of several diseases. It was hypothesized, that similar mechanisms may account for AMD ontogenesis, since SNPs in the promotor region of HtrA1 lead to an increase in protein expression in the retina. Interestingly, HtrA1 expression was found to be increased under inflammatory conditions in *in vitro* and *in vivo* (Hou et al, 2013; Rangaraju et al, 2018). These findings point towards an involvement of HtrA1 in inflammatory conditions. However, no significant inhibition of microglial TGF- β signaling was found when HtrA1 was applied in high concentrations, which correspond to levels measured in the aqueous humor of AMD patients (Tosi et al, 2017). After all, the inflammation may be independent from HtrA1 activity. This may be explained by the possibility that HtrA1 indirectly inhibits TGF- β signaling through digestion of extracellular matrix proteins (Murwantoko et al, 2004; Oka et al, 2004). Nevertheless, HtrA1 overexpression did not induce changes in TGF- β expression levels in the RPE/choroid of mice (Vierkotten et al, 2011). Though, not examined in the retina, these findings may point towards a differential and cell specific role of HtrA1.

Additionally, the present results show no differences between the WT and AMD-associated HtrA1 isoform regarding TGF- β signaling. The synonymous AMD-associated SNPs are located in the IGF-1 binding domain, and indeed, hSNP was found to have reduced ability to bind IGF-1 (Jacobo et al, 2013). More interestingly, the hSNP isoform was found to bind less

efficiently to TGF- β and be less proteolytically active (Friedrich et al, 2015). Despite the fact that synonymous SNPs do not change the amino acid sequence in proteins they can interrupt the formation of correct mRNA secondary structures, reduce translational accuracy and speed, and even alter the start of transcription (Hunt et al, 2009; Hunt et al, 2014; Im & Choi, 2017; Komar, 2007). However, the previously reported finding is challenged by the present results. Nevertheless, supporting evidence comes from a study, in which recombinant haplotypes in the currently largest available data set of AMD were analyzed (Grassmann et al, 2017). The authors demonstrate that genetic variants in or close to ARMS2 but not HTRA1 are responsible for disease susceptibility at the 10q26 locus. By this mean, the involvement of HTRA1 variants rs1049331 and rs2293870 was excluded. ARMS2 is a primate-specific gene only, hindering the analysis in rodents due to the lack of a homologous gene (Francis et al, 2008; Pahl et al, 2012). Furthermore, studies on the localization of ARMS2 demonstrate conflicting results (Fritsche et al, 2008; Kanda et al, 2007; Wang et al, 2009b). Proposed function of ARMS2 include regulator of complement mediated opsonization by binding to the surfaces of dead cells and anchoring properdin resulting in phagocytosis (Micklisch et al, 2017). More importantly, ARMS2 was found to be expressed on human monocytes and microglia. Strikingly, immune cells derived from patients homozygous for the ARMS2 AMD risk variant (rs10490924) lack the expression of the protein.

4.4. Perspective

The current study aids to uncover the relationship between heritability due to mutations and microglia mediated inflammation in AMD. In particular, the potential to use data on AMD-associated polymorphisms for the development of immunomodulatory compounds was investigated.

Indeed, microglia play an exclusive role in anaphylatoxin signaling by being the sole cells to express their receptors in the retina. Even more, increased expression during retinal degeneration is evident. The current findings together with published results strongly support the hypothesis that C3aR and C5aR targeted therapy could aid to slow down microgliosis and disease pathogenesis. However, further experiments using depletion strategies and pharmacologic blockade of the anaphylatoxin receptors should provide crucial information on the therapeutic potential.

For the second part of the study the results suggest an absence of HtrA1 mediated TGF- β pathway inhibition in microglia. This implicates, that HtrA1 does not induce inflammation via activation of microglia. Latest and promising studies hint towards a crucial role of ARMS2 in AMD disease pathogenesis, however, the exact functional role of this protein needs further scrutinizing.

Bibliography

Abdelsalam A, Del Priore L, Zarbin MA (1999) Drusen in age-related macular degeneration: pathogenesis, natural course, and laser photocoagulation-induced regression. *Survey of ophthalmology* 44: 1-29

Adams MK, Simpson JA, Aung KZ, Makeyeva GA, Giles GG, English DR, Hopper J, Guymer RH, Baird PN, Robman LD (2011) Abdominal obesity and age-related macular degeneration. *American journal of epidemiology* 173: 1246-1255

Akhtar-Schäfer I, Wang L, Krohne TU, Xu H, Langmann T (2018) Modulation of three key innate immune pathways for the most common retinal degenerative diseases. *EMBO molecular medicine*

Alexander C, Rietschel ET (2001) Bacterial lipopolysaccharides and innate immunity. *Journal of endotoxin research* 7: 167-202

Altay L, Scholz P, Schick T, Felsch M, Hoyng CB, den Hollander AI, Langmann T, Fauser S (2016) Association of Hyperreflective Foci Present in Early Forms of Age-Related Macular Degeneration With Known Age-Related Macular Degeneration Risk Polymorphisms. *Invest Ophthalmol Vis Sci* 57: 4315-4320

Ambati J, Atkinson JP, Gelfand BD (2013) Immunology of age-related macular degeneration. *Nat Rev Immunol* 13

Anderson DH, Radeke MJ, Gallo NB, Chapin EA, Johnson PT, Curletti CR, Hancox LS, Hu J, Ebright JN, Malek G, Hauser MA, Rickman CB, Bok D, Hageman GS, Johnson LV (2010) The pivotal role of the complement system in aging and age-related macular degeneration: hypothesis re-visited. *Prog Retin Eye Res* 29: 95-112

Andriessen EM, Wilson AM, Mawambo G, Dejda A, Miloudi K, Sennlaub F, Sapienza P (2016) Gut microbiota influences pathological angiogenesis in obesity-driven choroidal neovascularization. *EMBO molecular medicine*

Ardeljan D, Chan CC (2013) Aging is not a disease: distinguishing age-related macular degeneration from aging. *Prog Retin Eye Res* 37: 68-89

Baldi A, De Luca A, Morini M, Battista T, Felsani A, Baldi F, Catricala C, Amantea A, Noonan DM, Albini A, Natali PG, Lombardi D, Paggi MG (2002) The HtrA1 serine protease is down-regulated

during human melanoma progression and represses growth of metastatic melanoma cells. *Oncogene* 21: 6684-6688

Beaufort N, Scharrer E, Kremmer E, Lux V, Ehrmann M, Huber R, Houlden H, Werring D, Haffner C, Dichgans M (2014) Cerebral small vessel disease-related protease HtrA1 processes latent TGF-beta binding protein 1 and facilitates TGF-beta signaling. *Proceedings of the National Academy of Sciences of the United States of America* 111: 16496-16501

Benard M, Gonzalez BJ, Schouft MT, Falluel-Morel A, Vaudry D, Chan P, Vaudry H, Fontaine M (2004) Characterization of C3a and C5a receptors in rat cerebellar granule neurons during maturation. Neuroprotective effect of C5a against apoptotic cell death. *J Biol Chem* 279: 43487-43496

Bhakdi S, Tranum-Jensen J (1988) Damage to cell membranes by pore-forming bacterial cytolysins. *Progress in allergy* 40: 1-43

Bhutto I, Luty G (2012) Understanding age-related macular degeneration (AMD): relationships between the photoreceptor/retinal pigment epithelium/Bruch's membrane/choriocapillaris complex. *Molecular aspects of medicine* 33: 295-317

Boje KM, Arora PK (1992) Microglial-produced nitric oxide and reactive nitrogen oxides mediate neuronal cell death. *Brain research* 587

Bonilha VL (2014) Retinal pigment epithelium (RPE) cytoskeleton in vivo and in vitro. *Experimental eye research* 126: 38-45

Bora NS, Jha P, Lyzogubov VV, Kaliappan S, Liu J, Tytarenko RG, Fraser DA, Morgan BP, Bora PS (2010) Recombinant membrane-targeted form of CD59 inhibits the growth of choroidal neovascular complex in mice. *J Biol Chem* 285: 33826-33833

Bowmaker JK, Dartnall HJ (1980) Visual pigments of rods and cones in a human retina. *The Journal of Physiology* 298: 501-511

Braunger BM, Leimbeck SV, Schlecht A, Volz C, Jagle H, Tamm ER (2015) Deletion of ocular transforming growth factor beta signaling mimics essential characteristics of diabetic retinopathy. *The American journal of pathology* 185: 1749-1768

Brionne TC, Teseur I, Masliah E, Wyss-Coray T (2003) Loss of TGF-beta 1 leads to increased neuronal cell death and microgliosis in mouse brain. *Neuron* 40: 1133-1145

Brockmann C, Brockmann T, Dege S, Busch C, Kociok N, Vater A, Klusmann S, Strauss O, Jousen AM (2015) Intravitreal inhibition of complement C5a reduces choroidal neovascularization in mice. *Graefes Arch Clin Exp Ophthalmol* 253: 1695-1704

Buschini E, Piras A, Nuzzi R, Vercelli A (2011) Age related macular degeneration and drusen: neuroinflammation in the retina. *Progress in neurobiology* 95: 14-25

- Cai H, Zhou X, Dougherty GG, Reddy RD, Haas GL, Montrose DM, Keshavan M, Yao JK (2018) Pregnenolone-progesterone-allopregnanolone pathway as a potential therapeutic target in first-episode antipsychotic-naïve patients with schizophrenia. *Psychoneuroendocrinology* 90: 43-51
- Caicedo A, Espinosa-Heidmann DG, Piña Y, Hernandez EP, Cousins SW (2005) Blood-derived macrophages infiltrate the retina and activate Muller glial cells under experimental choroidal neovascularization. *Experimental eye research* 81: 38-47
- Calippe B, Augustin S, Beguier F, Charles-Messance H, Poupel L, Conart JB, Hu SJ, Lavalette S, Fauvet A, Rayes J, Levy O, Raoul W, Fitting C, Deneffe T, Pickering MC, Harris C, Jorieux S, Sullivan PM, Sahel JA, Karoyan P *et al* (2017) Complement Factor H Inhibits CD47-Mediated Resolution of Inflammation. *Immunity* 46: 261-272
- Canfield AE, Hadfield KD, Rock CF, Wylie EC, Wilkinson FL (2007) HtrA1: a novel regulator of physiological and pathological matrix mineralization? *Biochemical Society Transactions* 35: 669-671
- Chen M, Forrester JV, Xu H (2007) Synthesis of complement factor H by retinal pigment epithelial cells is down-regulated by oxidized photoreceptor outer segments. *Experimental eye research* 84: 635-645
- Chen M, Muckersie E, Forrester JV, Xu H (2010) Immune activation in retinal aging: a gene expression study. *Invest Ophthalmol Vis Sci* 51: 5888-5896
- Chen M, Xu H (2015) Parainflammation, chronic inflammation, and age-related macular degeneration. *J Leukoc Biol* 98: 713-725
- Chen M, Zhao J, Luo C, Pandi SP, Penalva RG, Fitzgerald DC, Xu H (2012) Para-inflammation-mediated retinal recruitment of bone marrow-derived myeloid cells following whole-body irradiation is CCL2 dependent. *Glia* 60: 833-842
- Chien J, Aletti G, Baldi A, Catalano V, Muretto P, Keeney GL, Kalli KR, Staub J, Ehrmann M, Cliby WA, Lee YK, Bible KC, Hartmann LC, Kaufmann SH, Shridhar V (2006) Serine protease HtrA1 modulates chemotherapy-induced cytotoxicity. *Journal of Clinical Investigation* 116: 1994-2004
- Chien J, He X, Shridhar V (2009a) Identification of tubulins as substrates of serine protease HtrA1 by mixture-based oriented peptide library screening. *Journal of cellular biochemistry* 107: 253-263
- Chien J, Ota T, Aletti G, Shridhar R, Boccellino M, Quagliuolo L, Baldi A, Shridhar V (2009b) Serine protease HtrA1 associates with microtubules and inhibits cell migration. *Molecular and cellular biology* 29: 4177-4187
- Chien J, Staub J, Hu SI, Erickson-Johnson MR, Couch FJ, Smith DI, Crowl RM, Kaufmann SH, Shridhar V (2004) A candidate tumor suppressor HtrA1 is downregulated in ovarian cancer. *Oncogene* 23: 1636-1644

- Chirco KR, Tucker BA, Stone EM, Mullins RF (2016) Selective accumulation of the complement membrane attack complex in aging choriocapillaris. *Experimental eye research* 146: 393-397
- Chiu CJ, Taylor A (2011) Dietary hyperglycemia, glycemic index and metabolic retinal diseases. *Prog Retin Eye Res* 30: 18-53
- Chow A, Brown BD, Merad M (2011) Studying the mononuclear phagocyte system in the molecular age. *Nat Rev Immunol* 11: 788-798
- Christenbury JG, Folgar FA, O'Connell R, Chiu SJ, Farsiu S, Toth CA (2013) Progression of intermediate age-related macular degeneration with proliferation and inner retinal migration of hyperreflective foci. *Ophthalmology* 120: 1038-1045
- Cilenti L, Lee Y, Hess S, Srinivasula S, Park KM, Junqueira D, Davis H, Bonventre JV, Alnemri ES, Zervos AS (2003) Characterization of a novel and specific inhibitor for the pro-apoptotic protease Omi/HtrA2. *J Biol Chem* 278: 11489-11494
- Clausen T, Kaiser M, Huber R, Ehrmann M (2011) HTRA proteases: regulated proteolysis in protein quality control. *Nat Rev Mol Cell Biol* 12: 152-162
- Clausen T, Southan C, Ehrmann M (2002) The HtrA family of proteases: implications for protein composition and cell fate. *Mol Cell* 10: 443-455
- Coffey PJ, Gias C, McDermott CJ, Lundh P, Pickering MC, Sethi C, Bird A, Fitzke FW, Maass A, Chen LL, Holder GE, Luthert PJ, Salt TE, Moss SE, Greenwood J (2007) Complement factor H deficiency in aged mice causes retinal abnormalities and visual dysfunction. *Proceedings of the National Academy of Sciences of the United States of America* 104: 16651-16656
- Colijn JM, Buitendijk GHS, Prokofyeva E, Alves D, Cachulo ML, Khawaja AP, Cougnard-Gregoire A, Merle BMJ, Korb C, Erke MG, Bron A, Anastasopoulos E, Meester-Smoor MA, Segato T, Piermarocchi S, de Jong P, Vingerling JR, Topouzis F, Creuzot-Garcher C, Bertelsen G *et al* (2017) Prevalence of Age-Related Macular Degeneration in Europe: The Past and the Future. *Ophthalmology* 124: 1753-1763
- Combadiere C, Feumi C, Raoul W, Keller N, Rodero M, Pezard A, Lavalette S, Houssier M, Jonet L, Picard E (2007) CX3CR1-dependent subretinal microglia cell accumulation is associated with cardinal features of age-related macular degeneration. *J Clin Invest* 117
- Conley YP, Jakobsdottir J, Mah T, Weeks DE, Klein R, Kuller L, Ferrell RE, Gorin MB (2006) CFH, ELOVL4, PLEKHA1 and LOC387715 genes and susceptibility to age-related maculopathy: AREDS and CHS cohorts and meta-analyses. *Human molecular genetics* 15: 3206-3218
- Cortright DN, Meade R, Waters SM, Chenard BL, Krause JE (2009) C5a, but not C3a, increases VEGF secretion in ARPE-19 human retinal pigment epithelial cells. *Current eye research* 34: 57-61

- Coscas G, De Benedetto U, Coscas F, Li Calzi CI, Vismara S, Roudot-Thoraval F, Bandello F, Souied E (2013) Hyperreflective dots: a new spectral-domain optical coherence tomography entity for follow-up and prognosis in exudative age-related macular degeneration. *Ophthalmologica Journal international d'ophtalmologie International journal of ophthalmology Zeitschrift fur Augenheilkunde* 229: 32-37
- Coughlin B, Schnabolk G, Joseph K, Raikwar H, Kunchithapautham K, Johnson K, Moore K, Wang Y, Rohrer B (2016) Connecting the innate and adaptive immune responses in mouse choroidal neovascularization via the anaphylatoxin C5a and gammadeltaT-cells. *Scientific reports* 6: 23794
- Crabb JW, Miyagi M, Gu X, Shadrach K, West KA, Sakaguchi H, Kamei M, Hasan A, Yan L, Rayborn ME, Salomon RG, Hollyfield JG (2002) Drusen proteome analysis: an approach to the etiology of age-related macular degeneration. *Proceedings of the National Academy of Sciences of the United States of America* 99
- Cummings M, Cunha-Vaz J (2008) Treatment of neovascular age-related macular degeneration in patients with diabetes. *Clinical ophthalmology (Auckland, NZ)* 2: 369-375
- Cunha-Vaz J, Bernardes R, Lobo C (2011) Blood-retinal barrier. *European journal of ophthalmology* 21 Suppl 6: S3-9
- Damani MR, Zhao L, Fontainhas AM, Amaral J, Fariss RN, Wong WT (2011) Age-related alterations in the dynamic behavior of microglia. *Aging cell* 10: 263-276
- Danciger M, Matthes MT, Yasamura D, Akhmedov NB, Rickabaugh T, Gentleman S, Redmond TM, La Vail MM, Farber DB (2000) A QTL on distal chromosome 3 that influences the severity of light-induced damage to mouse photoreceptors. *Mammalian genome : official journal of the International Mammalian Genome Society* 11: 422-427
- Dang Y, Xu Y, Wu W, Li W, Sun Y, Yang J, Zhu Y, Zhang C (2014) Tetrandrine suppresses lipopolysaccharide-induced microglial activation by inhibiting NF-kappaB and ERK signaling pathways in BV2 cells. *PLoS One* 9: e102522
- Datta S, Cano M, Ebrahimi K, Wang L, Handa JT (2017) The impact of oxidative stress and inflammation on RPE degeneration in non-neovascular AMD. *Prog Retin Eye Res* 60: 201-218
- Davis AE, 3rd, Mejia P, Lu F (2008) Biological activities of C1 inhibitor. *Molecular immunology* 45: 4057-4063
- Davoust N, Jones J, Stahel PF, Ames RS, Barnum SR (1999) Receptor for the C3a anaphylatoxin is expressed by neurons and glial cells. *Glia* 26: 201-211
- De Luca A, De Falco M, De Luca L, Penta R, Shridhar V, Baldi F, Campioni M, Paggi MG, Baldi A (2004) Pattern of expression of HtrA1 during mouse development. *The journal of histochemistry and cytochemistry : official journal of the Histochemistry Society* 52: 1609-1617

- De Luca A, De Falco M, Severino A, Campioni M, Santini D, Baldi F, Paggi MG, Baldi A (2003) Distribution of the serine protease HtrA1 in normal human tissues. *The journal of histochemistry and cytochemistry : official journal of the Histochemistry Society* 51: 1279-1284
- DeAngelis MM, Ji F, Adams S, Morrison MA, Harring AJ, Sweeney MO, Capone A, Miller JW, Dryja TP, Ott J, Kim IK (2008) Alleles in the HtrA Serine Peptidase 1 Gene Alter the Risk of Neovascular Age-Related Macular Degeneration. *Ophthalmology* 115: 1209-1215.e1207
- Dewan A, Liu M, Hartman S, Zhang SS, Liu DT, Zhao C, Tam PO, Chan WM, Lam DS, Snyder M, Barnstable C, Pang CP, Hoh J (2006) HTRA1 promoter polymorphism in wet age-related macular degeneration. *Science (New York, NY)* 314: 989-992
- Doyle SL, Campbell M, Ozaki E, Salomon RG, Mori A, Kenna PF, Farrar GJ, Kiang AS, Humphries MM, Lavelle EC, O'Neill LA, Hollyfield JG, Humphries P (2012) NLRP3 has a protective role in age-related macular degeneration through the induction of IL-18 by drusen components. *Nature medicine* 18: 791-798
- Edwards AO, Ritter R, 3rd, Abel KJ, Manning A, Panhuysen C, Farrer LA (2005) Complement factor H polymorphism and age-related macular degeneration. *Science (New York, NY)* 308: 421-424
- Eigenbrot C, Ultsch M, Lipari MT, Moran P, Lin SJ, Ganesan R, Quan C, Tom J, Sandoval W, van Lookeren Campagne M, Kirchhofer D (2012) Structural and functional analysis of HtrA1 and its subdomains. *Structure (London, England : 1993)* 20: 1040-1050
- Elmore MR, Najafi AR, Koike MA, Dagher NN, Spangenberg EE, Rice RA, Kitazawa M, Matusow B, Nguyen H, West BL, Green KN (2014) Colony-stimulating factor 1 receptor signaling is necessary for microglia viability, unmasking a microglia progenitor cell in the adult brain. *Neuron* 82: 380-397
- Espinosa-Heidmann DG, Suner IJ, Catanuto P, Hernandez EP, Marin-Castano ME, Cousins SW (2006) Cigarette smoke-related oxidants and the development of sub-RPE deposits in an experimental animal model of dry AMD. *Invest Ophthalmol Vis Sci* 47: 729-737
- Fausser S, Viebahn U, Muether PS (2015) Intraocular and systemic inflammation-related cytokines during one year of ranibizumab treatment for neovascular age-related macular degeneration. *Acta ophthalmologica* 93: 734-738
- Ferrer-Martin RM, Martin-Oliva D, Sierra-Martin A, Carrasco MC, Martin-Estebane M, Calvente R, Martin-Guerrero SM, Marin-Teva JL, Navascues J, Cuadros MA (2015) Microglial Activation Promotes Cell Survival in Organotypic Cultures of Postnatal Mouse Retinal Explants. *PLoS One* 10: e0135238
- Ferris FL, Davis MD, Clemons TE, Lee LY, Chew EY, Lindblad AS, Milton RC, Bressler SB, Klein R (2005) A simplified severity scale for age-related macular degeneration: AREDS Report No. 18. *Archives of ophthalmology (Chicago, Ill : 1960)* 123: 1570-1574

- Fett AL, Hermann MM, Muether PS, Kirchhof B, Fauser S (2012) Immunohistochemical localization of complement regulatory proteins in the human retina. *Histol Histopathol* 27: 357-364
- Fischer MD, Huber G, Beck SC, Tanimoto N, Muehlfriedel R, Fahl E, Grimm C, Wenzel A, Reme CE, van de Pavert SA, Wijnholds J, Pacal M, Bremner R, Seeliger MW (2009) Noninvasive, in vivo assessment of mouse retinal structure using optical coherence tomography. *PLoS One* 4: e7507
- Fisher SA, Abecasis GR, Yashar BM, Zarepari S, Swaroop A, Iyengar SK, Klein BEK, Klein R, Lee KE, Majewski J, Schultz DW, Klein ML, Seddon JM, Santangelo SL, Weeks DE, Conley YP, Mah TS, Schmidt S, Haines JL, Pericak-Vance MA *et al* (2005) Meta-analysis of genome scans of age-related macular degeneration. *Human molecular genetics* 14: 2257-2264
- Framme C, Wolf S, Wolf-Schnurrbusch U (2010) Small dense particles in the retina observable by spectral-domain optical coherence tomography in age-related macular degeneration. *Invest Ophthalmol Vis Sci* 51: 5965-5969
- Francis PJ, Appukuttan B, Simmons E, Landauer N, Stoddard J, Hamon S, Ott J, Ferguson B, Klein M, Stout JT, Neuringer M (2008) Rhesus monkeys and humans share common susceptibility genes for age-related macular disease. *Human molecular genetics* 17: 2673-2680
- Friedman DS, O'Colmain BJ, Munoz B, Tomany SC, McCarty C, de Jong PT, Nemesure B, Mitchell P, Kempen J (2004) Prevalence of age-related macular degeneration in the United States. *Archives of ophthalmology (Chicago, Ill : 1960)* 122: 564-572
- Friedrich U, Datta S, Schubert T, Plossl K, Schneider M, Grassmann F, Fuchshofer R, Tiefenbach KJ, Langst G, Weber BH (2015) Synonymous variants in HTRA1 implicated in AMD susceptibility impair its capacity to regulate TGF-beta signaling. *Human molecular genetics*
- Fritsche LG, Chen W, Schu M, Yaspan BL, Yu Y, Thorleifsson G, Zack DJ, Arakawa S, Cipriani V, Ripke S, Igo RP, Jr., Buitendijk GH, Sim X, Weeks DE, Guymer RH, Merriam JE, Francis PJ, Hannum G, Agarwal A, Armbrecht AM *et al* (2013) Seven new loci associated with age-related macular degeneration. *Nature genetics* 45: 433-439, 439e431-432
- Fritsche LG, Fariss RN, Stambolian D, Abecasis GR, Curcio CA, Swaroop A (2014) Age-related macular degeneration: genetics and biology coming together. *Annual review of genomics and human genetics* 15: 151-171
- Fritsche LG, Igl W, Bailey JN, Grassmann F, Sengupta S, Bragg-Gresham JL, Burdon KP, Hebbbring SJ, Wen C, Gorski M, Kim IK, Cho D, Zack D, Souied E, Scholl HP, Bala E, Lee KE, Hunter DJ, Sardell RJ, Mitchell P *et al* (2016) A large genome-wide association study of age-related macular degeneration highlights contributions of rare and common variants. *Nature genetics* 48: 134-143
- Fritsche LG, Loenhardt T, Janssen A, Fisher SA, Rivera A, Keilhauer CN, Weber BH (2008) Age-related macular degeneration is associated with an unstable ARMS2 (LOC387715) mRNA. *Nature genetics* 40: 892-896

- Frizziero L, Parrozzani R, Midena G, Miglionico G, Vujosevic S, Pilotto E, Midena E (2016) HYPERREFLECTIVE INTRARETINAL SPOTS IN RADIATION MACULAR EDEMA ON SPECTRAL DOMAIN OPTICAL COHERENCE TOMOGRAPHY. *Retina (Philadelphia, Pa)* 36: 1664-1669
- Fujita T (2002) Evolution of the lectin-complement pathway and its role in innate immunity. *Nat Rev Immunol* 2: 346-353
- Gal P, Barna L, Kocsis A, Zavodszky P (2007) Serine proteases of the classical and lectin pathways: similarities and differences. *Immunobiology* 212: 267-277
- Gasque P, Singhrao SK, Neal JW, Wang P, Sayah S, Fontaine M, Morgan BP (1998) The receptor for complement anaphylatoxin C3a is expressed by myeloid cells and nonmyeloid cells in inflamed human central nervous system: analysis in multiple sclerosis and bacterial meningitis. *J Immunol* 160: 3543-3554
- Gerth C (2009) The role of the ERG in the diagnosis and treatment of Age-Related Macular Degeneration. *Documenta ophthalmologica Advances in ophthalmology* 118: 63-68
- Ginhoux F, Greter M, Leboeuf M, Nandi S, See P, Gokhan S, Mehler MF, Conway SJ, Ng LG, Stanley ER, Samokhvalov IM, Merad M (2010) Fate mapping analysis reveals that adult microglia derive from primitive macrophages. *Science (New York, NY)* 330: 841-845
- Girard C, Liu S, Adams D, Lacroix C, Sineus M, Boucher C, Papadopoulos V, Rupprecht R, Schumacher M, Groyer G (2012) Axonal regeneration and neuroinflammation: roles for the translocator protein 18 kDa. *Journal of neuroendocrinology* 24: 71-81
- Gold B, Merriam JE, Zernant J, Hancox LS, Taiber AJ, Gehrs K, Cramer K, Neel J, Bergeron J, Barile GR, Smith RT, Hageman GS, Dean M, Allikmets R (2006) Variation in factor B (BF) and complement component 2 (C2) genes is associated with age-related macular degeneration. *Nature genetics* 38: 458-462
- Goldmann T, Wieghofer P, Muller PF, Wolf Y, Varol D, Yona S, Brendecke SM, Kierdorf K, Staszewski O, Datta M, Luedde T, Heikenwalder M, Jung S, Prinz M (2013) A new type of microglia gene targeting shows TAK1 to be pivotal in CNS autoimmune inflammation. *Nature neuroscience* 16: 1618-1626
- Gong D, Shi W, Yi S-j, Chen H, Groffen J, Heisterkamp N (2012) TGF β signaling plays a critical role in promoting alternative macrophage activation. *BMC Immunology* 13: 1-10
- Goumans MJ, Liu Z, ten Dijke P (2009) TGF-beta signaling in vascular biology and dysfunction. *Cell research* 19: 116-127
- Graham JR, Chamberland A, Lin Q, Li XJ, Dai D, Zeng W, Ryan MS, Rivera-Bermudez MA, Flannery CR, Yang Z (2013) Serine protease HTRA1 antagonizes transforming growth factor-beta

signaling by cleaving its receptors and loss of HTRA1 in vivo enhances bone formation. PLoS One 8: e74094

Grassmann F, Heid IM, Weber BH (2017) Recombinant Haplotypes Narrow the ARMS2/HTRA1 Association Signal for Age-Related Macular Degeneration. Genetics 205: 919-924

Grau S, Baldi A, Bussani R, Tian X, Stefanescu R, Przybylski M, Richards P, Jones SA, Shridhar V, Clausen T, Ehrmann M (2005) Implications of the serine protease HtrA1 in amyloid precursor protein processing. Proceedings of the National Academy of Sciences of the United States of America 102: 6021-6026

Grau S, Richards PJ, Kerr B, Hughes C, Caterson B, Williams AS, Junker U, Jones SA, Clausen T, Ehrmann M (2006) The role of human HtrA1 in arthritic disease. J Biol Chem 281: 6124-6129

Grimm C, Reme CE (2013) Light damage as a model of retinal degeneration. Methods in molecular biology (Clifton, NJ) 935: 87-97

Grimm C, Wenzel A, Hafezi F, Reme CE (2000) Gene expression in the mouse retina: the effect of damaging light. Molecular vision 6: 252-260

Gros P, Milder FJ, Janssen BJ (2008) Complement driven by conformational changes. Nat Rev Immunol 8: 48-58

Guilliams M, Ginhoux F, Jakubzick C, Naik SH, Onai N, Schraml BU, Segura E, Tussiwand R, Yona S (2014) Dendritic cells, monocytes and macrophages: a unified nomenclature based on ontogeny. Nature reviews Immunology 14: 571-578

Gupta N, Brown KE, Milam AH (2003) Activated microglia in human retinitis pigmentosa, late-onset retinal degeneration, and age-related macular degeneration. Experimental eye research 76: 463-471

Hageman GS, Anderson DH, Johnson LV, Hancox LS, Taiber AJ, Hardisty LI, Hageman JL, Stockman HA, Borchardt JD, Gehrs KM, Smith RJ, Silvestri G, Russell SR, Klaver CC, Barbazetto I, Chang S, Yannuzzi LA, Barile GR, Merriam JC, Smith RT *et al* (2005) A common haplotype in the complement regulatory gene factor H (HF1/CFH) predisposes individuals to age-related macular degeneration. Proceedings of the National Academy of Sciences of the United States of America 102: 7227-7232

Haines JL, Hauser MA, Schmidt S, Scott WK, Olson LM, Gallins P, Spencer KL, Kwan SY, Nouredine M, Gilbert JR, Schnetz-Boutaud N, Agarwal A, Postel EA, Pericak-Vance MA (2005) Complement factor H variant increases the risk of age-related macular degeneration. Science (New York, NY) 308: 419-421

Hammond CJ, Webster AR, Snieder H, Bird AC, Gilbert CE, Spector TD (2002) Genetic influence on early age-related maculopathy: a twin study. Ophthalmology 109: 730-736

- Hara K, Shiga A, Fukutake T, Nozaki H, Miyashita A, Yokoseki A, Kawata H, Koyama A, Arima K, Takahashi T, Ikeda M, Shiota H, Tamura M, Shimoe Y, Hirayama M, Arisato T, Yanagawa S, Tanaka A, Nakano I, Ikeda S-i *et al* (2009) Association of HTRA1 Mutations and Familial Ischemic Cerebral Small-Vessel Disease. *New England Journal of Medicine* 360: 1729-1739
- Harada T, Harada C, Kohsaka S, Wada E, Yoshida K, Ohno S, Mamada H, Tanaka K, Parada LF, Wada K (2002) Microglia–Müller Glia Cell Interactions Control Neurotrophic Factor Production during Light-Induced Retinal Degeneration. *The Journal of Neuroscience* 22: 9228-9236
- Helgason H, Sulem P, Duvvari MR, Luo H, Thorleifsson G, Stefansson H, Jonsdottir I, Masson G, Gudbjartsson DF, Walters GB, Magnusson OT, Kong A, Rafnar T, Kiemenev LA, Schoenmaker-Koller FE, Zhao L, Boon CJF, Song Y, Fauser S, Pei M *et al* (2013) A rare nonsynonymous sequence variant in C3 is associated with high risk of age-related macular degeneration. *Nature genetics* 45: 1371
- Herrera-Molina R, Flores B, Orellana JA, von Bernhardt R (2012) Modulation of interferon-gamma-induced glial cell activation by transforming growth factor beta1: a role for STAT1 and MAPK pathways. *Journal of neurochemistry* 123: 113-123
- Hoh Kam J, Lenassi E, Malik TH, Pickering MC, Jeffery G (2013) Complement component C3 plays a critical role in protecting the aging retina in a murine model of age-related macular degeneration. *The American journal of pathology* 183: 480-492
- Holland PM, Abramson RD, Watson R, Gelfand DH (1991) Detection of specific polymerase chain reaction product by utilizing the 5'----3' exonuclease activity of *Thermus aquaticus* DNA polymerase. *Proceedings of the National Academy of Sciences* 88: 7276-7280
- Holz FG, Sadda SR, Busbee B, Chew EY, Mitchell P, Tufail A, Brittain C, Ferrara D, Gray S, Honigberg L, Martin J, Tong B, Ehrlich JS, Bressler NM (2018) Efficacy and Safety of Lampalizumab for Geographic Atrophy Due to Age-Related Macular Degeneration: Chroma and Spectri Phase 3 Randomized Clinical Trials. *JAMA Ophthalmol* 136: 666-677
- Hoon M, Okawa H, Della Santina L, Wong ROL (2014) Functional architecture of the retina: Development and disease. *Progress in Retinal and Eye Research* 42: 44-84
- Hou Y, Lin H, Zhu L, Liu Z, Hu F, Shi J, Yang T, Shi X, Zhu M, Godley BF, Wang Q, Li Z, Zhao Y (2013) Lipopolysaccharide increases the incidence of collagen-induced arthritis in mice through induction of protease HTRA-1 expression. *Arthritis and rheumatism* 65: 2835-2846
- Huang Y, Xu Z, Xiong S, Qin G, Sun F, Yang J, Yuan TF, Zhao L, Wang K, Liang YX, Fu L, Wu T, So KF, Rao Y, Peng B (2018a) Dual extra-retinal origins of microglia in the model of retinal microglia repopulation. *Cell discovery* 4: 9
- Huang Y, Xu Z, Xiong S, Sun F, Qin G, Hu G, Wang J, Zhao L, Liang YX, Wu T, Lu Z, Humayun MS, So KF, Pan Y, Li N, Yuan TF, Rao Y, Peng B (2018b) Repopulated microglia are solely derived from the proliferation of residual microglia after acute depletion. *Nature neuroscience*

- Hume DA, Perry VH, Gordon S (1983) Immunohistochemical localization of a macrophage-specific antigen in developing mouse retina: phagocytosis of dying neurons and differentiation of microglial cells to form a regular array in the plexiform layers. *The Journal of cell biology* 97: 253-257
- Hunt R, Sauna ZE, Ambudkar SV, Gottesman MM, Kimchi-Sarfaty C (2009) Silent (synonymous) SNPs: should we care about them? *Methods in molecular biology* (Clifton, NJ) 578: 23-39
- Hunt RC, Simhadri VL, Iandoli M, Sauna ZE, Kimchi-Sarfaty C (2014) Exposing synonymous mutations. *Trends in genetics : TIG* 30: 308-321
- Huse M, Chen YG, Massague J, Kuriyan J (1999) Crystal structure of the cytoplasmic domain of the type I TGF beta receptor in complex with FKBP12. *Cell* 96: 425-436
- Im EH, Choi SS (2017) Synonymous Codon Usage Controls Various Molecular Aspects. *Genomics & informatics* 15: 123-127
- Jacobo SM, Deangelis MM, Kim IK, Kazlauskas A (2013) Age-related macular degeneration-associated silent polymorphisms in HtrA1 impair its ability to antagonize insulin-like growth factor 1. *Molecular and cellular biology* 33: 1976-1990
- Jager HR (2005) Loss of vision: imaging the visual pathways. *European radiology* 15: 501-510
- Jager RD, Mieler WF, Miller JW (2008) Age-related macular degeneration. *N Engl J Med* 358: 2606-2617
- Jakobsdottir J, Conley YP, Weeks DE, Mah TS, Ferrell RE, Gorin MB (2005) Susceptibility genes for age-related maculopathy on chromosome 10q26. *American journal of human genetics* 77: 389-407
- Janeway CA Jr, Travers P, Walport M (2001) *Immunobiology: The Immune System in Health and Disease. The complement system and innate immunity*; New York: Garland Science 5th edition.
- Jiang LQ, Jorquera M, Streilein JW (1993) Subretinal space and vitreous cavity as immunologically privileged sites for retinal allografts. *Invest Ophthalmol Vis Sci* 34: 3347-3354
- Johnson LV, Leitner WP, Staples MK, Anderson DH (2001) Complement Activation and Inflammatory Processes in Drusen Formation and Age Related Macular Degeneration. *Experimental eye research* 73: 887-896
- Jones A, Kumar S, Zhang N, Tong Z, Yang JH, Watt C, Anderson J, Amrita, Fillerup H, McCloskey M, Luo L, Yang Z, Ambati B, Marc R, Oka C, Zhang K, Fu Y (2011) Increased expression of multifunctional serine protease, HTRA1, in retinal pigment epithelium induces polypoidal choroidal vasculopathy in mice. *Proceedings of the National Academy of Sciences of the United States of America* 108: 14578-14583

- Kanda A, Chen W, Othman M, Branham KE, Brooks M, Khanna R, He S, Lyons R, Abecasis GR, Swaroop A (2007) A variant of mitochondrial protein LOC387715/ARMS2, not HTRA1, is strongly associated with age-related macular degeneration. *Proceedings of the National Academy of Sciences of the United States of America* 104: 16227-16232
- Karlstetter M, Ebert S, Langmann T (2010) Microglia in the healthy and degenerating retina: insights from novel mouse models. *Immunobiology* 215: 685-691
- Karlstetter M, Kopatz J, Aslanidis A, Shahraz A, Caramoy A, Linnartz-Gerlach B, Lin Y, Luckoff A, Fauser S, Duker K, Claude J, Wang Y, Ackermann J, Schmidt T, Hornung V, Skerka C, Langmann T, Neumann H (2017) Polysialic acid blocks mononuclear phagocyte reactivity, inhibits complement activation, and protects from vascular damage in the retina. *EMBO molecular medicine* 9: 154-166
- Karlstetter M, Nothdurfter C, Aslanidis A, Moeller K, Horn F, Scholz R, Neumann H, Weber BH, Rupprecht R, Langmann T (2014) Translocator protein (18 kDa) (TSPO) is expressed in reactive retinal microglia and modulates microglial inflammation and phagocytosis. *Journal of neuroinflammation* 11: 3
- Karlstetter M, Scholz R, Rutar M, Wong WT, Provis JM, Langmann T (2015) Retinal microglia: just bystander or target for therapy? *Prog Retin Eye Res* 45: 30-57
- Karperien A, Ahammer H, Jelinek HF (2013) Quantitating the subtleties of microglial morphology with fractal analysis. *Front Cell Neurosci* 7: 3
- Kettenmann H, Hanisch U-K, Noda M, Verkhratsky A (2011) Physiology of Microglia. *Physiological reviews* 91: 461-553
- Khan JC, Thurlby DA, Shahid H, Clayton DG, Yates JR, Bradley M, Moore AT, Bird AC (2006) Smoking and age related macular degeneration: the number of pack years of cigarette smoking is a major determinant of risk for both geographic atrophy and choroidal neovascularisation. *Br J Ophthalmol* 90: 75-80
- Kigerl KA, de Rivero Vaccari JP, Dietrich WD, Popovich PG, Keane RW (2014) Pattern recognition receptors and central nervous system repair. *Experimental Neurology* 258: 5-16
- Kimberley FC, Sivasankar B, Paul Morgan B (2007) Alternative roles for CD59. *Molecular immunology* 44: 73-81
- Klein R, Cruickshanks KJ, Nash SD, Krantz EM, Nieto FJ, Huang GH, Pankow JS, Klein BE (2010) The prevalence of age-related macular degeneration and associated risk factors. *Archives of ophthalmology (Chicago, Ill : 1960)* 128: 750-758
- Klein RJ, Zeiss C, Chew EY, Tsai JY, Sackler RS, Haynes C, Henning AK, SanGiovanni JP, Mane SM, Mayne ST, Bracken MB, Ferris FL, Ott J, Barnstable C, Hoh J (2005) Complement factor H polymorphism in age-related macular degeneration. *Science (New York, NY)* 308: 385-389

Kolb H (1995) Simple Anatomy of the Retina. In *Webvision: The Organization of the Retina and Visual System*, Kolb H, Fernandez E, Nelson R (eds). Salt Lake City (UT): University of Utah Health Sciences Center

Copyright: (c) 2018 Webvision.

Komar AA (2007) Silent SNPs: impact on gene function and phenotype. *Pharmacogenomics* 8: 1075-1080

Korbie DJ, Mattick JS (2008) Touchdown PCR for increased specificity and sensitivity in PCR amplification. *Nature protocols* 3: 1452

Krojer T, Sawa J, Schafer E, Saibil HR, Ehrmann M, Clausen T (2008) Structural basis for the regulated protease and chaperone function of DegP. *Nature* 453: 885-890

Kumar S, Berriochoa Z, Ambati BK, Fu Y (2014) Angiographic features of transgenic mice with increased expression of human serine protease HTRA1 in retinal pigment epithelium. *Invest Ophthalmol Vis Sci* 55: 3842-3850

Kyriakis JM, Avruch J (2001) Mammalian mitogen-activated protein kinase signal transduction pathways activated by stress and inflammation. *Physiological reviews* 81: 807-869

Lacy M, Jones J, Whittemore SR, Haviland DL, Wetsel RA, Barnum SR (1995) Expression of the receptors for the C5a anaphylatoxin, interleukin-8 and FMLP by human astrocytes and microglia. *Journal of neuroimmunology* 61: 71-78

Lamb TD, Collin SP, Pugh EN, Jr. (2007) Evolution of the vertebrate eye: opsins, photoreceptors, retina and eye cup. *Nature reviews Neuroscience* 8: 960-976

Lamb TD, Pugh JEN (2006) Phototransduction, Dark Adaptation, and Rhodopsin Regeneration The Proctor Lecture. *Investigative Ophthalmology & Visual Science* 47: 5138-5152

Lambert V, Lecomte J, Hansen S, Blacher S, Gonzalez ML, Struman I, Sounni NE, Rozet E, de Tullio P, Foidart JM, Rakic JM, Noel A (2013) Laser-induced choroidal neovascularization model to study age-related macular degeneration in mice. *Nature protocols* 8: 2197-2211

Lambris JD (1988) The multifunctional role of C3, the third component of complement. *Immunol Today* 9: 387-393

Langmann T (2007) Microglia activation in retinal degeneration. *J Leukoc Biol* 81: 1345-1351

Launay S, Maubert E, Lebeurrier N, Tennstaedt A, Campioni M, Docagne F, Gabriel C, Dauphinot L, Potier MC, Ehrmann M, Baldi A, Vivien D (2008) HtrA1-dependent proteolysis of TGF- β controls both neuronal maturation and developmental survival. *Cell Death And Differentiation* 15: 1408

- Li MO, Wan YY, Sanjabi S, Robertson AK, Flavell RA (2006) Transforming growth factor-beta regulation of immune responses. *Annu Rev Immunol* 24: 99-146
- Lipo E, Cashman SM, Kumar-Singh R (2013) Aurintricarboxylic acid inhibits complement activation, membrane attack complex, and choroidal neovascularization in a model of macular degeneration. *Invest Ophthalmol Vis Sci* 54: 7107-7114
- Lorenzi T, Lorenzi M, Altobelli E, Marzioni D, Mensa E, Quaranta A, Paolinelli F, Morroni M, Mazzucchelli R, De Luca A, Procopio AD, Baldi A, Muzzonigro G, Montironi R, Castellucci M (2013) HtrA1 in human urothelial bladder cancer: a secreted protein and a potential novel biomarker. *Int J Cancer* 133: 2650-2661
- Loyet KM, Good J, Davancaze T, Sturgeon L, Wang X, Yang J, Le KN, Wong M, Hass PE, Campagne MvL, Haughney PC, Morimoto A, Damico-Beyer LA, DeForge LE (2014) Complement Inhibition in Cynomolgus Monkeys by Anti-Factor D Antigen-Binding Fragment for the Treatment of an Advanced Form of Dry Age-Related Macular Degeneration. *Journal of Pharmacology and Experimental Therapeutics* 351: 527-537
- Luckoff A, Caramoy A, Scholz R, Prinz M, Kalinke U, Langmann T (2016) Interferon-beta signaling in retinal mononuclear phagocytes attenuates pathological neovascularization. *EMBO molecular medicine*
- Luckoff A, Scholz R, Sennlaub F, Xu H, Langmann T (2017) Comprehensive analysis of mouse retinal mononuclear phagocytes. *Nature protocols* 12: 1136-1150
- Lueck K, Wasmuth S, Williams J, Hughes TR, Morgan BP, Lommatzsch A, Greenwood J, Moss SE, Pauleikhoff D (2011) Sub-lytic C5b-9 induces functional changes in retinal pigment epithelial cells consistent with age-related macular degeneration. *Eye (London, England)* 25: 1074-1082
- Luo D-G, Xue T, Yau K-W (2008) How vision begins: An odyssey. *Proceedings of the National Academy of Sciences* 105: 9855-9862
- Malet H, Canellas F, Sawa J, Yan J, Thalassinou K, Ehrmann M, Clausen T, Saibil HR (2012) Newly folded substrates inside the molecular cage of the HtrA chaperone DegQ. *Nature structural & molecular biology* 19: 152-157
- Maller JB, Fagerness JA, Reynolds RC, Neale BM, Daly MJ, Seddon JM (2007) Variation in complement factor 3 is associated with risk of age-related macular degeneration. *Nature genetics* 39: 1200
- Marc RE, Jones BW, Watt CB, Vazquez-Chona F, Vaughan DK, Organisciak DT (2008) Extreme retinal remodeling triggered by light damage: implications for age related macular degeneration. *Molecular vision* 14: 782-806
- Masland RH (2001) The fundamental plan of the retina. *Nature neuroscience* 4: 877-886

Massague J, Wotton D (2000) Transcriptional control by the TGF-beta/Smad signaling system. *The EMBO journal* 19: 1745-1754

Masuda T, Shimazawa M, Hara H (2017) Retinal Diseases Associated with Oxidative Stress and the Effects of a Free Radical Scavenger (Edaravone). *Oxidative medicine and cellular longevity* 2017: 9208489

McGinn TE, Mitchell DM, Meighan PC, Partington N, Leoni DC, Jenkins CE, Varnum MD, Stenkamp DL (2018) Restoration of Dendritic Complexity, Functional Connectivity, and Diversity of Regenerated Retinal Bipolar Neurons in Adult Zebrafish. *J Neurosci* 38: 120-136

McLeod DS, Grebe R, Bhutto I, Merges C, Baba T, Luty GA (2009) Relationship between RPE and choriocapillaris in age-related macular degeneration. *Invest Ophthalmol Vis Sci* 50: 4982-4991

Melo E, Oertle P, Trepp C, Meistermann H, Burgoyne T, Sborgi L, Cabrera AC, Chen CY, Hoflack JC, Kam-Thong T, Schmucki R, Badi L, Flint N, Ghiani ZE, Delobel F, Stucki C, Gromo G, Einhaus A, Hornsperger B, Golling S *et al* (2017) HtrA1 Mediated Intracellular Effects on Tubulin Using a Polarized RPE Disease Model. *EBioMedicine*

Micklisch S, Lin Y, Jacob S, Karlstetter M, Dannhausen K, Dasari P, von der Heide M, Dahse H-M, Schmölz L, Grassmann F, Alene M, Fauser S, Neumann H, Lorkowski S, Pauly D, Weber BH, Joussen AM, Langmann T, Zipfel PF, Skerka C (2017) Age-related macular degeneration associated polymorphism rs10490924 in ARMS2 results in deficiency of a complement activator. *Journal of neuroinflammation* 14: 4

Milner JM, Patel A, Rowan AD (2008) Emerging roles of serine proteinases in tissue turnover in arthritis. *Arthritis and rheumatism* 58: 3644-3656

Mitchell DM, Lovel AG, Stenkamp DL (2018) Dynamic changes in microglial and macrophage characteristics during degeneration and regeneration of the zebrafish retina. *Journal of neuroinflammation* 15: 163

Mitter SK, Rao HV, Qi X, Cai J, Sugrue A, Dunn WA, Grant MB, Boulton ME (2012) Autophagy in the Retina: A Potential Role in Age-Related Macular Degeneration. *Advances in experimental medicine and biology* 723: 83-90

Mitter SK, Song C, Qi X, Mao H, Rao H, Akin D, Lewin A, Grant M, Dunn W, Jr., Ding J, Bowes Rickman C, Boulton M (2014) Dysregulated autophagy in the RPE is associated with increased susceptibility to oxidative stress and AMD. *Autophagy* 10: 1989-2005

Moiseyev G, Chen Y, Takahashi Y, Wu BX, Ma J-x (2005) RPE65 is the isomerohydrolase in the retinoid visual cycle. *Proceedings of the National Academy of Sciences of the United States of America* 102: 12413-12418

Morgan BP (1999) Regulation of the complement membrane attack pathway. *Critical reviews in immunology* 19: 173-198

Muller-Eberhard HJ (1986) The membrane attack complex of complement. *Annu Rev Immunol* 4: 503-528

Müller-Ladner U, Jones JL, Wetsel RA, Gay S, Raine CS, Barnum SR (1996) Enhanced expression of chemotactic receptors in multiple sclerosis lesions. *Journal of the Neurological Sciences* 144: 135-141

Mullins RF, Aptsiauri N, Hageman GS (2001) Structure and composition of drusen associated with glomerulonephritis: implications for the role of complement activation in drusen biogenesis. *Eye (London, England)* 15: 390-395

Mullins RF, Dewald AD, Streb LM, Wang K, Kuehn MH, Stone EM (2011) Elevated membrane attack complex in human choroid with high risk complement factor H genotypes. *Experimental eye research* 93: 565-567

Mullins RF, Schoo DP, Sohn EH, Flamme-Wiese MJ, Workamelahu G, Johnston RM, Wang K, Tucker BA, Stone EM (2014) The membrane attack complex in aging human choriocapillaris: relationship to macular degeneration and choroidal thinning. *The American journal of pathology* 184: 3142-3153

Munoz SS, Li H, Ruberu K, Chu Q, Saghatelian A, Ooi L, Garner B (2018) The serine protease HtrA1 contributes to the formation of an extracellular 25-kDa apolipoprotein E fragment that stimulates neuritogenesis. *J Biol Chem* 293: 4071-4084

Murwantoko, Yano M, Ueta Y, Murasaki A, Kanda H, Oka C, Kawaichi M (2004) Binding of proteins to the PDZ domain regulates proteolytic activity of HtrA1 serine protease. *The Biochemical journal* 381: 895-904

Nakayama M, Iejima D, Akahori M, Kamei J, Goto A, Iwata T (2014) Overexpression of HtrA1 and exposure to mainstream cigarette smoke leads to choroidal neovascularization and subretinal deposits in aged mice. *Invest Ophthalmol Vis Sci* 55: 6514-6523

Natoli R, Fernando N, Jiao H, Racic T, Madigan M, Barnett NL, Chu-Tan JA, Valter K, Provis J, Rutar M (2017) Retinal Macrophages Synthesize C3 and Activate Complement in AMD and in Models of Focal Retinal Degeneration. *Invest Ophthalmol Vis Sci* 58: 2977-2990

Neumaier F, Akhtar-Schafer I, Luke JN, Dibue-Adjei M, Hescheler J, Schneider T (2018) Reciprocal modulation of Cav 2.3 voltage-gated calcium channels by copper(II) ions and kainic acid. *Journal of neurochemistry*

Newman AM, Gallo NB, Hancox LS, Miller NJ, Radeke CM, Maloney MA, Cooper JB, Hageman GS, Anderson DH, Johnson LV, Radeke MJ (2012) Systems-level analysis of age-related macular degeneration reveals global biomarkers and phenotype-specific functional networks. *Genome Med* 4

- Niu S, Yu C, Chen Q, Yuan S, Lin J, Fan W, Liu Q (2017) Multimodality analysis of Hyper-reflective Foci and Hard Exudates in Patients with Diabetic Retinopathy. *Scientific reports* 7: 1568
- Nordahl EA, Rydengard V, Nyberg P, Nitsche DP, Morgelin M, Malmsten M, Bjorck L, Schmidtchen A (2004) Activation of the complement system generates antibacterial peptides. *Proceedings of the National Academy of Sciences of the United States of America* 101: 16879-16884
- Nozaki M, Raisler BJ, Sakurai E, Sarma JV, Barnum SR, Lambris JD, Chen Y, Zhang K, Ambati BK, Baffi JZ, Ambati J (2006) Drusen complement components C3a and C5a promote choroidal neovascularization. *Proceedings of the National Academy of Sciences of the United States of America* 103: 2328-2333
- Oka C, Tsujimoto R, Kajikawa M, Koshiba-Takeuchi K, Ina J, Yano M, Tsuchiya A, Ueta Y, Soma A, Kanda H, Matsumoto M, Kawaichi M (2004) HtrA1 serine protease inhibits signaling mediated by Tgfbeta family proteins. *Development (Cambridge, England)* 131: 1041-1053
- Pahl L, Spangenberg A, Schubert S, Schönmann U, Schmidtke J, Stuhmann M (2012) Characterization of the 10q26-orthologue in rhesus monkeys corroborates a functional connection between ARMS2 and HTRA1. *Experimental eye research* 98: 75-78
- Pang CE, Messinger JD, Zanzottera EC, Freund KB, Curcio CA (2015) The Onion Sign in Neovascular Age-Related Macular Degeneration Represents Cholesterol Crystals. *Ophthalmology* 122: 2316-2326
- Pangburn MK, Muller-Eberhard HJ (1984) The alternative pathway of complement. *Springer seminars in immunopathology* 7: 163-192
- Pangburn MK, Rawal N (2002) Structure and function of complement C5 convertase enzymes. *Biochemical Society transactions* 30: 1006-1010
- Parkhurst CN, Yang G, Ninan I, Savas JN, Yates JR, 3rd, Lafaille JJ, Hempstead BL, Littman DR, Gan WB (2013) Microglia promote learning-dependent synapse formation through brain-derived neurotrophic factor. *Cell* 155: 1596-1609
- Penfold PL, Madigan MC, Gillies MC, Provis JM (2001) Immunological and aetiological aspects of macular degeneration. *Prog Retin Eye Res* 20
- Pennesi ME, Neuringer M, Courtney RJ (2012) Animal models of age related macular degeneration. *Molecular aspects of medicine* 33: 487-509
- Platanias LC (2005) Mechanisms of type-I- and type-II-interferon-mediated signalling. *Nat Rev Immunol* 5: 375-386
- Prinz M, Schmidt H, Mildner A, Knobloch KP, Hanisch UK, Raasch J, Merkler D, Detje C, Gutcher I, Mages J, Lang R, Martin R, Gold R, Becher B, Bruck W, Kalinke U (2008) Distinct and

nonredundant in vivo functions of IFNAR on myeloid cells limit autoimmunity in the central nervous system. *Immunity* 28: 675-686

Raes G, Van den Bergh R, De Baetselier P, Ghassabeh GH (2005) Arginase-1 and Ym1 Are Markers for Murine, but Not Human, Alternatively Activated Myeloid Cells. *The Journal of Immunology* 174: 6561-6562

Rangaraju S, Dammer EB, Raza SA, Gao T, Xiao H, Betarbet R, Duong DM, Webster JA, Hales CM, Lah JJ, Levey AI, Seyfried NT (2018) Quantitative proteomics of acutely-isolated mouse microglia identifies novel immune Alzheimer's disease-related proteins. *Mol Neurodegener* 13: 34

Rashid K, Wolf A, Langmann T (2018) Microglia Activation and Immunomodulatory Therapies for Retinal Degenerations. *Frontiers in Cellular Neuroscience* 12

Raychaudhuri S, Iartchouk O, Chin K, Tan PL, Tai AK, Ripke S, Gowrisankar S, Vemuri S, Montgomery K, Yu Y, Reynolds R, Zack DJ, Campochiaro B, Campochiaro P, Katsanis N, Daly MJ, Seddon JM (2011) A rare penetrant mutation in CFH confers high risk of age-related macular degeneration. *Nature genetics* 43

Réu P, Khosravi A, Bernard S, Mold JE, Salehpour M, Alkass K, Perl S, Tisdale J, Possnert G, Druid H, Frisén J (2017) The Lifespan and Turnover of Microglia in the Human Brain. *Cell reports* 20: 779-784

Reynolds R, Hartnett ME, Atkinson JP, Giclas PC, Rosner B, Seddon JM (2009) Plasma complement components and activation fragments: associations with age-related macular degeneration genotypes and phenotypes. *Invest Ophthalmol Vis Sci* 50: 5818-5827

Risør MW, Poulsen ET, Thomsen LR, Dyrland TF, Nielsen TA, Nielsen NC, Sanggaard KW, Enghild JJ (2014) The Autolysis of Human HtrA1 Is Governed by the Redox State of Its N-Terminal Domain. *Biochemistry* 53: 3851-3857

Rivera A, Fisher SA, Fritsche LG, Keilhauer CN, Lichtner P, Meitinger T, Weber BH (2005) Hypothetical LOC387715 is a second major susceptibility gene for age-related macular degeneration, contributing independently of complement factor H to disease risk. *Human molecular genetics* 14: 3227-3236

Robbie SJ, Georgiadis A, Barker SE, Duran Y, Smith AJ, Ali RR, Luhmann UF, Bainbridge JW (2016) Enhanced Ccl2-Ccr2 signaling drives more severe choroidal neovascularization with aging. *Neurobiol Aging* 40: 110-119

Rollins TE, Siciliano S, Kobayashi S, Cianciarulo DN, Bonilla-Argudo V, Collier K, Springer MS (1991) Purification of the active C5a receptor from human polymorphonuclear leukocytes as a receptor-Gi complex. *Proceedings of the National Academy of Sciences* 88: 971-975

- Saito M, Barbazetto IA, Spaide RF (2013) Intravitreal cellular infiltrate imaged as punctate spots by spectral-domain optical coherence tomography in eyes with posterior segment inflammatory disease. *Retina (Philadelphia, Pa)* 33: 559-565
- Santarpia M, Gonzalez-Cao M, Viteri S, Karachaliou N, Altavilla G, Rosell R (2015) Programmed cell death protein-1/programmed cell death ligand-1 pathway inhibition and predictive biomarkers: understanding transforming growth factor-beta role. *Translational lung cancer research* 4: 728-742
- Schafer Dorothy P, Lehrman Emily K, Kautzman Amanda G, Koyama R, Mardinly Alan R, Yamasaki R, Ransohoff Richard M, Greenberg Michael E, Barres Ben A, Stevens B (2012) Microglia Sculpt Postnatal Neural Circuits in an Activity and Complement-Dependent Manner. *Neuron* 74: 691-705
- Schick T, Steinhauer M, Aslanidis A, Altay L, Karlstetter M, Langmann T, Kirschfink M, Fauser S (2017) Local complement activation in aqueous humor in patients with age-related macular degeneration. *Eye (London, England)* 31: 810-813
- Schmidt N, Irle I, Ripkens K, Lux V, Nelles J, Johannes C, Parry L, Greenow K, Amir S, Campioni M, Baldi A, Oka C, Kawaichi M, Clarke AR, Ehrmann M (2016) Epigenetic silencing of serine protease HTRA1 drives polyploidy. *BMC cancer* 16: 399
- Scholz R, Caramoy A, Bhuckory MB, Rashid K, Chen M, Xu H, Grimm C, Langmann T (2015a) Targeting translocator protein (18 kDa) (TSPO) dampens pro-inflammatory microglia reactivity in the retina and protects from degeneration. *Journal of neuroinflammation* 12: 201
- Scholz R, Sobotka M, Caramoy A, Stempf T, Moehle C, Langmann T (2015b) Minocycline counter-regulates pro-inflammatory microglia responses in the retina and protects from degeneration. *Journal of neuroinflammation* 12: 209
- Schraufstatter IU, Discipio RG, Zhao M, Khaldoyanidi SK (2009) C3a and C5a are chemotactic factors for human mesenchymal stem cells, which cause prolonged ERK1/2 phosphorylation. *J Immunol* 182: 3827-3836
- Schulte G, Fredholm BB (2003) Signalling from adenosine receptors to mitogen-activated protein kinases. *Cellular signalling* 15: 813-827
- Seddon JM, Ajani UA, Mitchell BD (1997) Familial aggregation of age-related maculopathy. *American journal of ophthalmology* 123: 199-206
- Seddon JM, Cote J, Page WF, Aggen SH, Neale MC (2005) The US twin study of age-related macular degeneration: relative roles of genetic and environmental influences. *Archives of ophthalmology (Chicago, Ill : 1960)* 123: 321-327
- Seddon JM, Yu Y, Miller EC, Reynolds R, Tan PL, Gowrisankar S, Goldstein JJ, Triebwasser M, Anderson HE, Zerbib J, Kavanagh D, Souied E, Katsanis N, Daly MJ, Atkinson JP, Raychaudhuri S

(2013) Rare variants in CFI, C3 and C9 are associated with high risk of advanced age-related macular degeneration. *Nature genetics* 45: 1366-1370

Sennlaub F, Auvynet C, Calippe B, Lavalette S, Poupel L, Hu SJ, Dominguez E, Camelo S, Levy O, Guyon E, Saederup N, Charo IF, Rooijen NV, Nandrot E, Bourges JL, Behar-Cohen F, Sahel JA, Guillonnet X, Raoul W, Combadiere C (2013) CCR2⁺ monocytes infiltrate atrophic lesions in age-related macular disease and mediate photoreceptor degeneration in experimental subretinal inflammation in *Cx3cr1* deficient mice. *EMBO molecular medicine* 5: 1775-1793

Shridhar V, Sen A, Chien J, Staub J, Avula R, Kovats S, Lee J, Lillie J, Smith DI (2002) Identification of underexpressed genes in early- and late-stage primary ovarian tumors by suppression subtraction hybridization. *Cancer Res* 62: 262-270

Shull MM, Ormsby I, Kier AB, Pawlowski S, Diebold RJ, Yin M, Allen R, Sidman C, Proetzel G, Calvin D (1992) Targeted disruption of the mouse transforming growth factor-beta 1 gene results in multifocal inflammatory disease. *Nature* 359

Sierra A, de Castro F, Del Rio-Hortega J, Rafael Iglesias-Rozas J, Garrosa M, Kettenmann H (2016) The "Big-Bang" for modern glial biology: Translation and comments on Pio del Rio-Hortega 1919 series of papers on microglia. *Glia* 64: 1801-1840

Skerka C, Lauer N, Weinberger AWA, Keilhauer CN, Sühnel J, Smith R, Schlötzer-Schrehardt U, Fritsche L, Heinen S, Hartmann A, Weber BHF, Zipfel PF (2007) Defective complement control of Factor H (Y402H) and FHL-1 in age-related macular degeneration. *Molecular immunology* 44: 3398-3406

Smith CA, Chauhan BC (2015) Imaging retinal ganglion cells: enabling experimental technology for clinical application. *Prog Retin Eye Res* 44: 1-14

Song D, Sulewski ME, Jr., Wang C, Song J, Bhuyan R, Sterling J, Clark E, Song WC, Dunaief JL (2017) Complement C5a receptor knockout has diminished light-induced microglia/macrophage retinal migration. *Molecular vision* 23: 210-218

Song JS, Kim Y-J, Han KU, Yoon BD, Kim JW (2015) Zymosan and PMA activate the immune responses of Mutz3-derived dendritic cells synergistically. *Immunology Letters* 167: 41-46

Sparrow JR, Ueda K, Zhou J (2012) Complement dysregulation in AMD: RPE-Bruch's membrane-choroid. *Molecular aspects of medicine* 33: 436-445

Spittau B, Rilka J, Steinfath E, Zoller T, Krieglstein K (2015) TGFbeta1 increases microglia-mediated engulfment of apoptotic cells via upregulation of the milk fat globule-EGF factor 8. *Glia* 63: 142-153

Spittau B, Wullkopf L, Zhou X, Rilka J, Pfeifer D, Krieglstein K (2013) Endogenous transforming growth factor-beta promotes quiescence of primary microglia in vitro. *Glia* 61: 287-300

- Stein PJ, Rasenick MM, Bitensky MW (1982) Chapter 8 Biochemistry of the cyclic nucleotide-related enzymes in rod photoreceptors. *Progress in Retinal Research* 1: 227-243
- Strauch KL, Beckwith J (1988) An *Escherichia coli* mutation preventing degradation of abnormal periplasmic proteins. *Proceedings of the National Academy of Sciences of the United States of America* 85: 1576-1580
- Streilein JW (2003) Ocular immune privilege: therapeutic opportunities from an experiment of nature. *Nature Reviews Immunology* 3: 879
- Supanji, Shimomachi M, Hasan MZ, Kawaichi M, Oka C (2013) HtrA1 is induced by oxidative stress and enhances cell senescence through p38 MAPK pathway. *Experimental eye research* 112: 79-92
- Swaroop A, Chew EY, Rickman CB, Abecasis GR (2009) Unraveling a multifactorial late-onset disease: from genetic susceptibility to disease mechanisms for age-related macular degeneration. *Annual review of genomics and human genetics* 10: 19-43
- Swienton DJ, Thomas AG (2014) The visual pathway--functional anatomy and pathology. *Seminars in ultrasound, CT, and MR* 35: 487-503
- Tan JS, Wang JJ, Flood V, Rochtchina E, Smith W, Mitchell P (2008) Dietary antioxidants and the long-term incidence of age-related macular degeneration: the Blue Mountains Eye Study. *Ophthalmology* 115: 334-341
- Taylor HR, West S, Munoz B, Rosenthal FS, Bressler SB, Bressler NM (1992) The long-term effects of visible light on the eye. *Archives of ophthalmology (Chicago, Ill : 1960)* 110: 99-104
- Teige I, Treschow A, Teige A, Mattsson R, Navikas V, Leanderson T, Holmdahl R, Issazadeh-Navikas S (2003) IFN-beta gene deletion leads to augmented and chronic demyelinating experimental autoimmune encephalomyelitis. *J Immunol* 170: 4776-4784
- ten Dijke P, Arthur HM (2007) Extracellular control of TGFbeta signalling in vascular development and disease. *Nat Rev Mol Cell Biol* 8: 857-869
- Tennstaedt A, Popsel S, Truebestein L, Hauske P, Brockmann A, Schmidt N, Irle I, Sacca B, Niemeyer CM, Brandt R, Ksiezak-Reding H, Tirniceriu AL, Egensperger R, Baldi A, Dehmelt L, Kaiser M, Huber R, Clausen T, Ehrmann M (2012) Human high temperature requirement serine protease A1 (HTRA1) degrades tau protein aggregates. *J Biol Chem* 287: 20931-20941
- Thompson VF, Saldaña S, Cong J, Goll DE (2000) A BODIPY Fluorescent Microplate Assay for Measuring Activity of Calpains and Other Proteases. *Analytical biochemistry* 279: 170-178
- Tomany SC, Cruickshanks KJ, Klein R, Klein BE, Knudtson MD (2004) Sunlight and the 10-year incidence of age-related maculopathy: the Beaver Dam Eye Study. *Archives of ophthalmology (Chicago, Ill : 1960)* 122: 750-757

- Toomey CB, Johnson LV, Bowes Rickman C (2018a) Complement factor H in AMD: Bridging genetic associations and pathobiology. *Progress in Retinal and Eye Research* 62: 38-57
- Toomey CB, Landowski M, Klingeborn M, Kelly U, Deans J, Dong H, Harrabi O, Van Blarcom T, Yeung YA, Grishanin R, Lin JC, Saban DR, Bowes Rickman C (2018b) Effect of Anti-C5a Therapy in a Murine Model of Early/Intermediate Dry Age-Related Macular Degeneration. *Investigative Ophthalmology & Visual Science* 59: 662-673
- Tosi GM, Caldi E, Neri G, Nuti E, Marigliani D, Baiocchi S, Traversi C, Cevenini G, Tarantello A, Fusco F, Nardi F, Orlandini M, Galvagni F (2017) HTRA1 and TGF-beta1 Concentrations in the Aqueous Humor of Patients With Neovascular Age-Related Macular Degeneration. *Invest Ophthalmol Vis Sci* 58: 162-167
- Tuo J, Ross RJ, Reed GF, Yan Q, Wang JJ, Bojanowski CM, Chew EY, Feng X, Olsen TW, Ferris FL, Mitchell P, Chan C-C (2008) The HtrA1 Promoter Polymorphism, Smoking, and Age-related Macular Degeneration in Multiple Case-control Samples. *Ophthalmology* 115: 1891-1898
- Ufret-Vincenty RL, Aredo B, Liu X, McMahon A, Chen PW, Sun H, Niederkorn JY, Kedzierski W (2010) Transgenic Mice Expressing Variants of Complement Factor H Develop AMD-like Retinal Findings. *Investigative Ophthalmology & Visual Science* 51: 5878-5887
- Van Beek J, Bernaudin M, Petit E, Gasque P, Nouvelot A, MacKenzie ET, Fontaine M (2000) Expression of Receptors for Complement Anaphylatoxins C3a and C5a Following Permanent Focal Cerebral Ischemia in the Mouse. *Experimental Neurology* 161: 373-382
- van der Schaft TL, Mooy CM, de Bruijn WC, de Jong PT (1993) Early stages of age-related macular degeneration: an immunofluorescence and electron microscopy study. *The British Journal of Ophthalmology* 77: 657-661
- Ven JP, Nilsson SC, Tan PL, Buitendijk GH, Ristau T, Mohlin FC, Nabuurs SB, Schoenmaker-Koller FE, Smailhodzic D, Campochiaro PA, Zack DJ, Duvvari MR, Bakker B, Paun CC, Boon CJ, Uitterlinden AG, Liakopoulos S, Klevering BJ, Fauser S, Dahan MR *et al* (2013) A functional variant in the CFI gene confers a high risk of age-related macular degeneration. *Nature genetics* 45
- Vierkotten S, Muether PS, Fauser S (2011) Overexpression of HTRA1 leads to ultrastructural changes in the elastic layer of Bruch's membrane via cleavage of extracellular matrix components. *PLoS One* 6: e22959
- Vogt SD, Barnum SR, Curcio CA, Read RW (2006) Distribution of complement anaphylatoxin receptors and membrane-bound regulators in normal human retina. *Experimental eye research* 83: 834-840
- Walter P, Widder RA, Luke C, Konigsfeld P, Brunner R (1999) Electrophysiological abnormalities in age-related macular degeneration. *Graefes Arch Clin Exp Ophthalmol* 237: 962-968

Wang AL, Lukas TJ, Yuan M, Du N, Tso MO, Neufeld AH (2009a) Autophagy and Exosomes in the Aged Retinal Pigment Epithelium: Possible Relevance to Drusen Formation and Age-Related Macular Degeneration. *PLoS ONE* 4: e4160

Wang G (2014) Chromosome 10q26 locus and age-related macular degeneration: A progress update. *Experimental eye research* 119: 1-7

Wang G, Spencer KL, Court BL, Olson LM, Scott WK, Haines JL, Pericak-Vance MA (2009b) Localization of Age-Related Macular Degeneration-Associated ARMS2 in Cytosol, Not Mitochondria. *Investigative Ophthalmology & Visual Science* 50: 3084-3090

Wang M, Wang X, Zhao L, Ma W, Rodriguez IR, Fariss RN, Wong WT (2014) Macrogliia-microglia interactions via TSPO signaling regulates microglial activation in the mouse retina. *J Neurosci* 34: 3793-3806

Wang W, Gawlik K, Lopez J, Wen C, Zhu J, Wu F, Shi W, Scheibler S, Cai H, Vairavan R, Shi A, Haw W, Ferreyra H, Zhang M, Chang S, Zhang K (2016a) Genetic and environmental factors strongly influence risk, severity and progression of age-related macular degeneration. *Signal Transduction and Targeted Therapy* 1: 16016

Wang X, Zhao L, Zhang J, Fariss RN, Ma W, Kretschmer F, Wang M, Qian HH, Badea TC, Diamond JS, Gan WB, Roger JE, Wong WT (2016b) Requirement for Microglia for the Maintenance of Synaptic Function and Integrity in the Mature Retina. *J Neurosci* 36: 2827-2842

Ward PA (2009) Functions of C5a receptors. *Journal of molecular medicine (Berlin, Germany)* 87: 375-378

Weih LM, VanNewkirk MR, McCarty CA, Taylor HR (2000) Age-specific causes of bilateral visual impairment. *Archives of ophthalmology (Chicago, Ill : 1960)* 118: 264-269

Wenzel A, Grimm C, Samardzija M, Remé CE (2005) Molecular mechanisms of light induced photoreceptor apoptosis and neuroprotection for retinal degeneration. *Prog Ret Eye Res* 24

Wenzel A, Reme CE, Williams TP, Hafezi F, Grimm C (2001) The Rpe65 Leu450Met variation increases retinal resistance against light-induced degeneration by slowing rhodopsin regeneration. *J Neurosci* 21: 53-58

Wong-Riley M (2010) Energy metabolism of the visual system. *Eye and Brain* 2: 99-116

Wong WL, Su X, Li X, Cheung CM, Klein R, Cheng CY, Wong TY (2014) Global prevalence of age-related macular degeneration and disease burden projection for 2020 and 2040: a systematic review and meta-analysis. *The Lancet Global health* 2: e106-116

Wynn TA, Vannella KM (2016) Macrophages in Tissue Repair, Regeneration, and Fibrosis. *Immunity* 44: 450-462

- Xu H, Chen M (2016) Targeting the complement system for the management of retinal inflammatory and degenerative diseases. *European journal of pharmacology*
- Yamashita H, ten Dijke P, Franzen P, Miyazono K, Heldin CH (1994) Formation of hetero-oligomeric complexes of type I and type II receptors for transforming growth factor-beta. *J Biol Chem* 269: 20172-20178
- Yang Z, Camp NJ, Sun H, Tong Z, Gibbs D, Cameron DJ, Chen H, Zhao Y, Pearson E, Li X, Chien J, Dewan A, Harmon J, Bernstein PS, Shridhar V, Zabriskie NA, Hoh J, Howes K, Zhang K (2006) A variant of the HTRA1 gene increases susceptibility to age-related macular degeneration. *Science* (New York, NY) 314: 992-993
- Zamiri P, Sugita S, Streilein JW (2007) Immunosuppressive properties of the pigmented epithelial cells and the subretinal space. *Chemical immunology and allergy* 92: 86-93
- Zarepari S, Branham KE, Li M, Shah S, Klein RJ, Ott J, Hoh J, Abecasis GR, Swaroop A (2005) Strong association of the Y402H variant in complement factor H at 1q32 with susceptibility to age-related macular degeneration. *American journal of human genetics* 77: 149-153
- Zhan X, Larson DE, Wang C, Koboldt DC, Sergeev YV, Fulton RS, Fulton LL, Fronick CC, Branham KE, Bragg-Gresham J, Jun G, Hu Y, Kang HM, Liu D, Othman M, Brooks M, Ratnapriya R, Boleda A, Grassmann F, von Strachwitz C *et al* (2013) Identification of a rare coding variant in complement 3 associated with age-related macular degeneration. *Nature genetics* 45: 1375-1379
- Zhang Y, Derynck R (1999) Regulation of Smad signalling by protein associations and signalling crosstalk. *Trends in Cell Biology* 9: 274-279
- Zhang Y, Zhao L, Wang X, Ma W, Lazere A, Qian H-h, Zhang J, Abu-Asab M, Fariss RN, Roger JE, Wong WT (2018) Repopulating retinal microglia restore endogenous organization and function under CX3CL1-CX3CR1 regulation. *Science Advances* 4
- Zhou J, Jang YP, Kim SR, Sparrow JR (2006) Complement activation by photooxidation products of A2E, a lipofuscin constituent of the retinal pigment epithelium. *Proceedings of the National Academy of Sciences of the United States of America* 103: 16182-16187
- Zhou J, Kim SR, Westlund BS, Sparrow JR (2009) Complement Activation by Bisretinoid Constituents of RPE Lipofuscin. *Investigative Ophthalmology & Visual Science* 50: 1392-1399
- Zhou X, Spittau B, Krieglstein K (2012) TGFbeta signalling plays an important role in IL4-induced alternative activation of microglia. *Journal of neuroinflammation* 9: 210
- Zhou X, Zoller T, Krieglstein K, Spittau B (2015) TGFbeta1 inhibits IFNgamma-mediated microglia activation and protects mDA neurons from IFNgamma-driven neurotoxicity. *Journal of neurochemistry* 134: 125-134

Zipfel PF, Mhlan M, Skerka C (2007) The alternative pathway of complement: a pattern recognition system. *Advances in experimental medicine and biology* 598: 80-92

Zöller T, Schneider A, Kleimeyer C, Masuda T, Potru PS, Pfeifer D, Blank T, Prinz M, Spittau B (2018) Silencing of TGF β signalling in microglia results in impaired homeostasis. *Nature communications* 9: 4011

List of Abbreviations

Abbreviations, if not mentioned in 2.1

Aif1	Allograft inflammatory factor 1
AMD	Age-related macular degeneration
ANOVA	Analysis of variance
ARMS2	Age-related maculopathy susceptibility 2
Arg1	Arginase 1
BAC	Bacterial artificial chromosome
BM	Bruch's membrane
Bp	Base pairs
BRB	Blood retina barrier
C	Complement component
C3aR	C3a anaphylatoxin chemotactic receptor
C5aR	C5a anaphylatoxin chemotactic receptor
CF	Complement factor
CD	Clusters of differentiation
CARASIL	Cerebral autosomal recessive arteriopathy with subcortical infarcts and leukoencephalopathy
CCL2	C-C motif chemokine 2
cDNA	Complementary DNA
CNS	Central nervous system
CNV	Choroidal neovascularization
Cp	Crossing-point
CSF1R	Colony stimulating factor 1 receptor
CX3CR1	C-X3-C motif chemokine receptor 1/ fractalkine
dH ₂ O	Distilled water
DAF	Decay-accelerating factor
DAMP	Damage-associated molecular pattern
DMEM	Dulbecco's modified eagle's medium
DNA	Deoxyribonucleic acid
dNTP's	2'-desoxyribonucleotides triphosphate
ERG	Electroretinogram
ERK	Extracellular signal-regulated protein kinases
F	Forward
GA	Geographic atrophy

GCL	Ganglion cell layer
GWAS	Genome wide association studies
h	Human
hWT	Human wildtype HtrA1 protein
hS328A	Human protease inactive HtrA1 protein
hSNP	Human AMD-associated HtrA1 protein
H&E stain	Hematoxylin and eosin stain
HF	Hyper-reflective foci
HRP	Horseradisch peroxidase
HtrA1	high-temperature requirement A serine peptidase 1, protein
HTRA1	human gene
Htra1	murine gene
Iba1	Ionized calcium-binding adapter molecule 1
IFN- β	Interferon- β
IFN- γ	Interferon- γ
Ifnar	Interferon- α/β receptor
IGF-1	Insulin-like growth factor 1
IGFBP	Insulin-like growth factor binding proteins
IS	Inner segments
iNos	Inducible nitric oxide synthase
INL	Inner nuclear layer
IPL	Inner plexiform layer
KAZ	Kazal-like domain
kDa	Kilodalton
Klf10	Kruppel Like Factor 10
LD	Bright light induced retinal degeneration
LPS	Lipopolysaccharide
m	Murine/mouse
mWT	Murine wildtype HtrA1 protein
mS328A	Murine protease inactive HtrA1 protein
MAC	Membrane attack complex
MAPK	Mitogen-activated protein kinase
MASP	Mannan-binding lectin serine protease
MBL	Mannose-binding lectin
nAMD	neovascular AMD
NBF	Neutral buffered formalin
NED	N-1-naphthylethylenediamine dihydrochloride
NF- κ B	Nuclear factor kappa-light-chain-enhancer of activated B cells

NO	Nitric oxide
ONL	Outer nuclear layer
OPL	Outer plexiform layer
ORF	Outer reading frame
OS	Outer segments
PAI-1	Plasminogen activator inhibitor 1
PAMP	Pathogen-associated molecular pattern
PDZ domain	Postsynaptic density of 95 kDa, Discs large and zonula occludens 1 domain
PFA	Paraformaldehyde
PMA	Phorbol 12-myristate 13-acetate
PRR	Pattern recognition receptor
qRT-PCR	Quantitative reverse transcriptase polymerase chain reaction
R	Reverse
RFU	Relative fluorescence units
RPE	Retinal pigment epithelium
RPE65	Retinoid isomerohydrolase
RNA	Ribonucleic acid
ROS	Reactive oxygen species
rpm	Revolutions per minute
SD-OCT	Spectral domain - Optical coherence tomography
SEM	Standard error of the mean
Smad	Mothers against decapentaplegic homolog 2
SNP	Single nucleotide polymorphism
SOCS	Suppressor of cytokine signaling
SP	Signal peptide
STAT	Signal transducer and activator of transcription
TBE	Tris/Borate/EDTA
TBS	Tris buffer saline
TGF- β	Transforming growth factor- β
Tgf- β RII	TGF- β receptor type II
TLR	Toll-like receptor
TNF- α	Tumor necrosis factor- α
TRITC	Tetramethylrhodamine
TSPO	Translocator protein
UTR	Untranslated region
VEGF	Vascular endothelial growth factor
WT	Wildtype
Ym1	Chitinase-like protein 3

List of Figures

Figure 1 Schematic overview of the human eye and the structure of the retina.....	4
Figure 2 Early, intermediate and late AMD symptoms of diseased individuals	6
Figure 3 Fundus and SD-OCT photographs and histology of healthy and diseased eyes.....	7
Figure 4 Associated and linkage signals and disease liability explained by total variants	9
Figure 5 Complement activation, regulation, and immune functions	11
Figure 6 The 10q26 locus, harboring ARMS2/HTRA1 and the structure of HtrA1	15
Figure 7 Microglia phenotype and retinal location during health and disease.....	19
Figure 8 XBD173 treatment of light-exposed mice prevents microglia reactivity	22
Figure 9 Experimental setup for light induced retinal damage (LD) in BALB/cJ mice	51
Figure 10 Representative ERG traces of retina from control and LD mice	52
Figure 11 Analysis of a-wave and b-wave amplitude and implicit time after LD	53
Figure 12 Representative OCT images and HF quantification.....	54
Figure 13 Origin of HF in degenerating retina.....	55
Figure 14 Expression of anaphylatoxin receptors in microglia upon activation in vitro.....	57
Figure 15 Transient increase in complement system activation upon retinal degeneration.	58
Figure 16 Co-localization of C3aR and microglia marker Aif during retinal degeneration.	59
Figure 17 Co-localization of C5aR and microglia marker Aif during retinal degeneration.	59
Figure 18 Gene expression of Aif1 and Htra1 after LD	60
Figure 19 Work stream for HtrA1 expression, purification and <i>in vitro</i> analysis	61
Figure 20 Immunoblot of HtrA1 variants and their proteolytic characterization.....	62
Figure 21 TGF- β induced quiescence in challenged primary murine microglia cells	64
Figure 22 Primary microglia cell morphology upon treatment with IFN- γ and TGF- β	64
Figure 23 BV-2 cells mirror primary microglial activity	65
Figure 24 HtrA1 stimulation do not inhibit TGF- β induced microglial quiescence	66
Figure 25 HtrA1 variants do not alter NO levels and morphology	67
Figure 26 HtrA1 variants do not influence TGF- β induced PAI-1 promotor activity.....	68
Figure 27 Effect of HtrA1 variants on paracrine TGF- β signaling	69

List of Tables

Table 1 Mouse strain, eye drops and systemic anesthesia.....	26
Table 2 Cell lines and bacteria strain.....	26
Table 3 Reagents and formula for cell culture and lysogeny broth (LB) media/plates.....	27
Table 4 Buffers and solutions prepared as indicated.....	28
Table 5 Self prepared gels.	29
Table 6 List of primary and secondary antibodies, stains and fluorophores.	29
Table 7 Enzymes, reaction buffers and PCR reagents.....	30
Table 8 Commercially available kits.	30
Table 9 Origin of gene sequence and plasmids used for cloning.	31
Table 10 Cloning primers fur human (h) and murine (m) constructs.....	31
Table 11 Sequencing primers.	31
Table 12 RNAscope® probes for murine target genes.....	32
Table 13 Primers and Roche probes used for quantitative RT-PCR.	32
Table 14 List of cytokines and compounds for cell culture and other reagents.	33
Table 15 List of laboratory devices.	34
Table 16 General consumables (not in alphabetical order).	35
Table 17 List of software programs.....	36
Table 18 PCR to amplify the ORF of murine and human HTRA1 variants.	42
Table 19 PCR program.....	43
Table 20 PCR product digestion.....	43
Table 21 Insert and vector ligation.	43
Table 22 Test digestion.	44
Table 23 qRT-PCR components.....	47
Table 24 qRT-PCR cycling conditions.....	47

Attachments

Acknowledgements

First and foremost, I thank Prof. Dr. Thomas Langmann, Chair of the Department of Experimental Immunology of the Eye, for his extensive professional guidance, which taught me a great deal about scientific research. I am very grateful for the opportunity to work in his lab alongside brilliant people. I owe a huge thanks to my colleagues, as well as former lab members. It was always fun to work with each one of them.

I would like to thank my mentor, Prof. Dr. Elena Rugarli who worked actively to provide me with outstanding ideas and major support to complete this project. I especially thank Prof. Dr. Toni Schneider who has been my mentor for a long time. He has taught me more than I could ever give him credit for here. I am also grateful to each of the members of my Thesis Committee, including Prof. Dr. Thorsten Hoppe and Prof. Dr. Stanislav Kopriva.

I would especially like to thank Dr. Isabell Witt and Dr. Marion Rosowski, the scientific coordinators of the Graduate Schools, for their continuous effort and support in project-related issues and also personal growth.

I am grateful to all of those with whom I have had the pleasure to work during this project. I would like to mention Dr. Markus Pietsch (Centre for Pharmacology) as well as Prof. Manuel Koch (Biochemistry II) and the members of their labs, who supported me with their excellent expertise.

This work would not have been possible without the financial support of the DFG (FOR2240), the ProRetina Foundation, and the Graduate Program in Pharmacology and Experimental Therapeutics in collaboration with Bayer AG.

Last but not least I owe every member of my family the greatest acknowledgements for their support and unconditional love: My parents, whose love and guidance are with me in whatever I pursue, and to whom I am dedicating this work to. My sisters, Seemel and Qiratt, who never fail to make me laugh, cheer me up, and motivate me. Annette and Herbert, who always support and encourage me to grow and accomplish new goals.

Most importantly, I thank Chris.

Erklärung

Ich versichere, dass ich die von mir vorgelegte Dissertation selbstständig angefertigt, die benutzten Quellen und Hilfsmittel vollständig angegeben und die Stellen der Arbeit – einschließlich Tabellen, Karten und Abbildungen –, die anderen Werken im Wortlaut oder dem Sinn nach entnommen sind, in jedem Einzelfall als Entlehnung kenntlich gemacht habe; dass diese Dissertation noch keiner anderen Fakultät oder Universität zur Prüfung vorgelegen hat; dass sie – abgesehen von unten angegebenen Teilpublikationen – noch nicht veröffentlicht worden ist, sowie, dass ich eine solche Veröffentlichung vor Abschluss des Promotionsverfahrens nicht vornehmen werde. Die Bestimmungen der Promotionsordnung sind mir bekannt. Die von mir vorgelegte Dissertation ist von Prof. Dr. Elena Rugarli und Prof. Dr. Thomas Langmann betreut worden.

Ich versichere, dass ich alle Angaben wahrheitsgemäß nach bestem Wissen und Gewissen gemacht habe und verpflichte mich, jedmögliche, die obigen Angaben betreffenden Veränderungen, dem Promotionsausschuss unverzüglich mitzuteilen.



Köln, den 16.02.2019

Isha Akhtar-Schäfer

Lebenslauf

PAWWAN ISHA AKHTAR-SCHÄFER, M.Sc.

Geburtsdatum	27. März 1990
Nationalität	deutsch
Adresse	Hofferhofer Str. 7, 51503 Rösrath
Telefon	+49 (0)176 707 374 93
Email	isha.akhtar@googlemail.com

Werdegang

05/2015 – Gegenwart	Promotion Dr. rer. nat. Lehrstuhl für experimentelle Immunologie des Auges, Universität zu Köln
10/2012 – 03/2015	M.Sc. in klinische und experimentelle Neurowissenschaften Universität zu Köln
10/2009 – 09/2012	B.Sc. in Neurowissenschaften Universität zu Köln
09/2000 – 06/2009	Abitur Hansa-Gymnasium, Köln

Publikationen

Isha Akhtar-Schäfer, Luping Wang, Tim U Krohne, Heping Xu, Thomas Langmann (2018) “Modulation of three key innate immune pathways for the most common retinal degenerative diseases.” *Embo Mol Med*, PMID: 30224384, DOI: 10.15252/emmm.201708259

Felix Neumaier, **Isha Akhtar-Schäfer**, Jan Niklas Lüke, Maxine Dibué-Adjei, Jürgen Hescheler, Toni Schneider (2018) „Reciprocal modulation of Cav2.3 voltage-gated calcium channels by copper(II) ions and kainic acid“ *J Neurochem*. PMID: 29972687, DOI:10.1111/jnc.14546.

Siarhei A. Siapich, **Isha Akhtar**, Toni Schneider & Matthias Lüke (2015) “*Low concentrations of ethanol but not of dimethyl sulfoxide (DMSO) impair reciprocal retinal signal transduction*”, *Graefes Arch Clin Exp Ophthalmol*. PMID: 26104874; DOI: 10.1007/s00417-015-3070-7.

Toni Schneider, Maxine Dibue-Adjei, Felix Neumaier, **Isha Akhtar**, Jürgen Hescheler, Marcel A. Kamp, Etienne E. Tevoufouet (2015) „*R-Type Voltage-Gated Ca²⁺ Channels in Cardiac and Neuronal Rhythmogenesis*.“ *Curr Mol Pharmacol*.

Maxine Dibué, Etienne E. Tevoufouet, Felix Neumaier, Andreas Krieger, Alexandra Kiel, Dimitar Evdokimov, Thomas Galetin, Serdar Alpdogan, **Isha Akhtar**, Sabrina Scharf, Renate Clemens, Kayalvizhi Radhakrishnan, Jürgen Hescheler, Toni Schneider and Marcel A. Kamp, (2013) “*Protein Interaction Partners of Cav2.3 R-Type Voltage-Gated Calcium Channels*” in *Modulation of Presynaptic Calcium Channels*.

